แรงเฉือนที่ต้องต้านทานในปล่องลิฟท์คอนกรีตเสริมเหล็ก

นายคิมเล็ง คีห์

วิทยานิพนธ์นี้เป็นส่วนหนึ่งของการศึกษาตามหลักสูตรปริญญาวิศวกรรมศาสตรมหาบัณฑิต
สาขาวิชาวิศวกรรมโยธา ภาควิชาวิศวกรรมโยธา
คณะวิศวกรรมศาสตร์ จุฬาลงกรณ์มหาวิทยาลัย
ปีการศึกษา 2558

SEISMIC SHEAR DEMANDS OF REINFORCED CONCRETE CORE WALLS

Mr. Kimleng Khy

A Thesis Submitted in Partial Fulfillment of the Requirements
for the Degree of Master of Engineering Program in Civil Engineering
Department of Civil Engineering
Faculty of Engineering
Chulalongkorn University
Academic Year 2015

Thesis Title	SEISMIC SHEAR DEMANDS OF REINFORCED CONCRETE CORE WALLS
By	Mr. Kimleng Khy
Field of Study	Civil Engineering
Thesis Advisor	Assistant Professor Chatpan Chintanapakdee, Ph.D.

Accepted by the Faculty of Engineering, Chulalongkorn University in Partial Fulfillment of the Requirements for the Master's Degree

.....Dean of the Faculty of Engineering
(Professor Bundhit Eua-arporn, Ph.D.)

THESIS COMMITTEE

.....Chairman
(Assistant Professor Anat Ruangrassamee, Ph.D.)
.....Thesis Advisor
(Assistant Professor Chatpan Chintanapakdee, Ph.D.)
.....External Examiner
(Associate Professor Sutat Leelataviwat, Ph.D.)

คิมเล็ง คีห์ : แรงเฉือนที่ต้องต้านทานในปล่องลิฟท์คอนกรีตเสริมเหล็ก (SEISMIC SHEAR DEMANDS OF REINFORCED CONCRETE CORE WALLS) อ.ที่ปรึกษาวิทยานิพนธ์หลัก: ฉัตรพันธ์ จินตนาภักดี, 127 หน้า.

มาตรฐาน ASCE 7-10 อนุญาตให้วิศวกรใช้วิธีสเปกตรัมผลตอบสนอง (Response Spectrum Analysis, RSA) ในการคำนวณแรงจากแผ่นดินไหวเพื่อการออกแบบของโครงสร้างอาคารสูง แต่งานวิจัยหลายชิ้นชี้ให้เห็นว่าค่าแรงเฉือนในกำแพงรับแรงเฉือนที่วิเคราะห์ได้จากวิธี RSA นั้นมีค่าต่ำกว่าแรงเฉือนที่จะเกิดขึ้นจริงหลายเท่า งานวิจัยนี้จึงศึกษาแรงเฉือนที่ต้องต้านทานในปล่องลิฟท์คอนกรีตเสริมเหล็กของอาคารที่มีความสูงตั้งแต่ 5 ถึง 25 ชั้น โดยคำนึงถึงรูปแบบการจัดวาง ตำแหน่งของปล่องลิฟท์ที่แบ่งออกเป็นสองแถว (split core walls) โดยสมมติให้อาคารตั้งอยู่ที่กรุงเทพมหานครหรือเชียงใหม่ และทำการออกแบบปล่องลิฟท์ด้วยวิธี RSA ตามมาตรฐาน ASCE 7-10 จากนั้นทำการวิเคราะห์โครงสร้างด้วยวิธีที่ให้ค่าถูกต้องสมจริงที่สุดคือวิธีแบบประวัติเวลาไม่เชิงเส้น (Nonlinear Response History Analysis, NLRHA) เพื่อคำนวณค่าแรงภายในที่น่าจะเกิดขึ้นจริงเนื่องจากแผ่นดินไหว จากผลการศึกษา พบว่าวิธี NLRHA ให้ค่าแรงเฉือนที่ต้องต้านทานของผนังปล่องลิฟท์สูงกว่าค่าจากวิธี RSA ซึ่งหมายความว่าโครงสร้างที่ออกแบบโดยใช้ค่าจากวิธี RSA อาจไม่ปลอดภัยจากการวิบัติแบบเฉือน ปล่องลิฟท์มีพฤติกรรมในทิศทางหนึ่งแบบกำแพงยื่นขึ้นจากพื้น และอีกทิศทางหนึ่งแบบกำแพงที่มีคานเชื่อม (coupled walls) หากพิจารณาการขยายค่าแรงเฉือนโดยใช้อัตราส่วนของแรงเฉือนในกำแพงที่ได้จาก NLRHA และ RSA พบว่าการขยายค่าแรงเฉือนในทิศทางที่มีพฤติกรรมแบบคานยื่นมีความรุนแรงมากกว่า ตำแหน่งที่ตั้งของอาคารทำให้การขยายค่าแรงเฉือนมีความแตกต่างกันเนื่องจากความแตกต่างของกราฟสเปกตรัมผลตอบสนองส่งผลให้การมีส่วนร่วมของโหมดสูงมีความแตกต่างกัน จากการศึกษาสมการสำหรับประมาณค่าการขยายค่าแรงเฉือนที่เสนอโดยงานวิจัยหลายชิ้นพบว่าสมการที่เสนอโดย Rejec และคณะ (2012) สามารถประมาณค่าได้แม่นยำสำหรับทิศทางแบบกำแพงยื่นในกรณีอาคารตั้งอยู่ที่กรุงเทพมหานคร ส่วนสมการของ Luu และคณะ (2014) ให้ค่าประมาณที่ดีทั้งสองทิศทางในกรณีอาคารตั้งอยู่ที่เชียงใหม่ มาตรฐาน Eurocode 8 (2004) มีการกำหนดให้คูณขยายค่าแรงเฉือนในกำแพงที่คำนวณจากวิธี RSA ด้วย ซึ่งมีปลอดภัยเพียงพอในอาคารต่างๆ ในการศึกษานี้ เกือบทุกกรณีเว้นแต่ที่ฐานของอาคาร 20 และ 25 ชั้นที่ตั้งอยู่ที่กรุงเทพมหานคร ซึ่งอาจนำไปประยุกต์ใช้เพื่อให้การออกแบบมีความปลอดภัย

ภาควิชา วิศวกรรมโยธา ลายมือชื่อนิสิต .....

สาขาวิชา วิศวกรรมโยธา ลายมือชื่อ อ.ที่ปรึกษาหลัก .....

ปีการศึกษา 2558

5670539421 : MAJOR CIVIL ENGINEERING
KEYWORDS: SEISMIC SHEAR DEMAND / REINFORCED CONCRETE CORE WALL / HIGH-RISE BUILDING / RESPONSE SPECTRUM ANALYSIS / NONLINEAR RESPONSE HISTORY ANALYSIS

KIMLENG KHY: SEISMIC SHEAR DEMANDS OF REINFORCED CONCRETE CORE WALLS. ADVISOR: ASST. PROF. CHATPAN CHINTANAPAKDEE, Ph.D., 127 pp.

ASCE 7-10 allows practical engineers to use Response Spectrum Analysis (RSA) procedure to compute the design forces of the structures. However, it has been found to be inappropriate for seismic shear demands of reinforced concrete (RC) walls. This thesis aims to investigate the seismic shear demands of RC core walls from low-rise to high-rise buildings. RC split core walls in 5 buildings varying from 5 to 25 stories subjected to ground motions in Bangkok and Chiang Mai of Thailand are first designed by RSA procedure in ASCE 7-10. Then, nonlinear response history analysis (NLRHA) is conducted to compute more accurate seismic demands of the structures. The results demonstrate that shear demands of core walls from NLRHA are significantly larger than those from RSA procedure. The ratio between shear force from NLRHA and RSA procedure is defined as shear amplification. The shear amplifications of core walls in cantilever-wall direction are larger than those in coupled-wall direction. The two building locations having different spectrum shapes lead to different shear amplifications. Rejec et al. (2012)'s equation can well estimate shear forces in cantilever direction of the core walls in Bangkok. Luu et al. (2014)'s equation provides good estimation of shear forces in both directions of the core walls in Chiang Mai. Beside these two equations, the shear magnification factor equation in Eurocode 8 (2004) is appropriate to be adopted to multiply with shear forces from RSA procedure before using them as design shear forces of RC core walls in both Bangkok and Chiang Mai, with the exception that it slightly underestimates the base shear forces in cantilever direction of 20- and 25-story core walls in Bangkok.

Department:	Civil Engineering	Student's Signature	.....
Field of Study:	Civil Engineering	Advisor's Signature	.....
Academic Year:	2015		

ACKNOWLEDGEMENTS

First of all, I would like to express my sincere gratitude to my thesis advisor, Asst. Prof. Chatpan Chintanapakdee, for his productive guidance, generous assistance, good advice and strong support during my research study for this Master's degree program. I highly appreciate his valuable time, encouragement and attention to discuss about my research issues with me.

I gratefully acknowledge the ASEAN University Network/Southeast Asia Engineering Education Development Network (AUN/SEED-Net) for providing the financial support throughout my Master's degree at Chulalongkorn University.

My profound thanks are also extended to all committee members, Asst. Prof. Anat Ruangrassamee and Assoc. Prof. Sutat Leelataviwat for their thoughtful comments and suggestions for this research. I sincerely appreciate lectures and professors at Institute of Technology of Cambodia and Chulalongkorn Universy for providing me necessary engineering knowledge to conduct my research.

Last but not least, I would like to deeply thank my parents and my fiancée for their encouragement and support which motivate me to accomplish this research successfully.

CONTENTS

Page

Page

LIST OF TABLES

LIST OF FIGURES

CHAPTER 1
INTRODUCTION

1.1 Background

Usefulness of structural walls in medium-rise and high-rise buildings has long been recognized both structural and functional requirements. They can form an efficient lateral resisting system to control the lateral deflection and to reduce the possibility of excessive deformations of the building subjected to earthquake loading. Hence, the choice of structural wall system and its advantageous position in a building is quite challenging. Among these, reinforced concrete (RC) split core walls where elevators are built inside are commonly used in Thailand.

To design such buildings under earthquake loading, practical engineers in Thailand usually employ modal response spectrum analysis (RSA) procedure in ASCE 7-10 to determine the design forces of the walls. The design forces in this method are obtained by using a single response modification factor (R) for all modes of response to reduce the elastic forces computed from RSA procedure. This method uses the same *R* for reducing shear force and bending moment hoping that flexural yielding at the base region of the wall limits shear force in the same way as it limits bending moment of the wall. However, the modal contributions of shear and moment responses are not identical. From elastic modal analysis, the base shear response of the wall is considerably contributed from the second mode especially for tall buildings whereas the first mode contributes most of the bending moment at the base of the wall. Previous researchers have demonstrated that flexural yielding at the base region of the wall reduces mainly the first mode shear but higher-mode shears are not significantly affected by inelastic action. Consequently, nonlinear response history analysis (NLRHA) results show that shear force keeps increasing after flexural yielding occurs at the base of the wall. The ratio between shear force from NLRHA and from RSA procedure is regarded as shear amplification.

This large shear amplification has attracted considerable interest in many countries (Paulay and Priestley 1992). Many researchers have spent much effort to prevent brittle failure of structural wall to happen and they found that shear demands

obtained from RSA procedure are non-conservative to use in designing of structural walls. Many studies on RC cantilever walls have shown that flexural over-strength at the base of the wall and higher mode contribution play an important role in increasing of shear demands of RC wall.

Some seismic design codes, National Building Code of Canada (NBCC 2010), Canadian Standard Association (CSA A23.3-04 2004); Eurocode 8 (CEN 2004) and New Zealand Standard (NZS 2006) have already accounted for this large shear demands of structural walls by multiplying the shear force from RSA procedure with some factor before using it as design shear force.

1.2 Statement of research problem

Seismic shear demands of RC walls have captured many interests from researchers around the world. Some simplified equations to estimate the seismic shear demands of RC walls have been developed. For RC planar cantilever walls, it was proposed by Blakeley et al. (1975), Ghosh and Markevicius (1990), Eibl and Keintzel (1988), Priestley (2003), Rutenberg and Nsieri (2006), Rejec et al. (2012), Boivin and Paultre (2012) and Luu et al. (2014), whereas for RC core walls, only in the cantilever direction, was observed by Yathon (2011), and Calugaru and Panagiotou (2012). It should be noted that no one considered the split-core wall systems with this issue. Hence shear demands of such system should also be studied.

Although many researchers and code writers exposed many publications on the seismic shear demand amplification due to higher modes, it is interesting that this has not been included in current ASCE 7-10 yet (Rutenberg 2013). Regarding to this concern, it should be kept in mind that United States commonly design tall buildings by using NLRHA at the Risk-Targeted Maximum Considered Earthquake (MCE_R) level of ground motion which consumes much effort and time to conduct the analysis. However, Thailand adopting mostly the ASCE 7-10 standard still commonly uses RSA procedure to determine the design shear forces for RC walls which leads to unsafe result. Therefore, this thesis addresses this concern.

1.3 Objective of research

The objectives of this study are the followings:

- To investigate the seismic shear demands of RC core walls from low-rise to high-rise buildings.
- To evaluate efficiency of seismic demands obtained from RSA procedure in ASCE 7-10 by NLRHA.
- To explore the accuracy of various codes and previous researchers' formulas for estimating shear demands of RC walls if applied to the core wall structures in this study.
- To provide possible suggestions to modify RSA procedure result to be used as seismic shear demands in design of RC core walls.

1.4 Scope of research

The scope of this research is to use five RC split core-wall buildings ranging from 5 to 25 stories which are generated to represent common buildings in Thailand. Two different cities, Bangkok and Chiang Mai in Thailand, are studied. A set of seven ground motions scaled to match with target spectrum in Bangkok is employed while a set of ten ground motions scaled to match with target spectrum in Chiang Mai is used. Nominal properties of materials based on Thailand Industrial Standard are used for both methods of analysis. The limitations of this work are the followings:

- The effects of shear demand amplification on RC core walls are mainly discussed.
- Core wall systems are designed to resist entire lateral force (interaction from frame is not considered).
- Wind load is not considered in this study.
- ASCE 7-10 and ACI 318-11 are followed in this study.
- The structural walls are assumed to have fixed support (soil interaction is not included in the analysis).
- The seismic loading is applied in each direction separately at a time.
- Torsional effects are not considered.

1.5 Research methodology

To achieve the objectives mentioned above, the following procedures need to be conducted.

1. Review the background of various codes and previously proposed formulas for estimating the seismic shear demands of RC shear walls.
2. Select the common structural parameters to be studied.
3. Analyze the structures by RSA procedure using ETABS program (CSI 2013), then the seismic demands can be determined.
4. Design the structural systems such that the nominal strength multiplied by the corresponding strength reduction factor in accordance with ACI 318-11 is approximately equal to the demands obtained from RSA procedure.
5. Analyze the structures already designed in step 4 by NLRHA using PERFORM-3D program (CSI 2011) .
6. Compare the results from NLRHA with those from RSA procedure.
7. Evaluate the accuracy of various codes and previously proposed formulas for estimating shear demand of RC wall to this study's results.
8. Recommend appropriate modification of RSA procedure results to be used as seismic shear demands in design of RC core wall.

1.6 Outline of dissertation

This thesis consists of seven Chapters which are briefly described below:

Chapter 1 gives an overview of ASCE 7-10 to determine the design forces and its inefficiency that leads to large shear amplification. This Chapter includes statement of research problem, objective and scope of research and finally the research methodology.

Chapter 2 describes in quite detail about the phenomenon of seismic shear amplification and provides extensive literature review on higher mode shear amplification approach. Various codes already accounted for shear amplification are also included. Previous researchers are divided into four different groups: group of NZS, EC8, CSA and ASCE 7.

Chapter 3 presents theoretical background of linear response spectrum analysis (RSA) and nonlinear response history analysis (NLRHA). This includes how elastic modal analysis can be applied in RSA and the reason that modal analysis is not applicable for NLRHA.

Chapter 4 provides information about structural systems and ground motions employed in this study. This Chapter describes how the structural members are sized and how the ground motions are obtained and scaled to be used in NLRHA.

Chapter 5 focuses on the detail of response spectrum analysis (RSA) procedure. This includes the modeling of the structural systems, analysis and design considerations, general behavior of each response (story drift, bending moment and shear force), the seismic demands of RC core walls, and finally design of structural members.

Chapter 6 focuses on nonlinear response history analysis (NLRHA) procedure, which includes the modeling of the structural systems, and analysis considerations. This Chapter discusses about the comparison of seismic demands obtained from RSA procedure and NLRHA, then it discusses about the accuracy of various codes and previously proposed formulas to this study results. Next, the sensitivity effects of base flexural over-strength (BFOS) of RC core wall on base shear amplification (BSA) are observed. Finally, the effects of elastic walls in upper stories on NLRHA seismic demands are investigated.

Chapter 7 is the last Chapter of this thesis, which concludes the whole study results. This Chapter offers appropriate suggestion to modify RSA procedure results to be used as shear demands in design of RC core walls in current Thai code. Recommendations for future research are mentioned in this Chapter.

CHAPTER 2
LITERATURE REVIEW

2.1 Seismic shear amplification phenomenon

Seismic demands in linear range due to higher modes have been widely accounted for by modal response spectrum analysis (RSA) which is well covered in many textbooks and seismic design codes. As mentioned in ASCE 7-10, it allows design engineers to use RSA procedure reduced by response modification factor (R) to obtain the design forces of the structural system. The factor, *R*, provides a rational relationship between elastic and inelastic forces of a given structural system. The factor, *R*, in ASCE 7 accounts for variety of ingredients such as: ductility factor, system over-strength factor, damping ratio of 5%, past performance of similar system and redundancy, the most important of which are ductility and system over-strength factor (Building Seismic Safety Council: FEMA 415B Note 2007) . Figure 2.1 explains ASCE 7 approach used to compute the design forces for inelastic system. The over-strength factor is the ratio of apparent strength to design strength. The ductility is an essential property of a structure to deform beyond elastic limit without excessive strength or stiffness degradation.

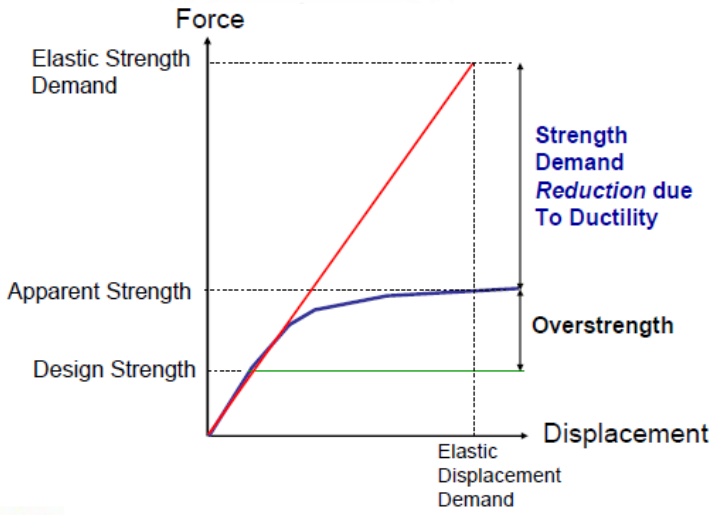

Figure 2.1 ASCE 7 design approach (Building Seismic Safety Council: FEMA 451B Notes 2007).

However, using the same factor, *R*, to reduce all modes of elastic forces in RSA is not accurate because the higher-mode responses are not reduced by inelastic action as much as the first-mode response when flexural yielding occurred at the base of the wall (Eibl and Keintzel 1988, Priestley 2003, Calugaru and Panagiotou 2012). As stated by Rejec et al. (2012) that the first mode contributed most of the bending moment at the base of the wall, which was limited by its flexural capacity; therefore, energy dissipation was predominantly limited to the flexural response in the first mode. Consequently, the first-mode responses are reduced due to energy dissipating mechanism while higher-mode responses are not. While plastic hinge constrained the first-mode responses to the level equal to its flexural capacity, the responses of higher modes remained approximately their elastic level (Rutenberg 2013). This observation was also confirmed by Munir and Warnitchai (2012) from their cyclic pushover analysis on high-rise core-wall building under load distribution based on mode shape of the structure. The hysteresis behaviors of the modal base shear-roof displacement relationship were shown in Figure 2.2. The first-mode deformation far exceeded the yielding level as clearly seen in the long flag-shape hysteresis behavior in Figure 2.2a. Yielding also occurred in the second mode but it was less extensive than the first mode as illustrated by the short flag-shape hysteresis behavior in Figure 2.2b. For the third and fourth modes, the responses were in the elastic range.

When the flexural capacity at the base of the wall was reached, the flexural over-strength inherent in the design process could increase shear force of the wall. This increase was predominately related to the first-mode shear response (Rejec et al. 2012). Hence, the responses can be approximately computed as a superposition of the first-mode shear reduced by the factor, *R*, while other higher-mode responses remain approximately elastic. Several analysis procedures were adapted to this approach (Eibl and Keintzel 1988, Priestley 2003, Calugaru and Panagiotou 2012). Moreover, as the structural height increases, higher modes become dominant for shear response. Study by Yathon (2011) outlined that the shear response was considerably contributed from the second mode even in low structures and in taller structures, it was unfair to assumed that moment and shear display the same inelastic behavior by applying the same force reduction factor.

Thus, when contribution of higher modes is significant and flexural over-strength at the base of the wall is large, RSA procedure leads to non-conservative estimation of shear demands in nonlinear RC walls.

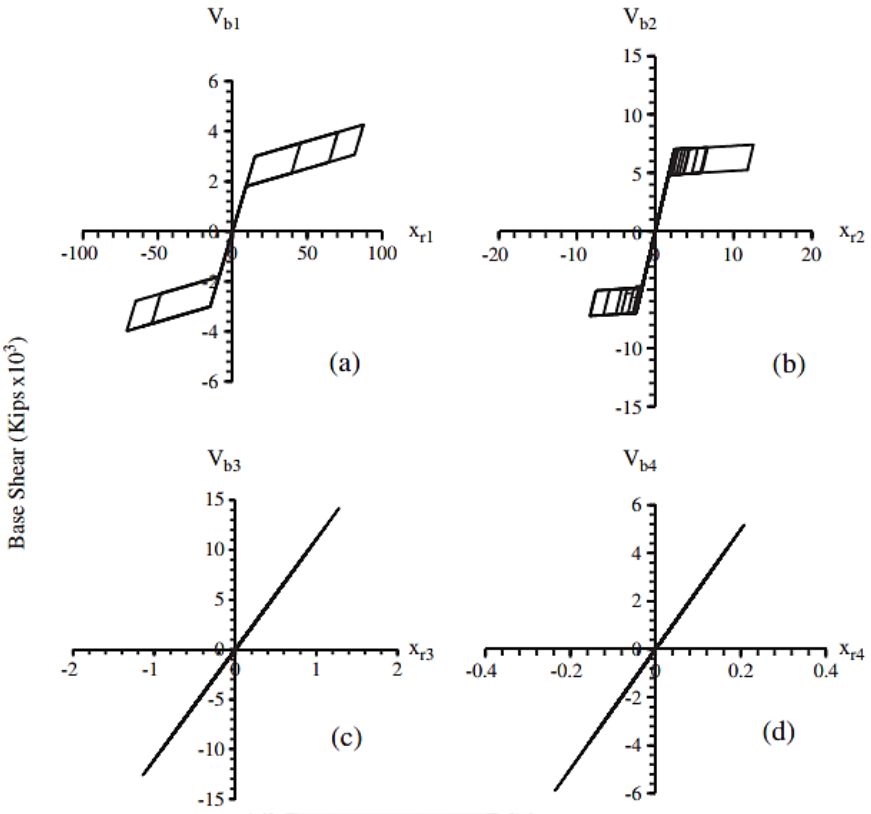

Figure 2.2 Base shear vs. roof displacement relationship: (a) first mode; (b) second mode; (c) third mode and (d) fourth mode (Munir and Warnitchai 2012).

2.2 Higher mode shear amplification approaches

Researches on seismic shear demands of RC walls began in 1975 and are still in progress till present day with different approaches. Many previous studies have mainly focused on the estimation of shear forces in RC cantilever walls designed for a single plastic hinge at the base of the walls. The results from each researcher were mainly based on the NLRHA using different parametric studies such as structural configurations and ground motions. Obviously, the results depended on these choices. Yet, there is no consensus regarding the extent of shear amplification based on previous researchers and provisions of various seismic codes. The reviews on higher mode shear amplification presented here are separated into four different groups: group of NZS, EC8, CSA and ASCE 7.

2.2.1 Group of NZS

Blakeley et al. (1975) was the first researcher group who observed that the base shear demands from their nonlinear analysis of 6- to 20-story cantilever walls were larger than those obtained from equivalent static analysis. They proposed simple formula, Eq. (2.1) for computing base shear amplification factor used to multiply with static shear force in New Zealand Standards to get the design shear force of the wall.

$$\omega_v = \begin{cases} 0.9 + \dfrac{n}{10} & \text{for n} \le 6 \\ 1.3 + \dfrac{n}{30} \le 1.8 & \text{for n} > 6 \end{cases} \tag{2.1}$$

where n is the number of stories and ω_v is the base shear amplification factor to be applied to the static shear force.

Paulay and Priestley (1992) modified the design shear force of Blakeley et al. (1975) by multiplying the shear force from the equivalent static analysis, V_E, with base shear amplification factor, ω_v, in Eq. (2.1) and flexural over-strength factor, ϕ_o. They further limited the design shear force, V_u, of the wall by elastic shear force as shown in the last term in Eq. (2.2).

$$V_u = \omega_v \phi_o V_E \le \mu_\Delta V_E \tag{2.2}$$

where μ_Δ is the displacement ductility ratio (seismic force reduction factor) used in design.

NZS 3101 (NZS 2006) followed the formula proposed by Paulay and Priestley (1992) but the standard does not limit the design shear force of the wall by elastic shear force. The design shear force of the wall in this standard shall not be less than the shear force determined by Eq. (2.3).

$$V_o^* = \omega_v \phi_o V_E \tag{2.3}$$

where V_o^* is the design shear force at any level of the wall and ϕ_o is the over-strength factor related to flexural action at any level of the wall.

2.2.2 Group of EC8

Eibl and Keintzel (1988) proposed base shear magnification factor formula scaled to shear force obtained from RSA. Their study was based on low-rise structures of 2- to 5-story. A set of ten strong ground motions was employed. They used the square root of the sum of the squares (SRSS) modal combination method to estimate base shear demand by assuming that only the first two modes were dominant modes and the reduction of shear force was applied only to the first mode shear. The design shear force at the base of structural wall was computed by Eq. (2.4).

$$V_{Ed} = \sqrt{\left(V_{Ed,1}^{'}\right)^2 + \left(qV_{Ed,2}^{'}\right)^2} \tag{2.4}$$

where V_{Ed} is the design shear force at the base of the wall, $V_{Ed,1}^{'}$ and $V_{Ed,2}^{'}$ are the reduced base shear forces contributed from the first and second mode, respectively, q is behavior factor (seismic force reduction factor) used in design. They further simplified Eq. (2.4) such that the ratio of the base shear from the second mode to that from the first mode was equal to $\sqrt{0.1}\,S_e(T_c)/S_e(T_1)$, the flexural over-strength, $\gamma_{Rd}M_{Rd}/M_{Ed}$, was applied only to the first-mode shear and the base shear magnification was limited by factor, q. The following expressions could be derived.

$$V_{Ed} = V_{Ed,1}^{'} q\sqrt{\left(\frac{\gamma_{Rd}}{q}\frac{M_{Rd}}{M_{Ed}}\right)^2 + 0.1\left(\frac{S_e(T_C)}{S_e(T_1)}\right)^2}$$

$$V_{Ed} = \varepsilon V_{Ed,1}^{'}$$

$$\varepsilon = q\sqrt{\left(\frac{\gamma_{Rd}}{q}\frac{M_{Rd}}{M_{Ed}}\right)^2 + 0.1\left(\frac{S_e(T_C)}{S_e(T_1)}\right)^2} \le q \tag{2.5}$$

where ε is base shear magnification factor, M_{Rd} is design flexural resistance at the base of the wall, M_{Ed} is the moment demand obtained from RSA at the base of the wall, γ_{Rd} is over-strength factor to account for steel strain-hardening $\left(\gamma_{Rd} = 1.2\right)$, T_c is the upper limited period of the constant spectral acceleration region of the spectrum,

T_1 is the fundamental period in the direction of shear force and $S_e(T)$ is ordinate of the elastic response spectrum.

Eurocode 8 (EC8) (CEN 2004) adopted Eq. (2.5) of Eibl and Keintzel (1988) under two modifications. First, EC8 amplified the design shear force of the wall by total shear force from RSA, $V_{Ed}^{'}$. Second, EC8 used this formula as constant magnification factor along the height of the wall. The value of ε was taken as 1.5 for moderately ductile walls (q<3). For highly ductile walls, it was calculated from Eq. (2.6) and the value of ε has to be at least 1.5, but needs not be larger than *q*.

$$V_{Ed} = \varepsilon V_{Ed}^{'}$$

$$\varepsilon = q\sqrt{\left(\frac{\gamma_{Rd}}{q}\frac{M_{Rd}}{M_{Ed}}\right)^2 + 0.1\left(\frac{S_e(T_C)}{S_e(T_1)}\right)^2} \qquad (2.6)$$

Priestley (2003) proposed Modified Modal Superposition (MMS) approach to determine the design shear forces for RC cantilever walls, as shown in Eq. (2.7). This method was developed based on the assumption that inelastic action only limited the shear force from the first mode and shear forces from higher modes were not affected by inelastic action.

$$V_i = \left(V_{1i}^2 + V_{2Ei}^2 + V_{3Ei}^2 + \ldots\right)^{0.5} \qquad (2.7)$$

where V_i is the design shear force of the wall at level *i*, V_{1i} is the lesser of elastic first mode and ductile first mode shear computed by direct displacement base design (DDBD) at level *i*, V_{2Ei} and V_{3Ei} are elastic modal shear at level *i* for mode 2 and 3, respectively.

Rutenberg and Nsieri (2006) conducted research on RC cantilever wall ranging from 5- to 25-story in order to provide possible revisions of EC8. From their parametric study, the base shear amplification factor was almost a linear function of the fundamental period *T* and the behavior factor *q* as shown in Figure 2.3. Consequently the following formula was proposed for computing the base shear force, V_a, of the wall.

$$V_a = \omega_v^* V_d$$

$$\omega_v^* = 0.75 + 0.22\left(T + q + Tq\right) \tag{2.8}$$

where ω_v^* is base shear amplification factor, V_d is the base shear obtained from Eq. (2.9).

$$V_d = \frac{M_y}{\frac{2}{3}H\left(1+\frac{1}{2n}\right)} \tag{2.9}$$

where M_y is the yielding moment at the base of the wall, H is the building height and n is the number of stories.

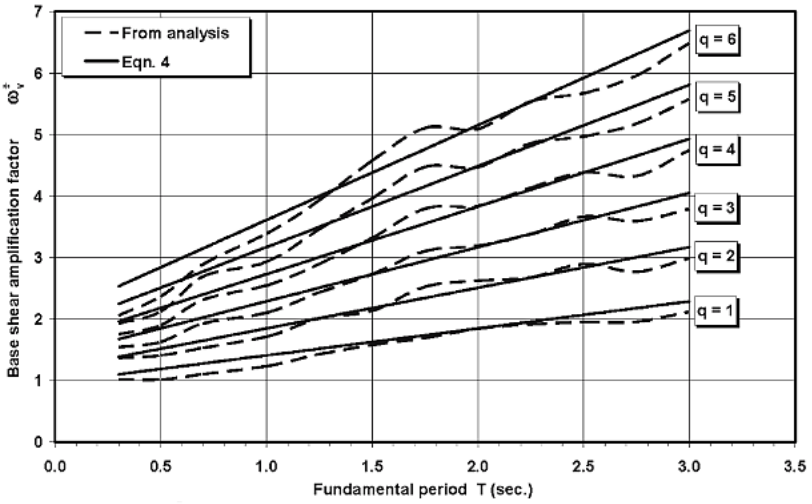

Figure 2.3 Mean base shear amplification factor from parametric study and proposed formula (Rutenberg and Nsieri 2006).

Rutenberg and Nsieri (2006) also proposed the design envelop of shear force distributed over the height of the wall as function of the fundamental period as shown in Figure 2.4, where ξ is defined by Eq. (2.10).

$$\xi = 1.0 - 0.3T \geq 0.5 \tag{2.10}$$

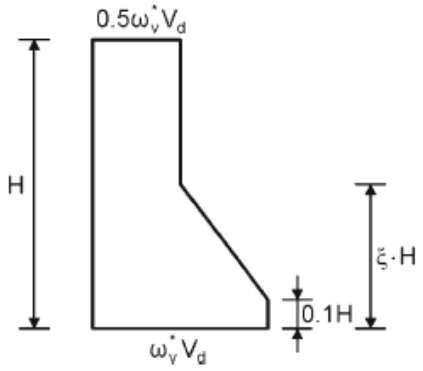

Figure 2.4 Design envelop of shear forces over the wall height (Rutenberg and Nsieri 2006).

Another study was conducted by Rejec et al. (2012) to propose possible improvement to EC8's formula as defined here by Eq. (2.6). They demonstrated that the design shear force in EC8 should be computed from the first mode shear, $V'_{Ed,1}$, from RSA amplified by the magnification factor, ε_a. They limited the base shear force of the wall by total elastic shear force from RSA. So, they modified Eq. (2.6) as Eq. (2.11).

$$V_{Ed,a} = \varepsilon_a V'_{Ed,1}$$

$$\varepsilon_a = q\sqrt{\left(\min\left[\frac{\gamma_{Rd}}{q}\frac{M_{Rd}}{M_{Ed}};1\right]\right)^2 + 0.1\left(\frac{S_e(T_C)}{S_e(T_1)}\right)^2} \geq 1.5 \qquad (2.11)$$

This equation was applicable to the base shear of the RC cantilever wall only. They further proposed formula as shown in Eq. (2.12) to compute the shear force along the height of the wall by replacing the constant ratio between the contribution of second mode to that of the first mode found by Eibl and Keintzel (1988) with a variable ratio, *m(z)* along the height the wall.

$$\varepsilon_a(z) = q\sqrt{\left(\min\left[\frac{\gamma_{Rd}}{q}\frac{M_{Rd}}{M_{Ed}};1\right]\right)^2 + m(z)^2\left(\frac{S_e(T_C)}{S_e(T_1)}\right)^2} \geq 1.5 \qquad (2.12)$$

where *z* is the vertical coordinate of the wall, *H* is the total height of the wall and *m(z)* is the ratio between the second/higher mode normalized shear and the first mode normalized shear as presented in Figure 2.5.

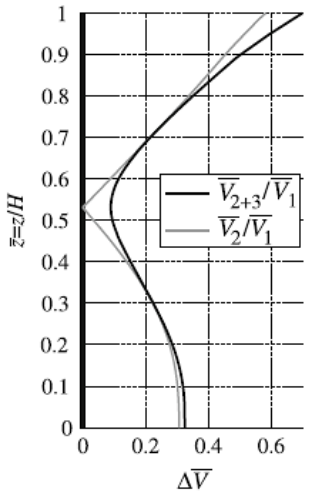

Figure 2.5 Ratio of the second/higher modes normalized shear to the first mode normalized shear (Rejec et al. 2012).

2.2.3 Group of CSA

NBCC (2010) has explicitly considered higher mode effects when using equivalent static force procedure as indicated in Eq. (2.13) by applying higher mode factor, M_v, to increase the base shear force and by applying base overturning reduction factor, J, to reduce overturning moment because higher mode contribution of overturning moment is relatively smaller than that of base shear. These factors depend on the structural type, fundamental period of the structure and the shape of design spectrum as shown in Table 2.1.

$$V = \frac{S(T_a) M_v I_E W}{R_d R_o} \tag{2.13}$$

where V is design base shear, $S(T_a)$ is design spectral acceleration at fundamental period T_a, I_E is importance factor of the building, W is the weight of the building and R_d and R_o are factors which account for ductility and over-strength, respectively.

Table 2.1 Higher mode factor and base overturning reduction factor (NBCC 2010) .

$S_a(0.2)/S_a(2.0)$	Type of Lateral Resisting Systems	M_v for $T_a \le 1.0$	M_v for $T_a = 2.0$	M_v for $T_a \ge 4.0$	J for $T_a \le 0.5$	J for $T_a = 2.0$	J for $T_a \ge 4.0$
< 8.0	Moment-resisting frames	1.0	1.0	(3)	1.0	0.9	(3)
	Coupled walls(4)	1.0	1.0	1.0	1.0	0.9	0.8
	Braced frames	1.0	1.0	(3)	1.0	0.8	(3)
	Walls, wall-frame systems	1.0	1.2	1.6	1.0	0.6	0.5
	Other systems(5)	1.0	1.2	(3)	1.0	0.6	(3)
≥ 8.0	Moment-resisting frames	1.0	1.2	(3)	1.0	0.7	(3)
	Coupled walls(4)	1.0	1.2	1.2	1.0	0.7	0.6
	Braced frames	1.0	1.5	(3)	1.0	0.6	(3)
	Walls, wall-frame systems	1.0	2.2	3.0	1.0	0.4	0.3
	Other systems(5)	1.0	2.2	(3)	1.0	0.4	(3)

In addition to NBCC (2010), CSA-A23.3 (2004) contains specific provision for seismic design of shear walls. For ductile wall, it requires that the base shear resistance must be increased by the ratio of base probable bending moment capacity to the base bending moment obtained from RSA, which is actually the base flexural over-strength of the wall. For moderately ductile wall, the same calculation is followed by using base nominal bending moment capacity instead of base probable bending moment capacity. Based on Adebar et al. (2014), the new provision of CSA-A23.3 (2014) requires that the design shear force of the wall shall not be greater than elastic shear force from RSA reduced by force reduction factor, $R_d R_o$ equal to 1.3.

Yathon (2011) proposed different approach to modify Canadian design codes, such as NBCC (2005) and CSA-A23.3 (2004). The proposed method was based on nine cantilever RC core walls subjected to 40 ground motions scaled to match with uniform hazard spectra for Vancouver and Montreal in Canada. His concept was about relationship between fixed base shear and pinned base shear obtained from RSA. The design base shear force of RC cantilever wall was computed by summation of RSA fixed-base shear reduced by ductility factor, R_d in Canadian code and RSA pinned-base shear as shown in Eq. (2.14).

$$V_a = \left(\frac{1}{R_d}\right)V_e + H_f R_{pf} V_e \tag{2.14}$$

$$H_f = P - e^{1.6(1-R_d)}$$

$$P = \begin{cases} 1.0 & S_a(0.2)/S_a(2) < 8 \\ 1.1 & S_a(0.2)/S_a(2) \ge 8 \end{cases}$$

$$R_{pf} = \begin{cases} 2T_2 & \mathrm{T}_2 < 0.25s \\ 0.5 & \mathrm{T}_2 \geq 0.25\mathrm{s} \end{cases}$$

where V_a is the amplified base shear force, V_e is the elastic base shear from RSA, R_{pf} is the ratio of pinned to fixed base shear, H_f is the fraction of pinned base shear based on NLRHA parametric results and P is the plateau where H_f levels off as shown in Figure 2.6 and T_2 is the second-mode period of the structure.

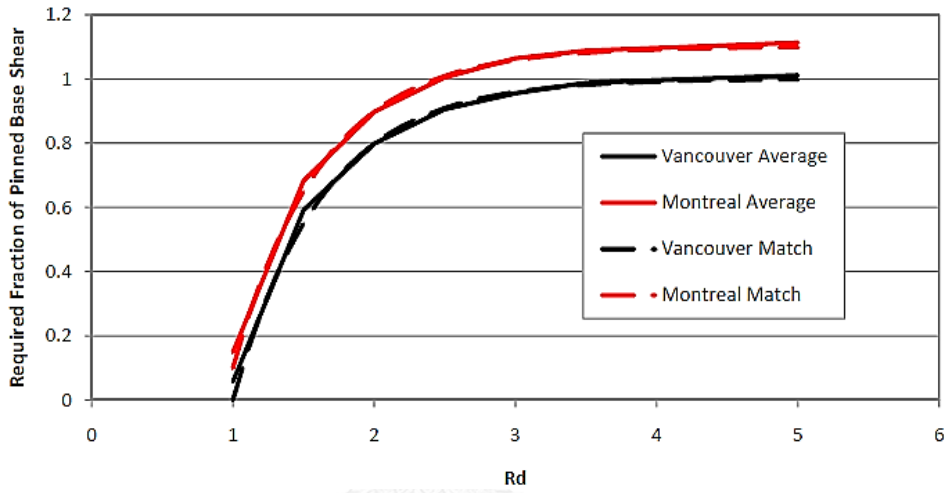

Figure 2.6 Required fraction of pinned base shear vs. force reduction factor R_d (Yathon 2011).

Boivin and Paultre (2012) proposed capacity design method for shear strength design of regular ductile RC cantilever wall for CSA-A23.3 (2004). Their proposed method was based on a parametric study for ductile walls subjected to Western North America ground motions. They included that seismic base shear force was primarily influenced by wall over-strength factor and fundamental period. A new base shear amplification factor value, $\bar{\omega}_v$, was proposed as indicated in Table 2.2. The design base shear force, V_{pb}, was calculated by Eq. (2.15).

$$V_{pb} = \bar{\omega}_v V_{Pbase} \leq V_{\mathrm{limit}_{base}}$$

$$V_{Pbase} = V_f \left(\frac{M_p}{M_f} \right)_{base} \qquad (2.15)$$

where V_{Pbase} is the probable shear force at the base of the wall as required in CSA-A23.3 (2004), $V_{\text{limit}_{base}}$ is the base share force limit (elastic shear force reduced by $R_d R_o = 1.3$), V_f and M_f are the design base shear force and base bending moment obtained from RSA, respectively, and M_p is the base probable moment capacity of the wall.

Boivin and Paultre (2012) also suggested using the design shear envelop proposed by Rutenberg and Nsieri (2006), as displayed in Figure 2.7 with a new equation for $\overline{\xi}$.

$$\overline{\xi} = 1.5 - T_1; \quad 0.5 \le \overline{\xi} \le 1 \tag{2.16}$$

Table 2.2 Propose base shear amplification factor value (Boivin and Paultre 2012).

$R_d R_o/\gamma_w$	$T_1 \le 0.5$	$T_1 \ge 1.0$
2.80	1.0	2.0
1.87	1.0	1.5
≤1.40	1.0	1.0

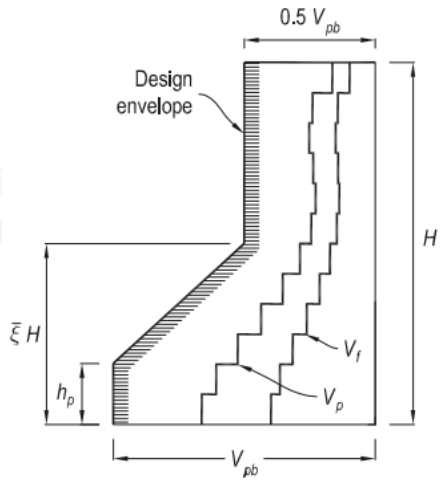

Figure 2.7 Proposed capacity design envelop for shear strength design (Boivin and Paultre 2012).

Luu et al. (2014) performed a parametric study to examine the seismic demands of moderately ductile (MD) RC shear walls subjected to high-frequency Eastern North America earthquakes. A new base shear amplification factor, ω_v, applied to the base

shear, V_d, obtained from RSA was proposed for National Building Code of Canada (NBCC 2010) and CSA-A23.3 (2004) for MD shear walls.

$$V_b = \omega_v V_d$$

$$\omega_v = \begin{cases} 1.6+0.7(\gamma_w - 1)+0.2(T - 0.5) & \text{if } 0.5 \le T \le 1.5 \\ 1.8+0.7(\gamma_w - 1) - 0.1(T - 1.5) & \text{if } 1.5 < T \le 3.5 \end{cases} \quad (2.17)$$

where V_b is the design base shear force of the wall, T is the fundamental period and γ_w is the base flexural over-strength factor of the wall.

Shear force design envelop similar to Rutenberg and Nsieri (2006) and Boivin and Paultre (2012) was also proposed with few modification as presented in Eq. (2.18).

$$\xi = 1.2 - 0.4T \quad 0.6 \le \xi \le 1 \quad (2.18)$$
$$\alpha = 0.4$$
$$\beta = 1/n$$

where n is the number of stories and T is fundamental period.

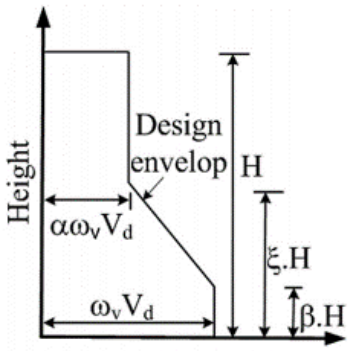

Figure 2.8 Proposed shear force design envelop (Luu et al. 2014).

2.2.4 Group of ASCE 7

As already mentioned in Chapter 1, current ASCE 7-10 does not account for shear amplification in structural walls when RSA procedure is used. However, common designs of tall buildings in United States have directly considered this problem by employing NLRHA at MCE_R level of ground motion which consumes much effort and time to conduct the analysis.

To propose suggestion to modify RSA procedure in ASCE 7-10, Calugaru and Panagiotou (2012) conducted the research using a central RC core wall of 10-, 20- and 40-story buildings subjected to three near-fault ground motions. They found that RSA procedure in ASCE 7-10 which uses a single value of response modification factor, *R*, for all modes of response was not conservative for tall buildings because higher-modes response should not be reduced as much as the first mode. Modified modal response spectrum analysis (MMRSA) approach as shown in Eq. (2.19) was proposed which is very similar to MMS of Priestley (2003). The only difference is that they also applied the reduction factor, R_H to higher-mode contributions. However that reduction factor was found to be much smaller and generally varied from 1 to 2.

$$Q^i = \sqrt{\left[Q_1^i \frac{\Omega_{b,0}}{R_1} \right]^2 + \frac{\left[Q_2^i \right]^2 + \left[Q_3^i \right]^2}{\left[R_H \right]^2}} \tag{2.19}$$

where Q^i is the design shear force of the wall at level i , Q_q^i is the q^{th} mode elastic shear force at level i , $\Omega_{b,0}$ is the base section flexural over-strength factor, R_1 and R_H are the reduction factor for the first and higher modes, respectively.

2.3 Summary

In summary, RSA underestimates the design shear forces of RC walls. Most of the formulas above are based on parametric studies; hence, they are applicable to the similar structural systems and to spectra having similar shape to the mean spectra used for their study. Anyway, most researchers focused only on RC cantilever walls both planar walls (Blakeley et al. 1975, Eibl and Keintzel 1988, Paulay and Priestley 1992, Priestley 2003, Rutenberg and Nsieri 2006, Boivin and Paultre 2012, Rejec et al. 2012, Luu et al. 2014) and core walls (Yathon 2011, Calugaru and Panagiotou 2012). NZS, EC8, NBCC and CSA have already been modified to account for shear amplification in RC walls but there is no such shear amplification in ASCE 7-10. None of these studies focused on split core walls with coupling beams. Therefore, this study attempts to investigate the shear demands in such systems and aims to explore the accuracy of various codes and the proposed formulas above if applied to the core-wall structures and spectrum shapes used in this study. Two directions of core wall whose behaviors

are different as it behaves like cantilever wall in one direction and coupled wall in the other direction are studied at the same time in this thesis.

CHAPTER 3
THEORETICAL BACKGROUND

3.1 Response spectrum analysis

3.1.1 Response spectra

The equation of motion for a linear single degree of freedom (SDOF) system subjected to ground excitation $\ddot{u}_g(t)$ is:

$$m\ddot{u}(t) + c\dot{u}(t) + ku(t) = -m\ddot{u}_g(t) \tag{3.1}$$

dividing both sides by *m* and replacing $\frac{c}{m} = 2\zeta\omega_n$ and $\frac{k}{m} = \omega_n^2$ yields:

$$\ddot{u}(t) + 2\zeta\omega_n\dot{u}(t) + \omega_n^2 u(t) = -\ddot{u}_g(t) \tag{3.2}$$

where *u* is the relative displacement, *m*, *c* and *k* are the mass, damping and lateral stiffness of the SDOF system, respectively.

Eq. (3.2) indicates that the response is defined by the damping ratio, ζ the natural frequency, ω_n (or natural period, T_n) and the ground acceleration, $\ddot{u}_g(t)$. Hence, for a particular $\ddot{u}_g(t)$ and a constant ζ, a response spectrum is obtained by repeatedly solving Eq. (3.2) for structures with varying natural period. Then the deformation, pseudo-velocity and pseudo-acceleration response spectrum are obtained by plotting their peak values versus the natural period from which the displacement, velocity and acceleration are computed.

The peak value of deformation of an SDOF system is denoted by:

$$D = \max_t |u(t)| \tag{3.3}$$

Then the peak pseudo-velocity (*V*) and the peak pseudo-acceleration (*A*) of an SDOF system are computed from the peak deformation (*D*) by:

$$V = \omega_n D = \frac{2\pi}{T_n} D \tag{3.4}$$

$$A = \omega_n^2 D = \left(\frac{2\pi}{T_n} \right)^2 D \tag{3.5}$$

It should be noted that earthquake excitation is characterized by a smooth design spectrum in practice which is obtained by doing statistics of many ground motions. As stated in ASCE 7-10, the design response spectrum is based on 5% damping ratio.

3.1.2 Modal analysis

The equation of motion of a linear multi-degree of freedom (MDOF) system is:

$$\mathbf{m}\ddot{\mathbf{u}}(t) + \mathbf{c}\dot{\mathbf{u}}(t) + \mathbf{k}\mathbf{u}(t) = \mathbf{p}_{\text{eff}}(t) \tag{3.6}$$

where **m**, **c** and **k** are mass, damping and stiffness matrix, respectively and $\mathbf{p}_{\text{eff}}(t)$ is a vector of effective earthquake force expressed by Eq. (3.7) in which ι is influence vector.

$$\mathbf{p}_{\text{eff}}(t) = -\mathbf{m}\iota\ddot{u}_g(t) \tag{3.7}$$

For linear system, the displacement **u** of an *N*-DOF system can be expressed as the superposition of the modal contributions.

$$\mathbf{u}(t) = \sum_{n=1}^{N} \phi_n q_n(t) \tag{3.8}$$

Expand the spatial distribution of the effective earthquake force $\mathbf{m}\iota$ as a summation of modal inertia force distribution $\mathbf{s}_n$:

$$\mathbf{m}\iota = \sum_{n=1}^{N} \mathbf{s}_n = \sum_{n=1}^{N} \Gamma_n \mathbf{m}\phi_n \tag{3.9}$$

where

$$\Gamma_n = \frac{L_n}{M_n} \qquad \mathrm{L}_n = \phi_n^T \mathbf{m}\iota \qquad \mathrm{M}_n = \phi_n^T \mathbf{m}\phi_n \tag{3.10}$$

The contribution of n^{th} mode to excitation vector $\mathbf{m}\iota$ is:

$$\mathbf{s}_n = \Gamma_n \mathbf{m}\phi_n \tag{3.11}$$

substituting Eq. (3.7) and Eq. (3.8) into Eq. (3.6) and multiplying both sides by ϕ_n^T, then dividing the obtained equation by normalized mass, M_n, finally utilizing the orthogonal properties of modes, $\phi_n^T \mathbf{m} \phi_r = 0,\ \phi_n^T \mathbf{c} \phi_r = 0,\ \phi_n^T \mathbf{k} \phi_r = 0$, leads to equation governing the modal coordinate q_n:

$$\ddot{q}_n + 2\zeta_n \omega_n \dot{q}_n + \omega_n^2 q_n = -\Gamma_n \ddot{u}_g(t) \tag{3.12}$$

Then, the modal equation can be obtained by substituting $q_n(t) = \Gamma_n D_n(t)$ into Eq. (3.12) and dividing both sides by Γ_n.

$$\ddot{D}_n + 2\zeta_n \omega_n \dot{D}_n + \omega_n^2 D = -\ddot{u}_g(t) \tag{3.13}$$

Note that Eq. (3.12) is equivalent to the governing equation of linearly elastic SDOF system whose vibration properties belong to n^{th} mode of MDOF system. Thus, the concept of response spectra mention in section 3.1.1 can be applied here.

The displacement due to the n^{th} mode is computed as:

$$\mathbf{u}_n(t) = \phi_n q_n(t) = \Gamma_n \phi_n D_n(t) \tag{3.14}$$

The response contributed from the n^{th} mode is determined as:

$$r_n(t) = r_n^{st} A_n(t) \tag{3.15}$$

where $A_n(t) = \omega_n^2 D_n(t)$ and r_n^{st} is the modal static response determined by static analysis due to external force $\mathbf{s}_n$.

3.1.3 Modal combination

The common modal combination methods for RSA are the square root of the sum of the squares method (SRSS) and the complete quadratic combination method (CQC).

SRSS

$$r_o \approx \sqrt{\sum_{n=1}^{N} r_{no}^2} \tag{3.16}$$

CQC
$$r_o \approx \sqrt{\sum_{i=1}^{N}\sum_{i=1}^{N} \rho_{in} r_{io} r_{no}} \tag{3.17}$$

where
$$\rho_{in} = \frac{8\sqrt{\varsigma_i \varsigma_n}(\varsigma_i + \beta_{in}\varsigma_n)\beta_{in}^{3/2}}{(1-\beta_{in}^2)+4\varsigma_i\varsigma_n\beta_{in}(1+\beta_{in}^2)+4(\varsigma_i^2+\varsigma_n^2)\beta_{in}^2} \tag{3.18}$$

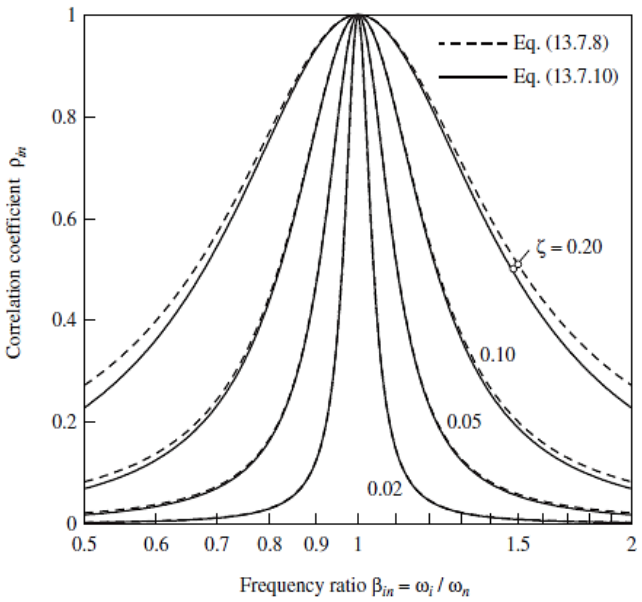

Figure 3.1 Variation of correlation coefficient ρ_{in} with modal frequency ratio, β_{in} (Chopra 2012).

3.1.4 Scaling of design value

To obtain the design forces, elastic forces obtained from the modal combination are reduced by a response modification factor (R*)*. In seismic design, the equivalent lateral force (ELF) procedure is required to verify the reliability of RSA which is done by comparison of seismic base shear obtained from both methods. In case the seismic base shear (V_d) computed from RSA is less than 85% of static base shear (V_s) from ELF method, a scaling factor of $0.85V_s/V_d$ is employed to scale up the seismic force demands but not for displacement or drift based on ASCE 7-10. The ASCE 7-10 standard requires to scale up displacement and drift by the quantity of C_d/I after divindg elastic spectrum by R/I factor, in which C_d is displacement amplification factor and I is important factor of the building.

3.2 Nonlinear response history analysis

For inelastic system, the stiffness term in Eq. (3.6) is modified to recognize the inelastic behavior of the structure. The nonlinear relationship between lateral force $\mathbf{f}_s$ and resulting lateral displacement **u** defends on the history of displacement.

$$\mathbf{f}_s = \mathbf{f}_s(\mathbf{u},\dot{\mathbf{u}}) \tag{3.19}$$

Hence, modifying Eq. (3.6) with this generalization, the governing equation for inelastic system is:

$$\mathbf{m}\ddot{\mathbf{u}}(t) + \mathbf{c}\dot{\mathbf{u}}(t) + \mathbf{f}_s(\mathbf{u},\dot{\mathbf{u}}) = \mathbf{p}_{eff}(t) \tag{3.20}$$

Because of the contribution from the modes other than the n^{th} mode to the system response, Eq. (3.8) cannot be employed; hence, the modal analysis is no longer applicable to nonlinear inelastic system.

Therefore, Eq. (3.20) contains N coupled nonlinear differential equations that must be solved simultaneously to obtain the displacement response and the internal forces of the structure. Numerical method is required to solve Eq. (3.20).

CHAPTER 4
STRUCTURAL SYSTEMS AND GROUND MOTIONS

4.1 Structural parameters

4.1.1 Description of structural systems

Structural walls in the form of elevator shafts are widely used to provide effectively lateral stiffness for multistory buildings. For high-rise buildings, it is necessary to design enough number of elevators in which its arrangement is very important to facilitate the passengers. Regarding to this problem, split core-wall buildings are commonly used in Thailand as shown in Figure 4.1. The benefits of this option are to provide sufficient opening space and to reduce torsional effect, which are the desire of architect and structural engineer, respectively. Therefore, this study uses five RC split core-wall buildings ranging from 5- to 25-story having core walls located at the center of a square-shape floor plan. The floor plan of each building is shown in Appendix A. The orientation of core-wall cross section of each building is presented in Figure 4.1. Each building consists of two core walls coupled by coupling beams (long coupling beams, LCB) in X direction with the exception that 5-story building has only one central core wall. The openings for elevator doors have short coupling beams (SCB) in Y direction above the openings.

For the 5-story buildings, the core wall behaves like a cantilever wall in both directions. For 10- to 25-story buildings, the behaviors of core walls in both directions are different as they are coupled in X direction, while they behaves like a cantilever wall in Y direction. Although, in Y direction, each core wall consists of both solid wall and perforated wall for elevator doors, the solid wall is the primary wall which resists about 80% of total horizontal shear force as shown in Figure 4.2.

These core-wall systems are designed to resist all lateral loads; hence, the lateral stiffness and strength of the gravity columns and slabs are ignored. However, their masses are included in the analysis. Core walls are assumed to have uniform cross section. The coupling beams in each direction are considered to have constant section

over the entire height of each building. These buildings are assumed to be located in downtown area of Bangkok and in Chiang Mai province of Thailand.

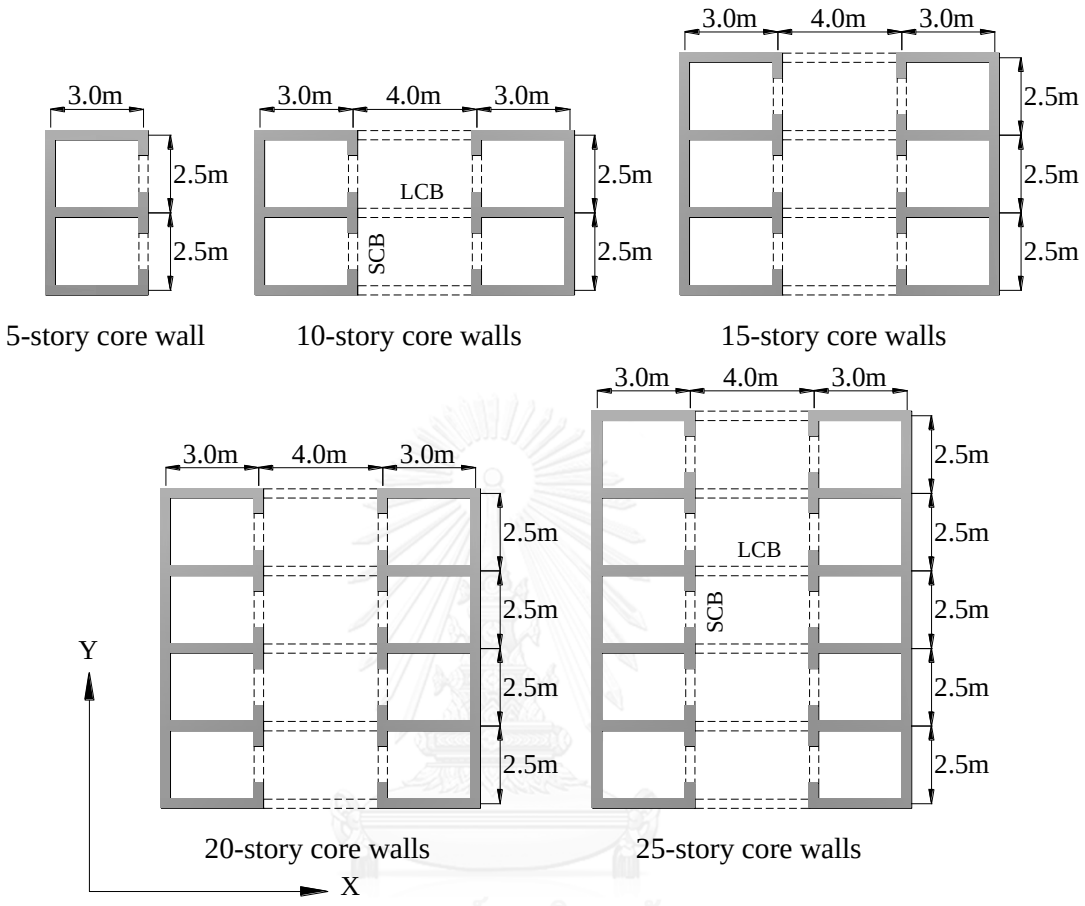

Figure 4.1 Core-wall cross sections for the five studied buildings.

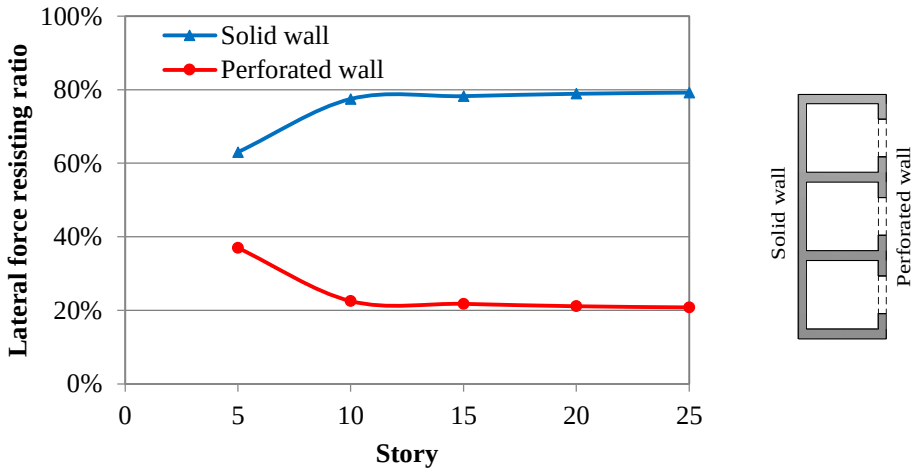

Figure 4.2 Comparison of shear force resisted by solid wall and perforated wall.

4.1.2 Sizing of structural systems

The structural systems are chosen with below restrictions:

- **Core walls**: The section is realistic; the width depends on the size and the number of elevators and the thickness increases with the building height such that the computed periods is in acceptable range which is approximately equal to the upper limited periods provided in ASCE 7-10.
- **Coupling beams**: They are sized such that its width equal to the wall thickness and its maximum depth is provided so that the clear height between the floor and the coupling beam is 2.5 m.
- **Floor plan**: The floor area is determined by the ratio of wall area to floor area obtaining from observing many case study buildings. The corresponding flat slab thickness is 0.2 m.
- **Columns**: The stiffness and strength of the column are ignored in this study because all the lateral loads are considered to be resisted by the core-wall system. Hence, the columns are assumed to have sufficient capacity to support gravity load.

The architectural requirements are also considered so that it represents a wide range of possibilities.

- The elevator box of 3 m x 2.5 m width in which its number equaling to 0.4 times the number of stories is employed, based on experiences.
- The building height is computed from the typical floor to floor height which is 3 m tall.
- The width of the corridor is taken as 4 m. The opening door has 1.2 m width and 2.2 m height.

The building characteristics and dimensional design data for RC split core-wall systems are presented in Table 4.1 and Table 4.2, respectively.

Table 4.1 Building characteristics.

No. story	Building height (m)	Wall/floor area ratio	Floor area (m^2)	Seismic weight per floor (kN)	Fundamental periods (s)	
					X	Y
5	15	0.01	380	3383	0.57	0.43
10	30	0.012	792	7318	1.62	1.29
15	45	0.015	1080	9903	2.68	1.71
20	60	0.02	1225	11,550	3.72	2.05
25	75	0.025	1376	13,278	4.60	2.27

Table 4.2 Dimensional design data for RC split core-wall systems.

No. story	Wall thickness (m)	Long Coupling Beam (LCB) (m^2)	Short Coupling Beam (SCB) (m^2)
5	0.20	-	0.20 x 0.80
10	0.25	0.25 x 0.50	0.25 x 0.80
15	0.30	0.30 x 0.50	0.30 x 0.80
20	0.35	0.35 x 0.50	0.35 x 0.80
25	0.40	0.40 x 0.50	0.40 x 0.80

4.1.3 Material properties

The properties of the concrete and rebar shown in Table 4.3 were employed for all structural members in a building. The modulus of elasticity of concrete was computed from Eq. (4.1).

$$E_c = 4700\sqrt{f_c'} \tag{4.1}$$

where E_c and f_c' have unit of MPa.

Table 4.3 Material properties.

No. story	Concrete compressive strength (MPa)	Modulus of elasticity of concrete (MPa)	Steel yield strength (MPa)	Modulus of elasticity of rebar (MPa)	Unit weight of concrete (kN/m^3)
5	30	25,743	390	200,000	24
10	30	25,743			
15	35	27,806			
20	35	27,806			
25	40	29,725			

4.2 Ground motions

The maximum considered earthquake (MCE) ground motions having 2 percent probability of occurrence within 50 years corresponding to 2475 years return period are employed in this study. It should be noted that RSA procedure in ASCE 7-10 uses the design spectrum that is referred to design basic earthquake (DBE) having 10 percent probability of occurrence within 50 years. DBE is computed by multiplying MCE with a factor of 2/3. MCE is used in NLRHA to evaluate the response of the structural system to prevent collapse. However, for Bangkok (low seismic zone), MCE is used for both RSA and NLRHA in this study because the structural systems did not yield much under DBE. For Chiang Mai (high seismic zone), DBE is employed for both RSA and NLRHA. The purpose of this study is not to verify the design of structural systems but it instead aims to evaluate the method of analysis, RSA. Therefore, using the same intensity of ground motions for RSA and NLRHA is appropriate to do the evaluation.

4.2.1 Ground motions for Bangkok

A set of seven recorded ground motions selected from PEER Ground Motion Database is used as seismic excitation. The detail information about the record of these ground motions is presented in the Table 4.4. These ground motions are modified and scaled such that their spectra match the bed-rock target spectrum as shown in Figure 4.3. This target spectrum is defined from mapped acceleration parameters at 0.2 and 1 second proposed by Palasri and Ruangrassamee (2010). Then, those spectral-matching

ground motions are scaled by a factor of 1.5 and they are input in ProShake program (EduPro 2004) to simulate the wave propagation through layers of soft soil underlying downtown area of Bangkok. The soft soil profile and the resulted time history of ground accelerations are shown in Appendix B. The pseudo-acceleration response spectra with 5% damping ratio of soft-soil ground motions are plotted in Figure 4.4.

Table 4.4 List of seven ground motions for Bangkok.

No.	Earthquake	Year	Station	Magnitude	Distance (km)	V_{s30} (m/s)
1	Kocaeli	1999	Maslak	7.4	64	>750
2	Chi-Chi	1999	TTN 042	7.6	65	845
3	Northridge	1994	Wrightwood Jackson Flat	6.7	68	822
4	Loma Prieta	1989	Piedmont Jr High	6.9	73	895
5	San Fernando	1971	Cedar Springs Allen Ranch	6.6	90	813
6	Chi-Chi	1999	TAP 077	7.6	117	1023
7	Landers	1992	San Gabriel E Grand Ave	7.3	142	>750

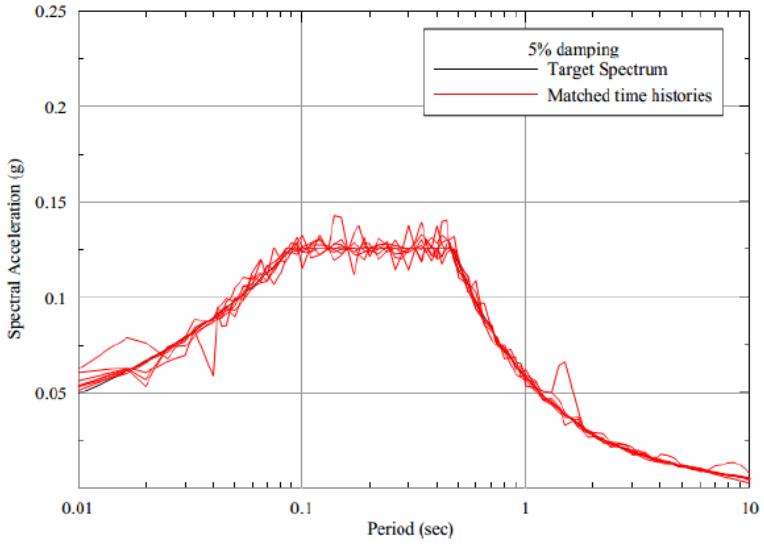

Figure 4.3 Bed-rock target spectrum and response spectra of seven ground motions modified to match the target spectrum.

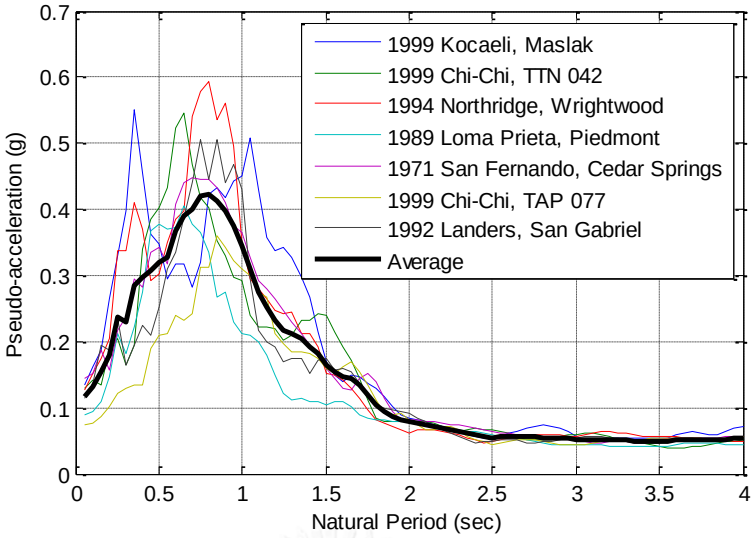

Figure 4.4 Elastic response spectra for 5% damping ratio of soft-soil ground motions.

4.2.2 Ground motions for Chiang Mai

Ten pairs of ground motions selected from PEER Ground Motion Database are used as seismic excitation. The selections are based on specific criteria such as magnitude, site distance and shear wave velocity, which are similar to that of design spectrum in Chiang Mai. The detail information about the record of these ground motions is presented in Table 4.5. Those ground motions are scaled by a factor obtained from trial and error by Minchainant (2012) such that mean SRSS spectrum of the ten pairs of ground motions is not less than 1.17 times the design spectrum according to the requirement of Chapter 16 in ASCE 7-10. The design spectrum is defined from site class D in Chiang Mai. The un-scaled SRSS spectrum of each pair is plotted in Figure 4.5. The mean un-scaled and scaled SRSS spectra of the ten pairs of those records are plotted along with the design spectrum and 1.17 times the design spectrum in Chiang Mai as shown in Figure 4.6. The component with larger PGA is selected from each of the ten pairs to make a set of the ten ground motions to be employed in NLRHA. The mean spectrum of these ten records is illustrated in Figure 4.7. The time history of these ten ground motions can be found in Appendix B.

Table 4.5 List of ten pair of ground motions for Chiang Mai.

NGA No.	Earthquake	Year	Station	Magnitude	Distance (km)	V_{s30} (m/s)
30	Parkfield	1966	Cholame-Shandon Array #5	6.19	9.6	290
95	Managua-Nicaragua-01	1972	Managua-ESSO	6.24	4.1	289
147	Coyote Lake	1979	Gilroy Array #2	5.74	9	271
148	Coyote Lake	1979	Gilroy Array #3	5.74	7.4	350
149	Coyote Lake	1979	Gilroy Array #4	5.74	5.7	222
159	Imperial Valley-06	1979	Agrarias	6.53	0.7	275
161	Imperial Valley-06	1979	Brawley Airport	6.53	10.4	209
162	Imperial Valley-06	1979	Calexico Fire Station	6.53	10.4	231
179	Imperial Valley-06	1979	El Centro Array #4	6.53	7	209
185	Imperial Valley-06	1979	Holtville Post Office	6.53	7.7	203

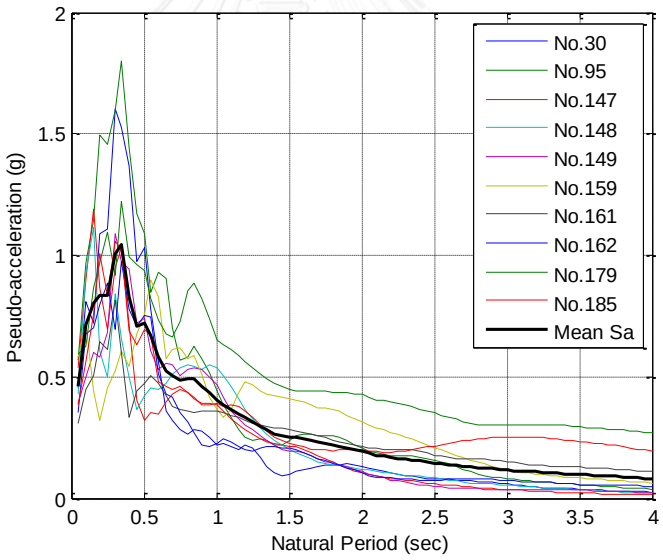

Figure 4.5 Un-scaled SRSS spectrum for 5% damping ratio of each pair of records.

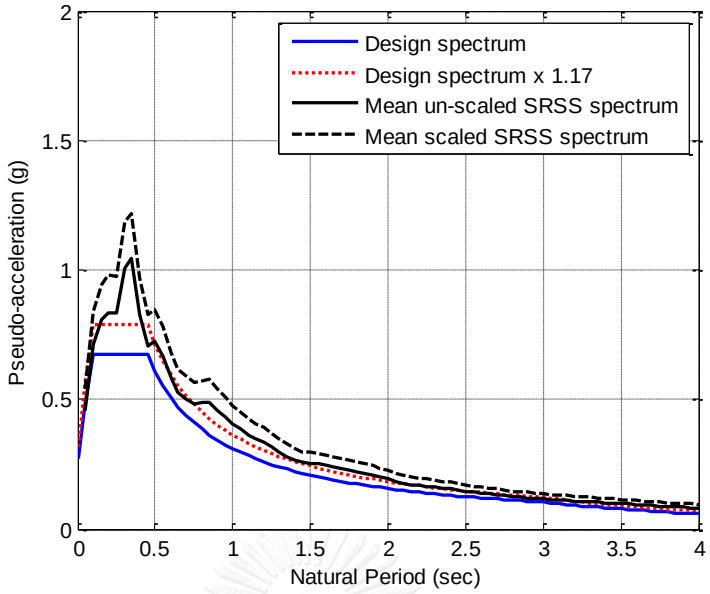

Figure 4.6 Mean SRSS spectrum for 5% damping ratio after scaling.

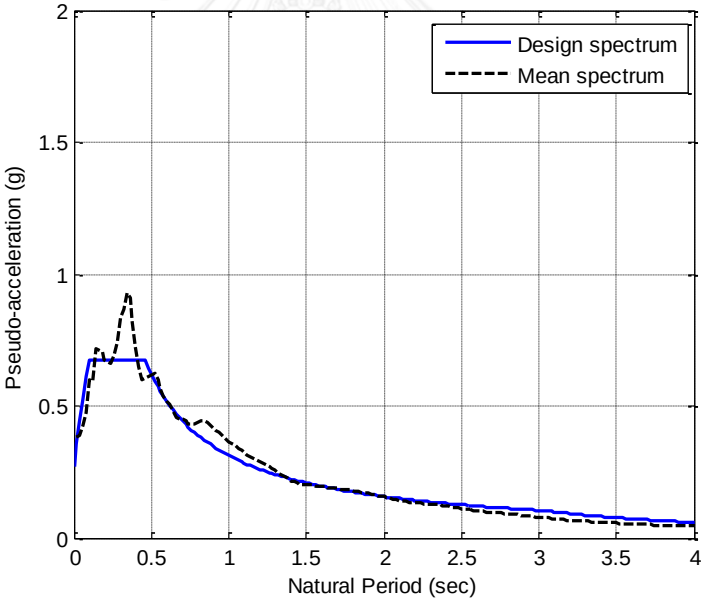

Figure 4.7 Mean spectrum for 5% damping ratio of the ten ground motions used in NLRHA after scaling.

CHAPTER 5
RESPONSE SPECTRUM ANALYSIS

5.1 Linear modeling of structural systems

5.1.1 Modeling assumptions

The followings are assumed in the linear modeling of the structural systems:

- RC spilt core wall is designed to resist the entire lateral loads; hence, only the structural split core-wall systems are modeled by ignoring the stiffness and strength of the gravity columns and slabs in the analytical model.
- Core walls are assumed to have uniform cross section. The coupling beams in each direction are considered to have the same stiffness and strength over the entire height of the building.
- Rigid diaphragm is assigned to the floor slab assuming that the floor is rigid in plane.
- Floor masses are computed from all dead loads and are assigned to the center of mass at each floor level.
- Foundation is assumed to be fixed support and interaction from soil is not considered.

5.1.2 Structural models

Three-dimensional model of the structure is created in ETABS program version 13 (CSI 2013) for analysis. The effective stiffness values of the structural members given in ACI 318-11 are used to account for cracked sections of RC members as presented in Table 5.1. Each structural component is modeled as follow:

- Wall is modeled as shell element.
- Short coupling beam (SCB), span to depth ratio of 1.5, is modeled as shell element.
- Long coupling beam (LCB), span to depth ration of 8, is modeled as frame element connected to the walls by an embedded rigid beam to ensure the rigid connection between the coupled walls and LCB.

Table 5.1 Effective stiffness of structural members in linear modeling (ACI 318-11).

Element	Effective stiffness	
	Flexural	Shear
Core wall	0.7 EI_g	1.0 GA_g
Coupling beam	0.35 EI_g	1.0 GA_g

5.2 Analysis and design considerations

The structural systems are designed according to ASCE 7-10 and ACI 318-11. The lateral force resisting system is considered to be special RC shear wall whose design factors are:

- Response modification factor R=6,
- Deflection amplification factor C_d=5
- Important factor I=1.25.

The structures are designed to resist the gravity loads and seismic load as shown in Table 5.2 and Figure 5.1, respectively. In Bangkok, the seismic load is specified by the mean spectrum of the seven recorded used in NLRHA, whereas in Chiang Mai, the design spectrum defined from site class D is employed. Basic load combinations for strength design in ASCE 7-10 as presented in Table 5.3 are considered. The seismic load is applied in each direction separately at a time. The vertical seismic load effect is not considered in this study. RSA is carried out by three-dimensional structural model described in Section 5.2. Constant modal damping ratio of 5% is employed.

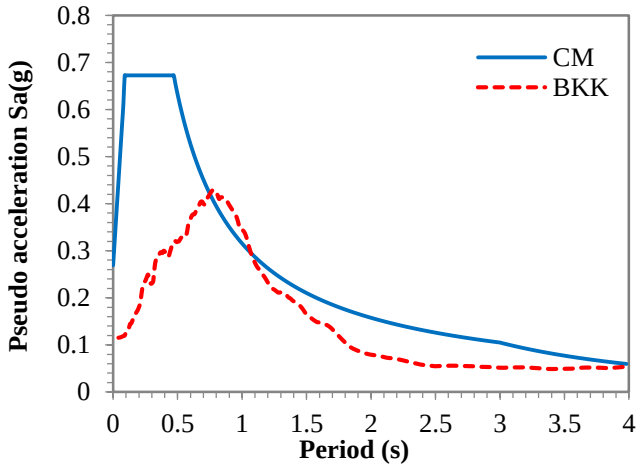

Figure 5.1 Elastic spectrum for 5% damping ratio in Bangkok and Chiang Mai.

Table 5.2 Gravity loads.

Load case	Value
Live Load	2.5 kN/m^2
Super imposed dead load	3 kN/m^2

Table 5.3 Load combinations.

No.	Load Combination
1	$1.2D + 0.5L \pm Q_E$
2	$0.9D \pm Q_E$

where D is all dead loads, L is unreduced live load and Q_E is seismic load.

5.3 Story drift, bending moment and shear response behavior

5.3.1 Modal properties

The modal properties of the first three modes in each direction of the structure are presented in Table 5.4.

Table 5.4 Modal properties of the first three modes.

No. Story	Mode	Fundamental period (s)		Modal participating mass ratios	
		X	Y	X	Y
5	1	0.57	0.43	69%	73%
	2	0.11	0.11	22%	19%
	3	0.05	0.06	6%	5%
10	1	1.62	1.28	66%	66%
	2	0.31	0.25	20%	22%
	3	0.12	0.11	7%	7%
15	1	2.69	1.72	65%	65%
	2	0.54	0.32	18%	21%
	3	0.21	0.14	7%	7%
20	1	3.72	2.05	66%	64%
	2	0.78	0.38	17%	21%
	3	0.31	0.16	7%	7%
25	1	4.60	2.27	66%	64%
	2	1.01	0.42	17%	21%
	3	0.40	0.18	6%	7%

5.3.2 Maximum envelop and modal contribution

Modal analysis is the basis of RSA approach which computes the seismic demands of each mode separately then combines them with appropriate modal combination rule. In this study, the complete quadratic combination (CQC) method is employed. Story drift, bending moment and shear force profiles contributed from the first three modes are presented along with the combined peak response envelop as shown in Figure 5.2. Only the results of buildings subjected to mean spectrum of Bangkok in X direction are presented here. Similar trend is observed for design spectrum in Chiang Mai.

(a) 5-story

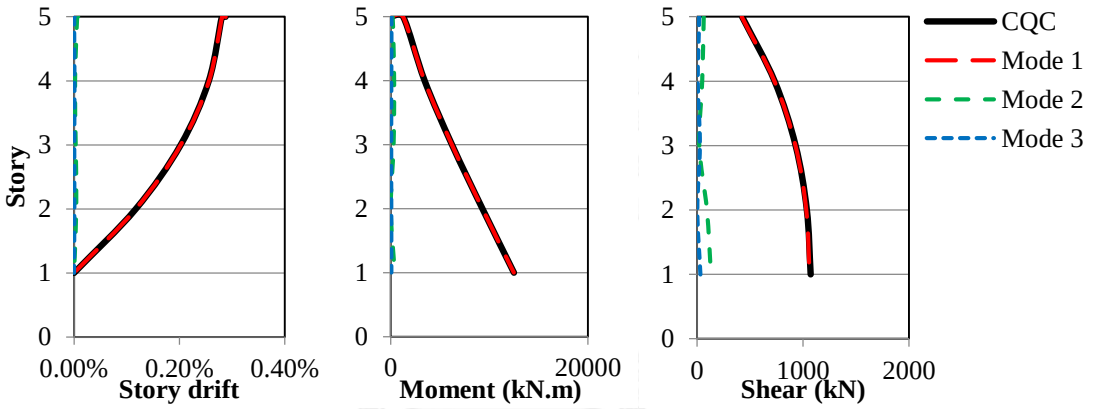

(b) 10-story

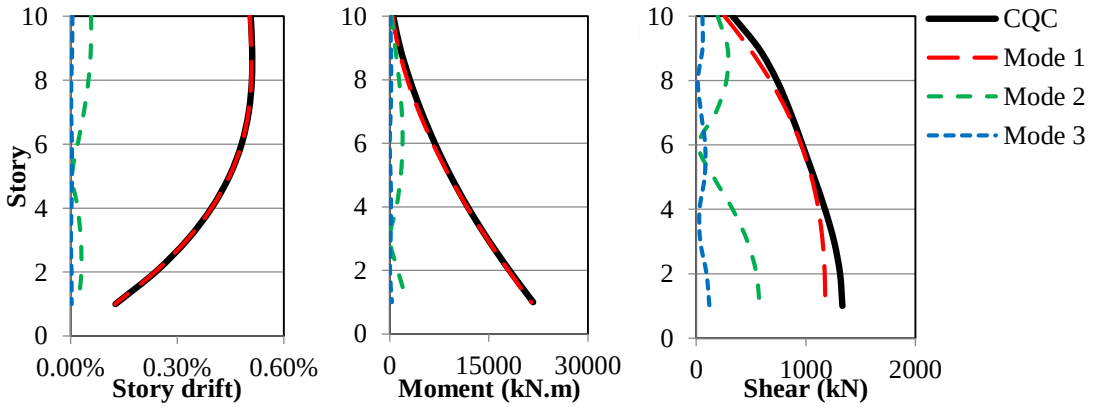

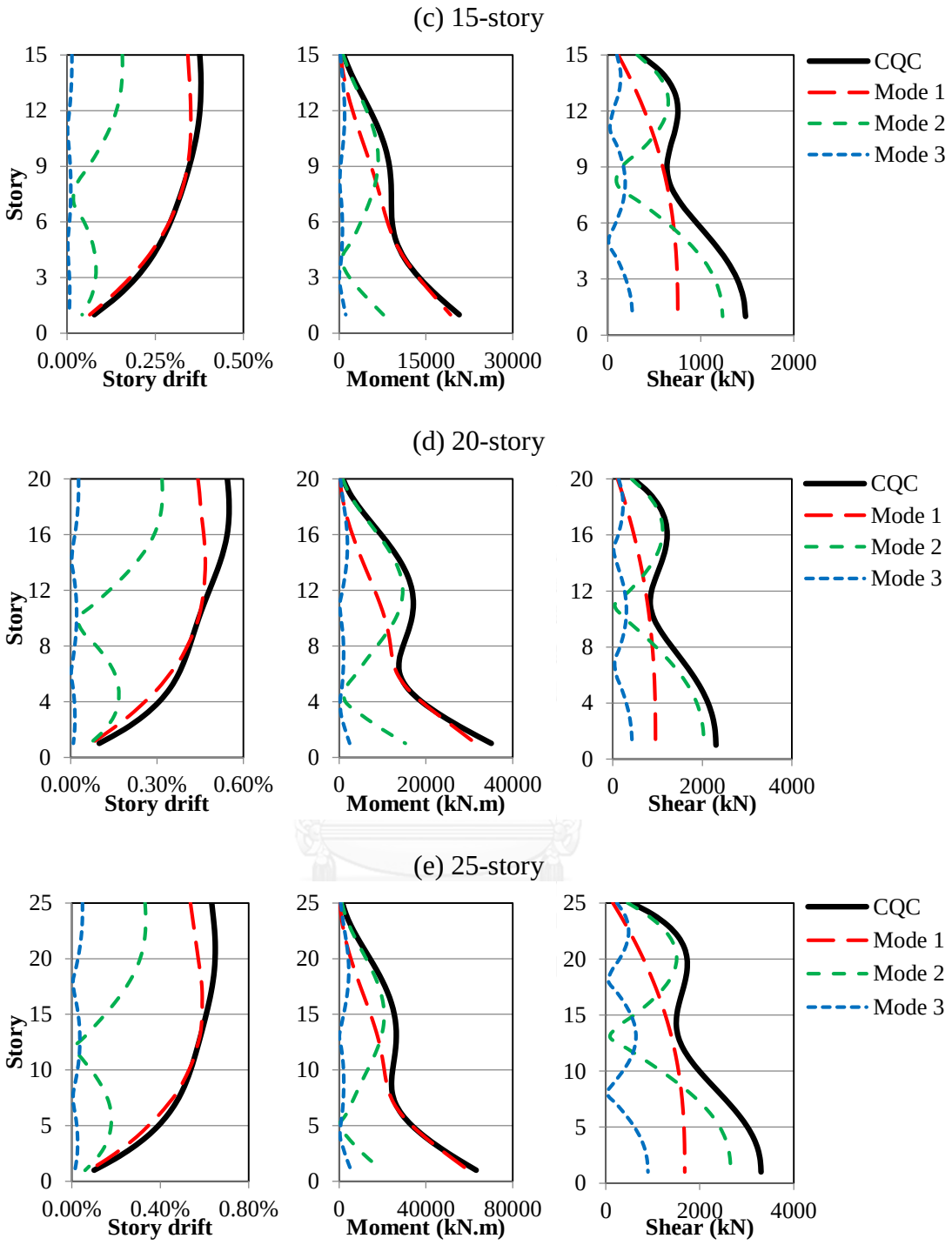

Figure 5.2 Story drift, bending moment and shear profiles contributed from the first three modes and the combined peak response envelop: (a) 5-story; (b) 10-story; (c) 15-story; (d) 20-story and (e) 25-story.

These figures show that as the structural heights increase, higher modes become more dominant for both bending moment and shear response, even though the mass

participation of higher modes are smaller than that of the first mode. The modal contributions to the total response envelop are totally different between story drift, bending moment and shear response. For story drift, the first-mode contribution is always dominant along the height of the structures. For bending moment, the first mode is dominant at the base of the structure for all buildings, while higher modes play important role around mid-height of the structure for taller buildings. For shear which is the primary focus in this study, second-mode contribution is considerably significant at the base of the wall even for shorter buildings. Therefore, for taller buildings, it is not appropriate to assume that bending moment and shear response display the same inelastic behavior by applying the same response modification factor as mentioned in ASCE 7-10.

5.3.3 Base moment and base shear modal contribution ratio

The modal contribution ratio of each mode is defined here as:

$$\bar{F}_i = \frac{F_i}{F_{CQC}} \tag{5.1}$$

where $\bar{F}_i$ is the modal contribution ratio of response in mode *i*, F_i is the peak modal response of mode *i*, F_{CQC} is the combined peak response.

The variations of modal contribution ratio with fundamental period for base shear and base moment of the five studied structures are presented here both in Bangkok and Chiang Mai. Only the results in X direction are presented here. Similar trends are observed in Y direction.

For Bangkok, second-mode contribution overtakes the first-mode contribution for periods greater than 2.2 seconds for base shear responses while base moment responses are always dominated by the first mode for all periods. For Chiang Mai, second-mode contribution is dominant for periods greater than 1.6 seconds for base shear response, whereas base moment responses are observed the same thing as in Bangkok. From this investigation, it can be concluded that for the same structural systems subjected to ground motions having different spectrum shapes, higher-mode contributions for base shear are different.

Figure 5.3 highlights the fact that higher modes are the primary contributors to base shear for tall buildings with long fundamental periods. Note that these trends are not always the general case because they are derived from the five studied structures and spectral shapes considered in this study.

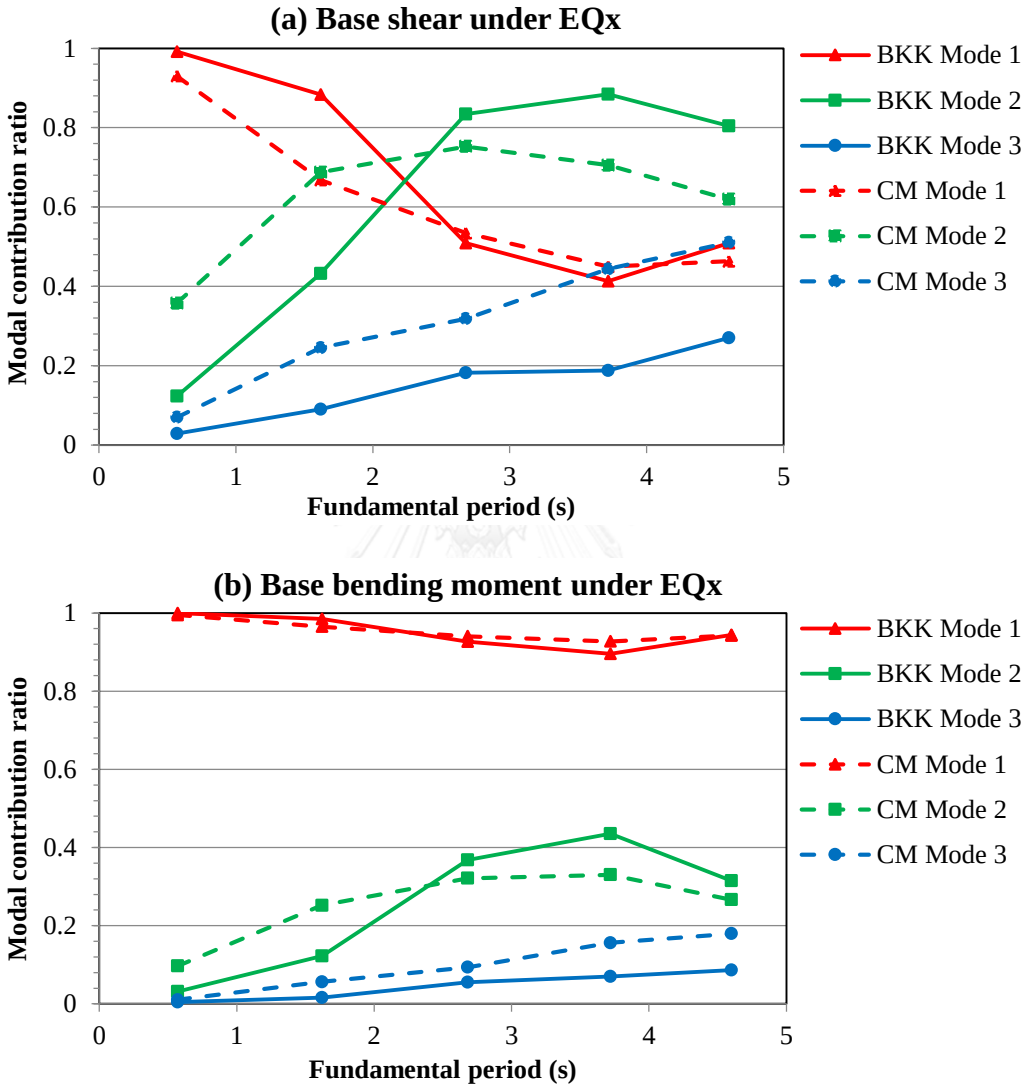

Figure 5.3 Modal contribution ratios for the first three modes: (a) base shear under EQx and (b) base bending moment under EQx.

5.4 Seismic demands of RC core walls

❖ Story drift

Story drift ratio is obtained from RSA by scaling up with a factor of C_d/I = 4, in which C_d=5 and I=1.25 based on ASCE 7-10. The allowable story drift ratio is 1.5% according to ASCE 7-10. The maximum story drift ratios are illustrated in Figure 5.4 for both Bangkok and Chiang Mai. They are all below the maximum allowable story drift ratio. To easily identify the results in each building and its location, the coding is defined such that the capital letters are for location (BKK for Bangkok and CM for Chiang Mai) and the following numbers refer to number of stories.

(a) 5-story

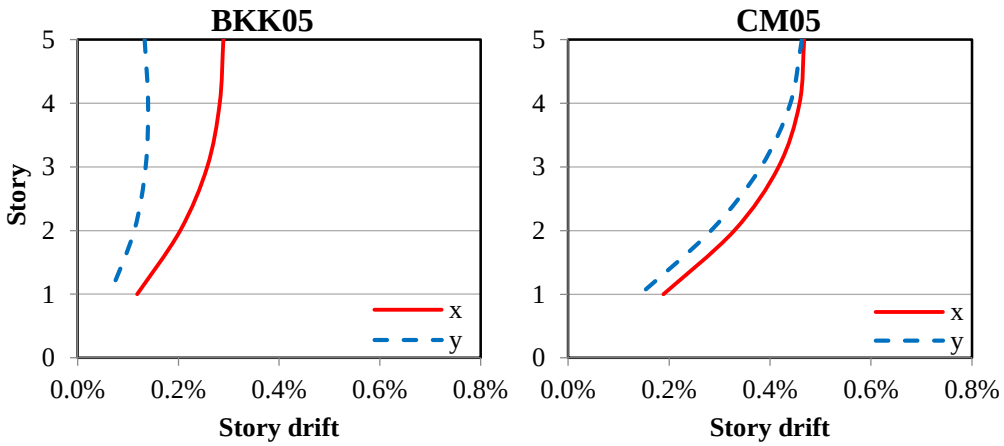

(b) 10-story

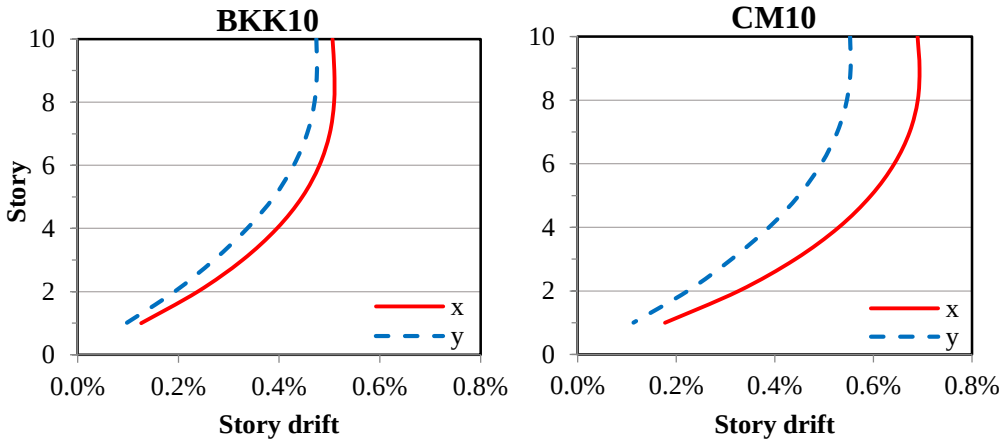

(c) 15-story

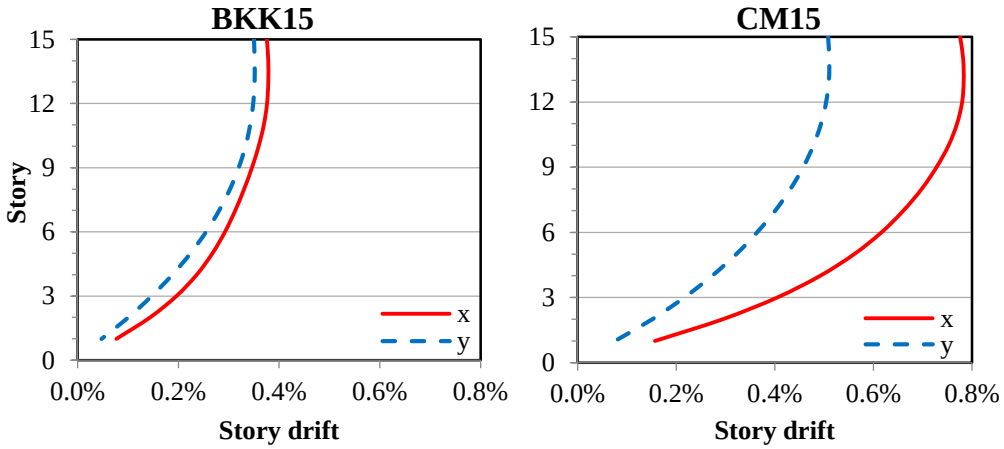

(d) 20-story

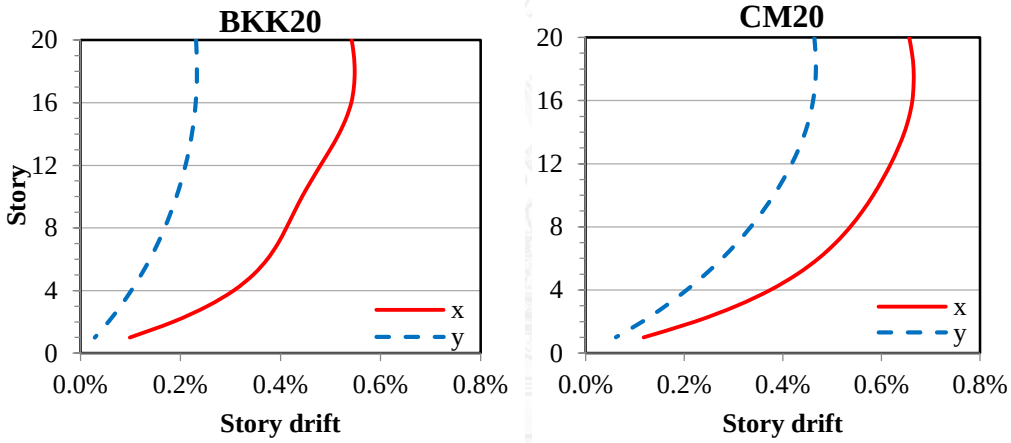

(e) 25-story

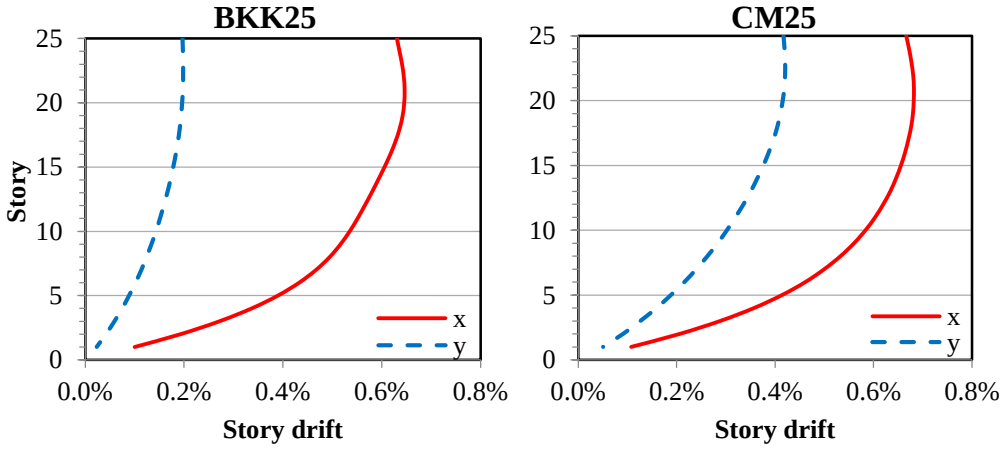

Figure 5.4 Maximum story drift ratio from ASCE 7-10: (a) 5-story; (b) 10-story; (c) 15-story; (d) 20-story and (e) 25-story.

❖ **Internal forces of core walls**

ASCE 7-10 requires that dynamic base shear (V_d) determined from RSA is at least equal to 85% of the static base shear (V_s) computed from equivalent lateral force (ELF) procedure. Such scaling results in effective response modification factor, R_{eff}, which is the ratio between elastic base shear and design base shear. The value of R_{eff} is computed by:

$$R_{eff} = \min\left(\frac{R}{I} \times \frac{V_d}{0.85V_s}, \frac{R}{I}\right) \tag{5.2}$$

The dynamic base shear V_d from RSA is computed by ETABS program (CSI 2013) whereas the static base shear V_s from ELF is calculated by the Eq. (5.3).

$$V_s = C_s W \tag{5.3}$$

where W is the effective weight of the building and C_s is seismic response coefficient determined from Eq. (5.4).

$$C_s = \frac{S_a I}{R} \geq 0.044 S_{DS} I \tag{5.4}$$

where S_a is pseudo acceleration and S_{DS} is the design spectral response acceleration parameter in the short period.

The fundamental period in ELF method is computed from:

$$T = \min(C_u T_a, T_{etabs}) \tag{5.5}$$

$$T_a = N/10 \tag{5.6}$$

where T_a is approximated period recommended by the ASCE 7-10, N is number of story of the building and C_u is coefficient of upper limit period which is equal to 1.4 taken from the ASCE 7-10.

Then, the effective response modification factor can be calculated as summarized in Table 5.5 and Table 5.6 for Bangkok and Chiang Mai, respectively.

Table 5.5 Effective response modification factor for buildings in Bangkok.

No. story	$0.85V_{sx}$ (kN)	$0.85V_{sy}$ (kN)	V_{dx} (kN)	V_{dy} (kN)	R_{effx}	R_{effy}
5	1077	921	825	771	3.68	4.02
10	2659	2915	1613	2245	2.91	3.70
15	2959	3647	2168	3041	3.52	4.00
20	4592	4592	3916	3791	4.09	3.96
25	6588	6588	4781	5236	3.48	3.82

Table 5.6 Effective response modification factor for buildings in Chiang Mai.

No. story	0.85Vsx (kN)	0.85Vsy (kN)	Vdx (kN)	Vdy (kN)	Reffx	Reffy
5	1,772	2,150	1,430	1,761	3.87	3.93
10	3,107	3,399	2,875	3,347	4.44	4.73
15	4,957	5,164	4,363	5,888	4.23	4.80
20	7,691	7,691	4,710	8,550	2.94	4.80
25	11,035	11,035	5,718	11,906	2.49	4.80

The design shear forces and bending moments of the RC core walls already scaled to 85% of static base shear are plotted in the Figure 5.5 and Figure 5.6 for Bangkok and Chiang Mai, respectively.

(a) 5-story

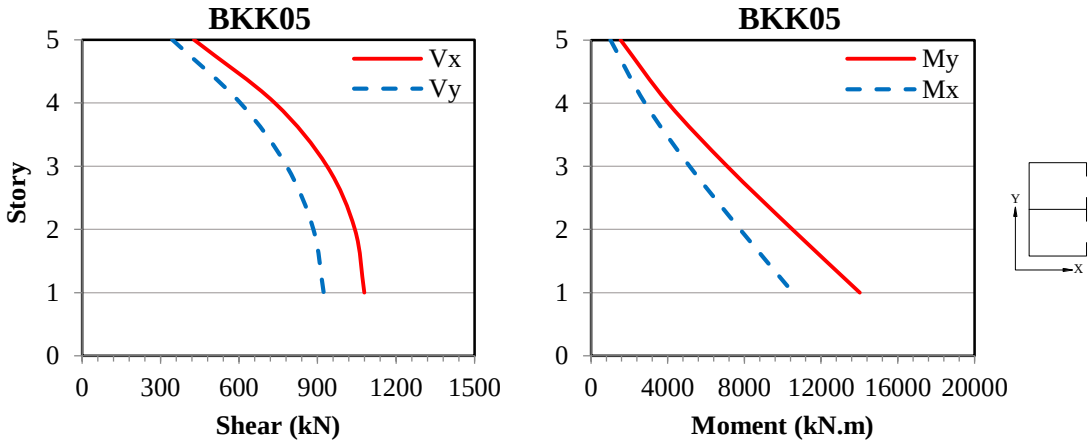

(b) 10-story

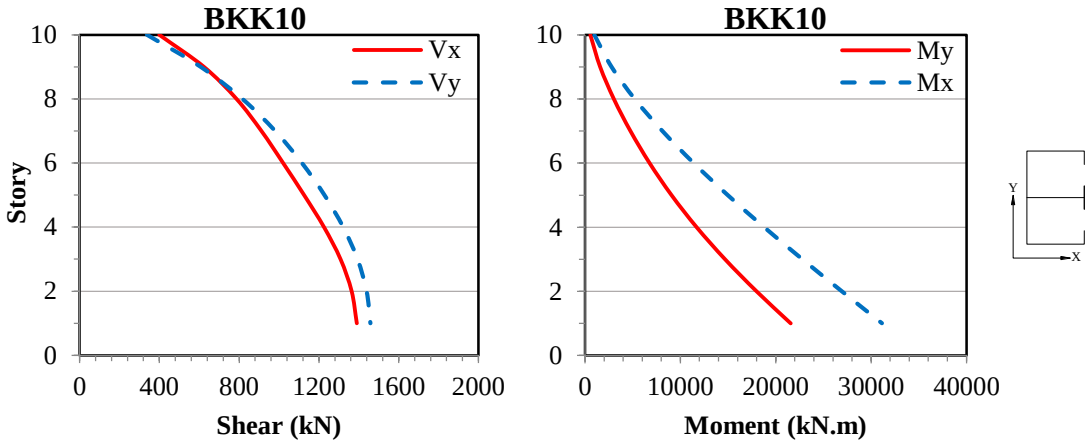

(c) 15-story

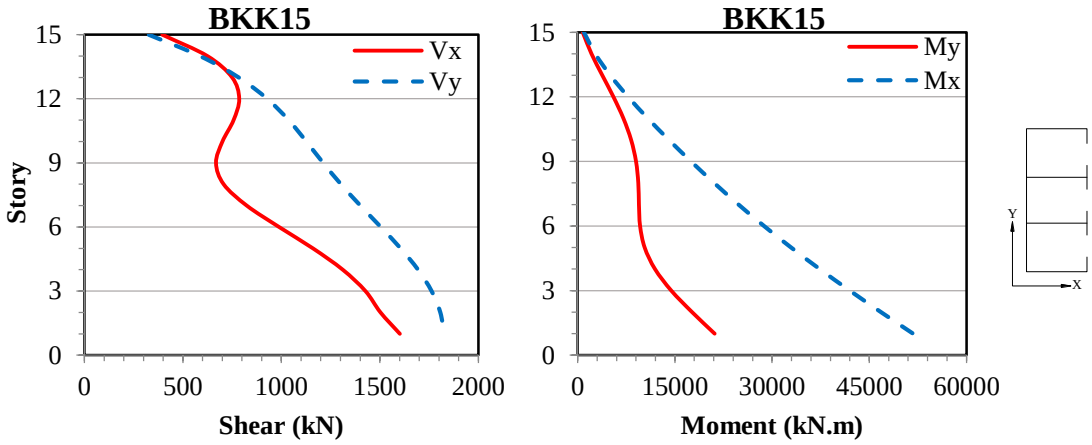

(d) 20-story

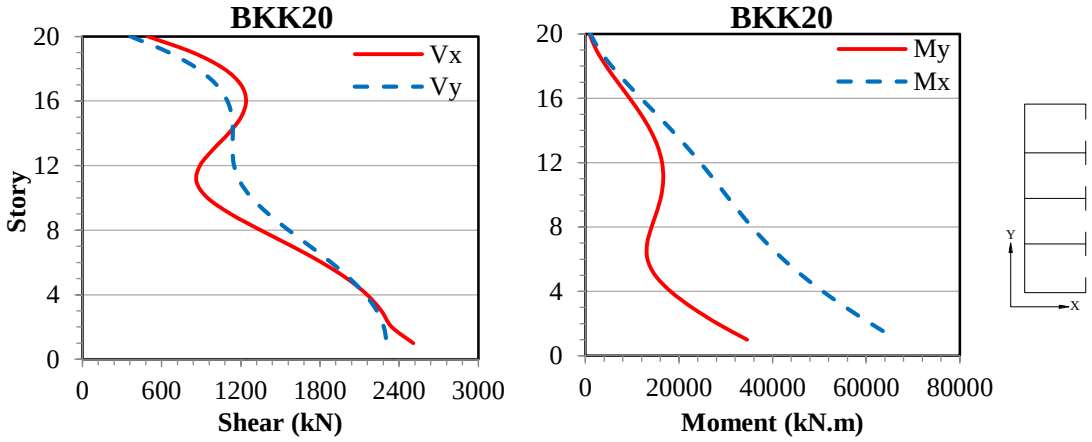

(e) 25-story

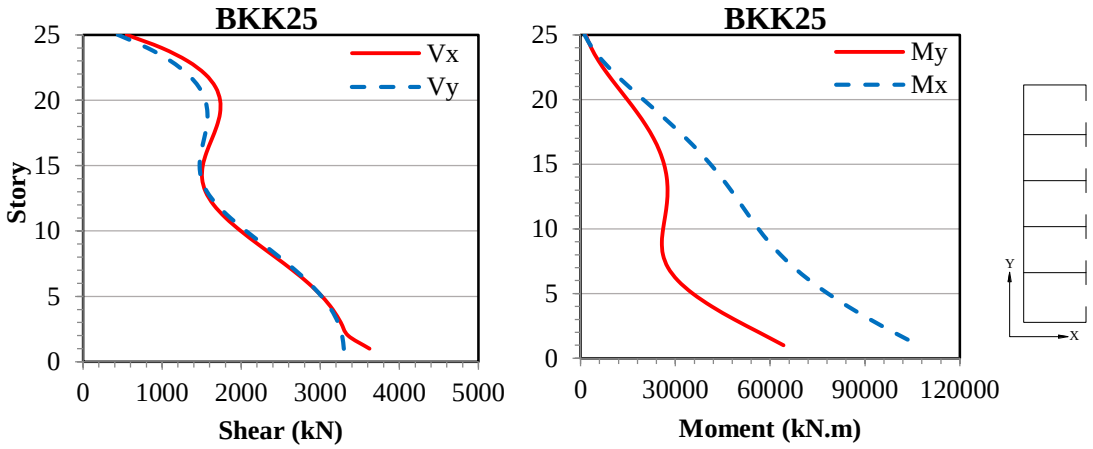

Figure 5.5 Design shear forces and bending moments of core walls from RSA procedure in Bangkok: (a) 5-story; (b) 10-story; (c) 15-story; (d) 20-story and (e) 25-story.

(a) 5-story

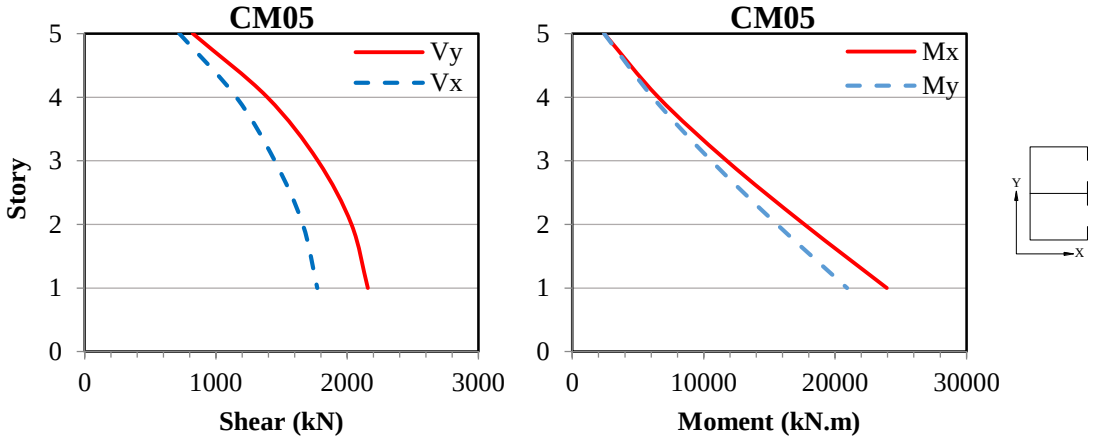

(b) 10-story

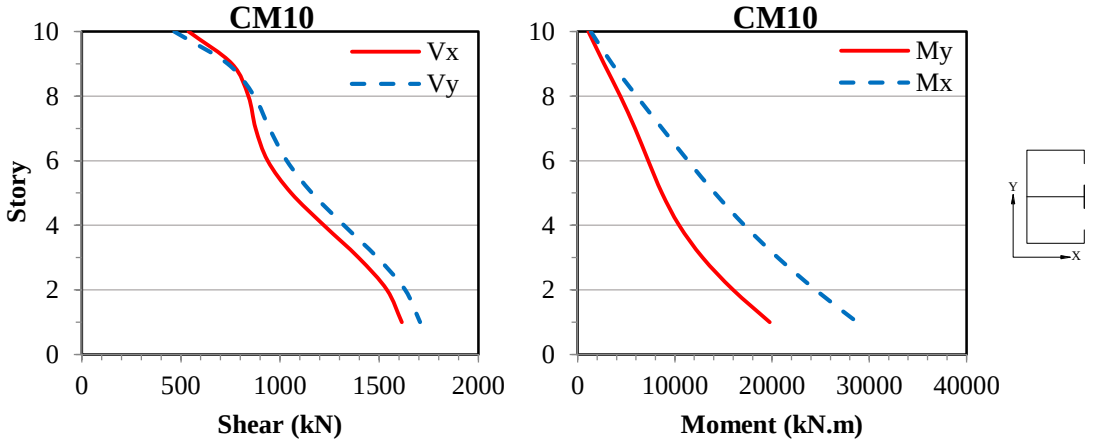

(c) 15-story

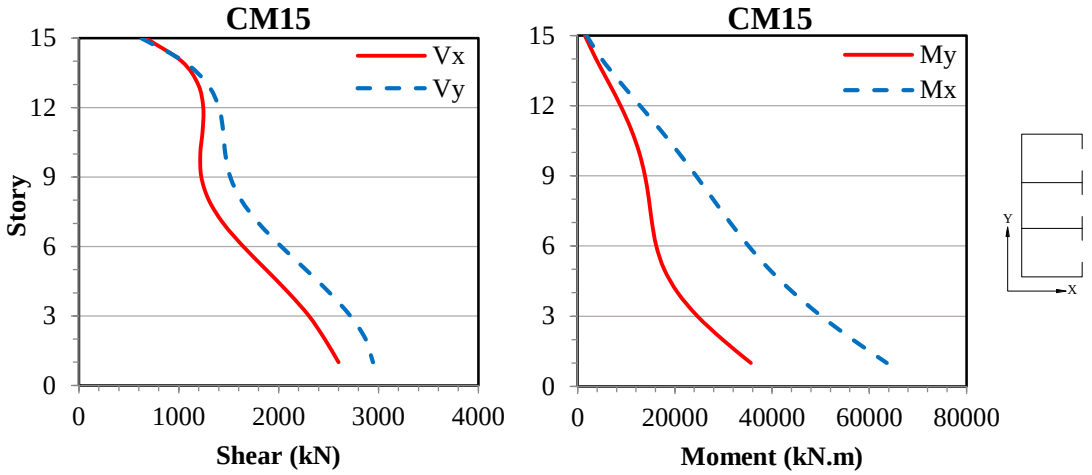

(d) 20-story

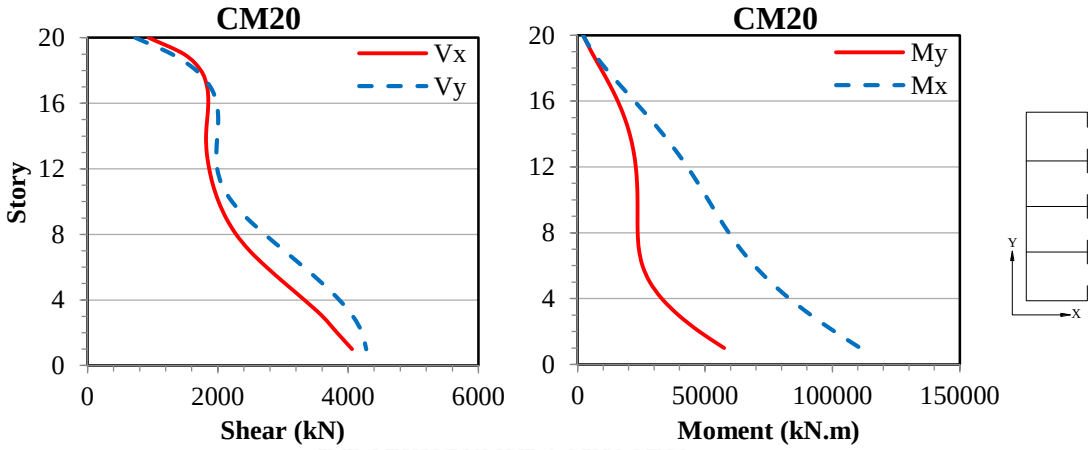

(e) 25-story

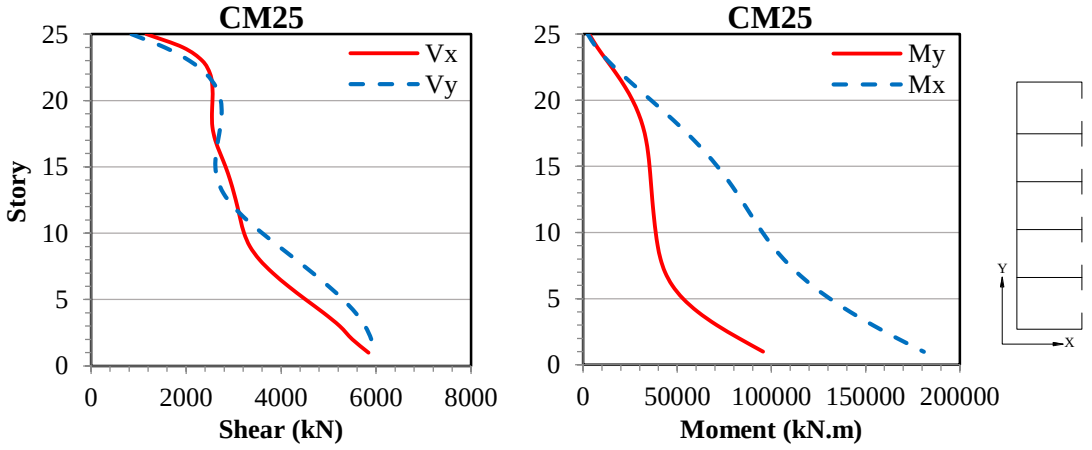

Figure 5.6 Design shear forces and bending moments of core walls from RSA procedure in Chiang Mai: (a) 5-story; (b) 10-story; (c) 15-story; (d) 20-story and (e) 25-story.

5.5 Design of structural members

The split core-wall structures are designed such that their nominal strengths multiplied by the corresponding strength reduction factor in accordance with ACI 318-11 are approximately equal to the demands obtained from RSA procedure.

5.5.1 Design of core walls

Each core wall is designed as a single cross section (combined many wall segments) in which its flexural strength is represented by P-M interaction diagram. That interaction surface is used to determine the critical flexural demand/capacity ratio for each design load combination. The minimum vertical reinforcement is 0.25% for special structural wall according to ACI 318-11. The P-M interaction diagrams are developed for eight different ratios of reinforcement varying from 0.25% to 2%. Uniform reinforcement for each wall segment is considered for simplicity. Core walls are assumed to have uniform cross section with reduction of vertical reinforcement in every three stories when required. For all design load combinations, linear interpolation between the eight interaction surfaces is used to determine the largest required reinforcing ratio that give demand/capacity ratio approximately equal to one. This process is done with the help of ETABS Program (CSI 2013). Shear design for core wall is not considered in this study. The example of P-M interaction diagrams of 5-story core wall about X- and Y-axis obtained from eight different ratios of reinforcing steel is presented in Figure 5.7 and Figure 5.8, respectively.

The required vertical reinforcing ratios along the height of core wall in each building are summarized in Table 5.7 and Table 5.8 for Bangkok and Chiang Mai, respectively.

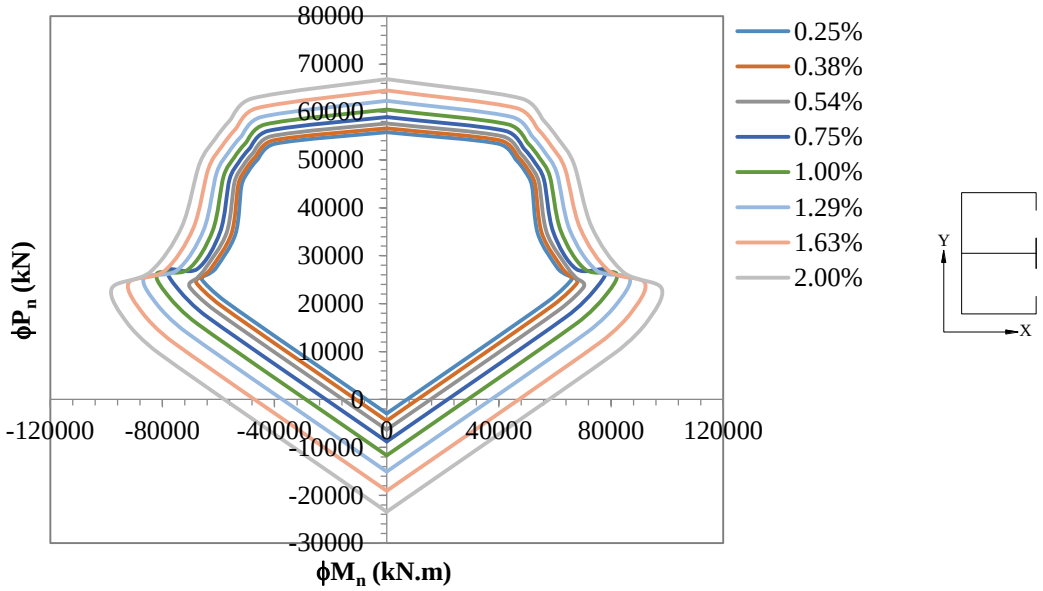

Figure 5.7 P-M interaction diagrams of 5-story core wall about X-axis.

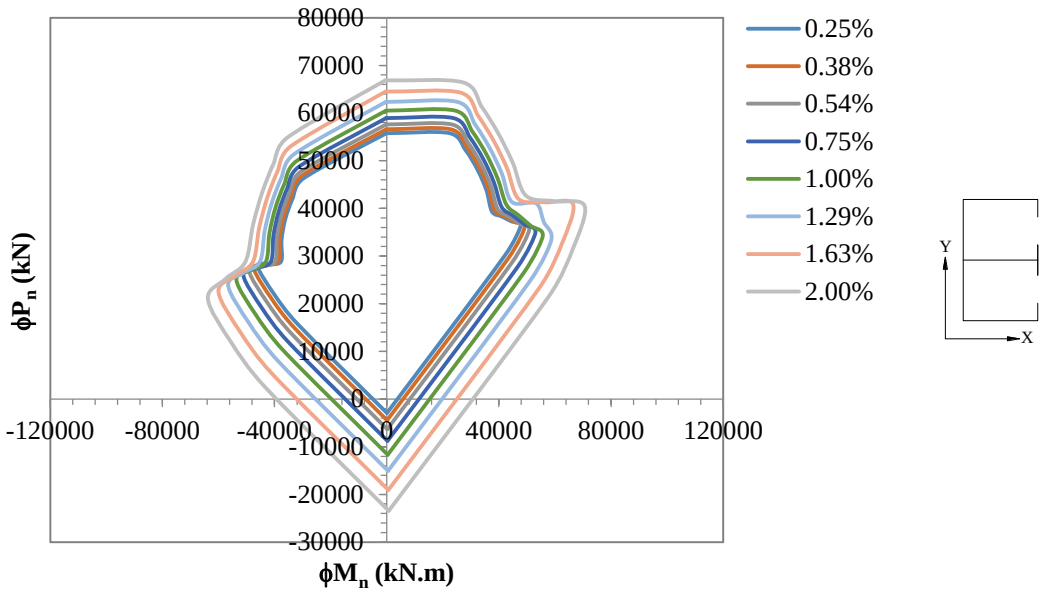

Figure 5.8 P-M interaction diagrams of 5-story core wall about Y-axis.

Table 5.7 Required vertical reinforcement of core walls in Bangkok.

No. story	Reinforcing ratios (%)				
	5-story	10-story	15-story	20-story	25-story
25					0.25
24					0.25
23					0.25
22					0.25
21					0.25
20				0.25	0.25
19				0.25	0.25
18				0.25	0.25
17				0.25	0.25
16				0.25	0.25
15			0.25	0.25	0.25
14			0.25	0.25	0.25
13			0.25	0.25	0.25
12			0.25	0.25	0.25
11			0.25	0.25	0.25
10		0.25	0.25	0.25	0.25
9		0.25	0.25	0.25	0.25
8		0.25	0.25	0.25	0.25
7		0.25	0.25	0.25	0.25
6		0.38	0.25	0.25	0.25
5	0.25	0.38	0.25	0.25	0.25
4	0.25	0.38	0.25	0.25	0.25
3	0.35	0.8	0.25	0.25	0.28
2	0.35	0.8	0.25	0.25	0.28
1	0.35	0.8	0.25	0.25	0.28

Table 5.8 Required vertical reinforcement of core walls in Chiang Mai.

No. story	Reinforcing ratios (%)				
	5-story	10-story	15-story	20-story	25-story
25					0.25
24					0.25
23					0.25
22					0.25
21					0.31
20				0.25	0.31
19				0.25	0.31
18				0.25	0.33
17				0.25	0.33
16				0.25	0.33
15			0.25	0.28	0.33
14			0.25	0.28	0.33
13			0.25	0.28	0.33
12			0.25	0.28	0.33
11			0.25	0.28	0.33
10		0.25	0.25	0.28	0.33
9		0.25	0.25	0.28	0.33
8		0.25	0.25	0.28	0.33
7		0.25	0.25	0.28	0.33
6		0.31	0.34	0.37	0.42
5	0.37	0.31	0.34	0.37	0.42
4	0.37	0.31	0.34	0.37	0.42
3	0.86	0.68	0.63	0.69	0.88
2	0.86	0.68	0.63	0.69	0.88
1	0.86	0.68	0.63	0.69	0.88

5.5.2 Design of coupling beams

All the coupling beams in each direction are designed to have uniform strength along the height of the building for simplicity. No detail of reinforcement in coupling beams is made. Only the design strength to make demand/capacity ratio equal to one is required for further usage in nonlinear modeling for NLRHA. The design strengths are computed by dividing the maximum demands obtained from RSA procedure with strength reduction factor in ACI 318-11.

For short coupling beam (SCB), span to depth ratio of 1.5, diagonal shear reinforcement is used recommended by PEER/ATC-72-1 (2010). Design shear strength is needed for nonlinear modeling. The nominal shear strength (V_n) of SCB is computed by dividing the maximum shear demand (V_{max}) with strength reduction factor equal to 0.85 according to Section 9.3.4 of ACI 318-11.

For long coupling beam (LCB), span to depth ratio of 8, conventionally reinforcement is employed. Design flexural strength is required for nonlinear modeling. The nominal bending moment strength (M_n) of LCB is calculated by dividing the maximum bending moment demand (M_{max}) with strength reduction factor equal to 0.9 according to Section 9.3.2 of ACI 318-11.

The maximum demands and nominal strengths of SCB and LCB in each building are summarized in Table 5.9 and Table 5.10 for Bangkok and Chiang Mai, respectively.

Table 5.9 Seismic demands and design strengths of coupling beams in Bangkok.

No. Story	SCB		LCB	
	V_{max} (kN)	V_n (kN)	M_{max} (kN.m)	M_n (kN.m)
5	268	315	-	-
10	166	196	131	145
15	211	248	101	113
20	193	227	139	155
25	215	253	217	242

Table 5.10 Seismic demands and design strengths of coupling beams in Chiang Mai.

No. Story	SCB		LCB	
	V_{max} (kN)	V_n (kN)	M_{max} (kN.m)	M_n (kN.m)
5	570	670	-	-
10	246	290	116	129
15	321	377	170	189
20	335	394	229	255
25	376	442	316	351

CHAPTER 6
NONLINEAR RESPONSE HISTORY ANALYSIS

6.1 Nonlinear modeling of structural systems

6.1.1 Modeling assumptions

The same assumptions as in linear modeling described in Chapter 5 are made. In nonlinear model, p-delta effects due to the gravity columns are included by creating a dummy column with no lateral stiffness at the center of each core wall and by slaving the column ends with other nodes at each floor, recommended by Powell (2007). The dummy column is subjected to an axial load of all dead load plus 25 percent of live load (D+0.25L), which are supported by all columns in the building.

6.1.2 Structural models

Three-dimensional nonlinear model is constructed in PERFORM-3D version 5 (CSI 2011), in which each structural member is modeled as described below.

6.1.2.1 Core wall

Core walls are modeled using inelastic fiber shear wall elements represented by the concrete and steel properties. The material stress-stain relationships presented below are used. Nonlinear modeling is incorporated over the entire height of the core wall. In each core-wall cross section, the webs consist of eight concrete fibers along with eight steel fibers while the flanges consist of three concrete fibers and three steel fibers. Concrete fibers in the webs are modeled as confined concrete in the edge (smaller fiber) and unconfined concrete in the middle region (relatively large fiber), whereas concrete fibers in the flanges are all confined concrete. Steel fibers are distributed with uniform spacing for both webs and flanges, for simplicity. An example of core-wall fiber section of 5-story building is shown in Figure 6.1. Core wall in the first story consists of two elements, whereas core wall in upper stories is represented by one element.

In plan shear behavior of the walls is considered to be elastic. The elastic shear material for wall with reduced shear stiffness of $G_c/10$ ($G_c=0.4E_c$) to account for shear cracking recommended by PEER/ATC-72-1 (2010) is employed.

Out of plan behavior of the walls is assumed to be elastic. The concrete modulus of elasticity of one quarter ($E_c/4$) is considered to allow for stiffness reduction when concrete cracks.

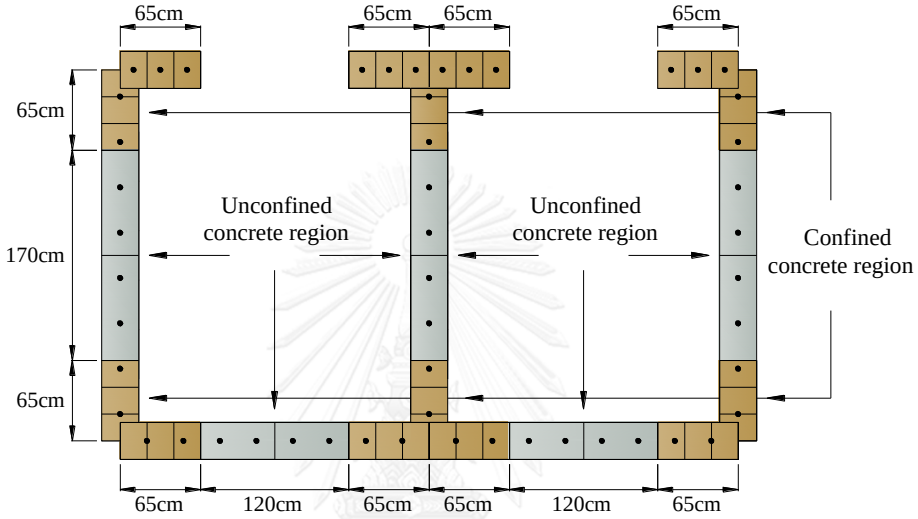

Figure 6.1 Core wall fiber section of 5-story building.

6.1.2.1.1 Concrete

The material stress-stain relationship for confined and unconfined concrete proposed by Mander et al. (1988) as shown in Figure 6.2 is adopted such that it is represented by a tri-linear relationship in PERFORM-3D (CSI 2011) as presented in Figure 6.3 and Figure 6.4. The tension strength of concrete is neglected. The non-cyclic degraded concrete material is used and the cyclic degraded reinforcing steel material whose cyclic degradation parameters are taken from Moehle et al. (2011) is employed. Moehle et al. (2011) modeled the rectangular wall tested by Orakcal and Wallace (2006) in PERFORM-3D program and they adjusted the cyclic degradation parameters of reinforcing steel so that the modeled wall matched the lateral load versus top displacement curve of the tested wall.

The stress-strain relationship of concrete proposed by Mander et al. (1988) is given by the following expressions:

$$f_c = \frac{f_{cc}^{'} xr}{r - 1 + x^r} \tag{6.1}$$

where

$$x = \frac{\varepsilon_c}{\varepsilon_{cc}} \qquad r = \frac{E_c}{E_c - E_{\sec}}$$

$$\varepsilon_{cc} = \varepsilon_{co}\left[1 + 5\left(\frac{f_{cc}^{'}}{f_{co}^{'}} - 1\right)\right] \qquad E_{\sec} = \frac{f_{cc}^{'}}{\varepsilon_{cc}}$$

$$f_{cc}^{'} = Kf_{co}^{'} \qquad \varepsilon_{cu} = 0.004 + \frac{1.4\rho_s f_{yh}\varepsilon_{sm}}{f_{cc}^{'}}$$

in which

f_c = longitudinal compression stress of concrete

$f_{cc}^{'}$ = maximum compression stress of confined concrete

$f_{co}^{'}$ = compressive strength of concrete at 28 days

f_{yh} = yield strength of the hoop reinforcement

ε_c = longitudinal compression strain of concrete

ε_{cc} = compression strain at maximum concrete stress of confined concrete

ε_{cu} = ultimate compression strain of confined concrete

ε_{sm} = steel strain at maximum tensile stress

E_c = concrete modulus of elasticity

$E_{\sec}$ = concrete secant modulus elasticity

K = confinement ratio of concrete

ρ_s = ratio of volume of rectangular steel hoops to volume of concrete core measured to the outside of the peripheral hoop

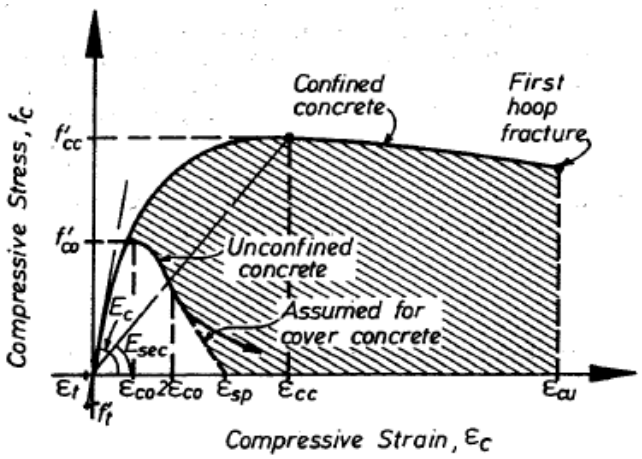

Figure 6.2 Stress-strain model for concrete (Mander et al. 1988).

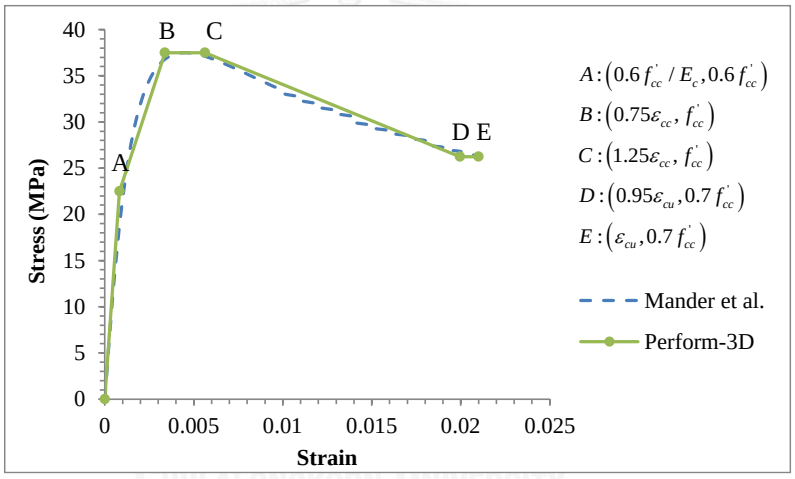

Figure 6.3 Confined concrete stress-strain relationship.

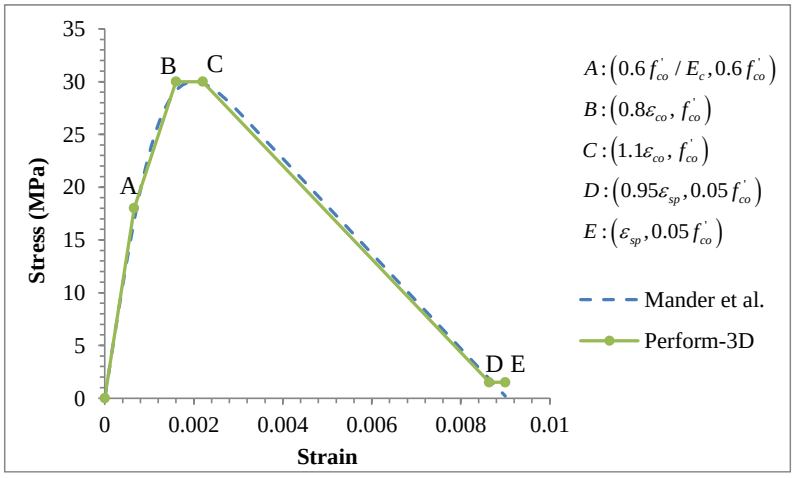

Figure 6.4 Unconfined concrete stress-strain relationship.

6.1.2.1.2 Reinforcing steel

The reinforcing steel with strain hardening ratio of 3% recommended by PEER/ATC-72-1 (2010) is adopted. The stress-strain curve of the steel is based on material specification of Thailand Industrial Standard in which the nominal yield strength of 390 MPa corresponding to the ultimate strength of 560 MPa is used. The ultimate strain of the steel is assumed to be 0.09 (=60% of industrial standard as recommended by Priestley et al. (2007)).

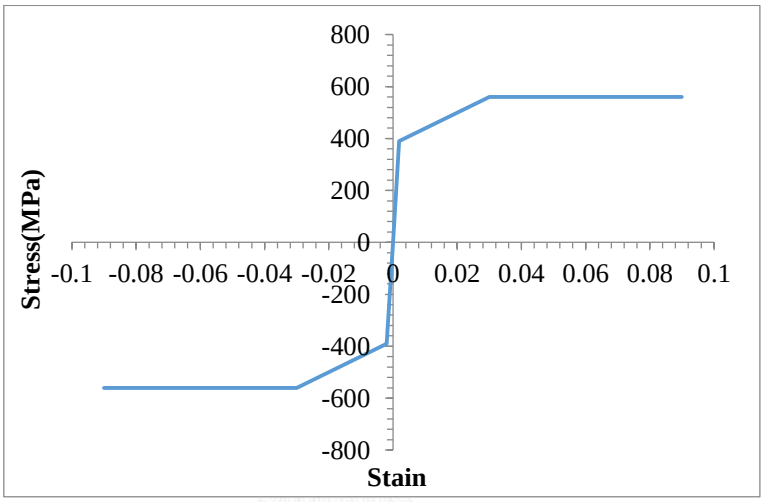

Figure 6.5 Inelastic steel stress-strain relationship.

The cyclic degradation parameters of reinforcing steel to be used with PERFORM-3D are taken from Moehle et al. (2011) as indicated in Table 6.1. The tri-linear hysteresis loop described in Section 6.1.2.4 is used for cyclic behavior of reinforcing steel.

Table 6.1 Cyclic degradation parameters for reinforcing steel (Moehle et al. 2011).

Points	Strain	Cyclic degradation factor
Y	0.00195	0.70
1	0.0025	0.68
2	0.004	0.64
3	0.006	0.62
X	0.09	0.60

where *Y* represents the yield point, *X* represents maximum strain point and 1, 2 and 3 represent intermediate strain between *Y* and *X* point.

6.1.2.1.3 Validation of core wall capacity

To ensure correct capacity of core wall used in PERFORM-3D program (CSI 2011), general fiber model using distributed reinforcement in XTRACT program (Imbsen 2006) is employed to compare moment-curvature capacity of the core-wall cross section. The moment-curvature presented in Figure 6.6 comes from the case of 5-story core wall without gravity load. The results obtained from both programs are closely matched in both directions.

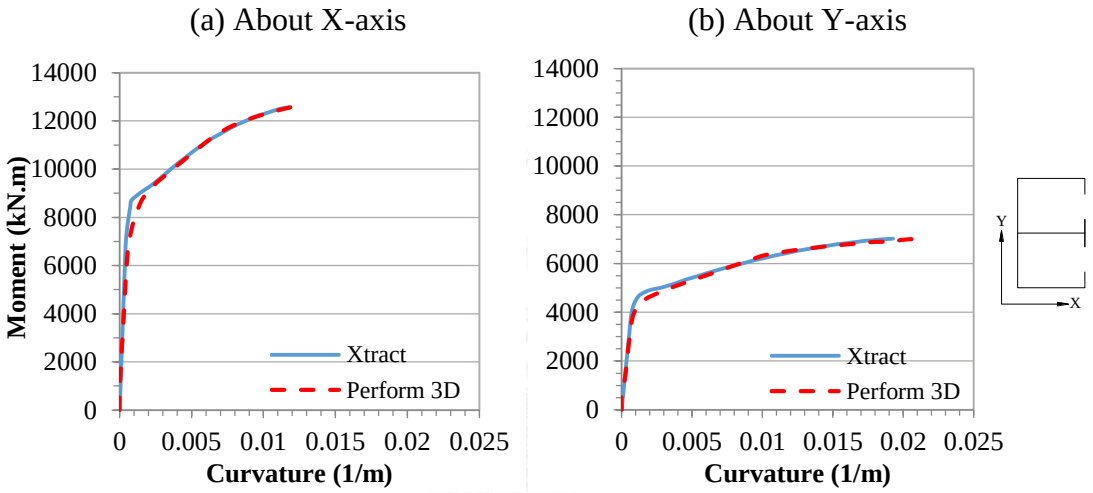

Figure 6.6 Comparison of moment-curvature of core-wall cross section obtained from XTRACT and PERFORM-3D program: (a) about X-axis and (b) about Y-axis.

6.1.2.2 Short coupling beam

Short coupling beams (SCB) above the opening door (span to depth ratio of 1.5) are modeled using a nonlinear shear displacement-hinge at the center of the beam with modeling parameters based on test results of Naish et al. (2013). The shear-displacement back bone curve is represented by a tri-linear shear force-rotation relationship as displayed in Figure 6.7. The elastic modulus for bending of $0.2E_cI_g$ is used for elastic portion to account for slip/extension deformations at beam-wall interface. SCB is connected to the walls using embedded element suggested by Powell (2007).

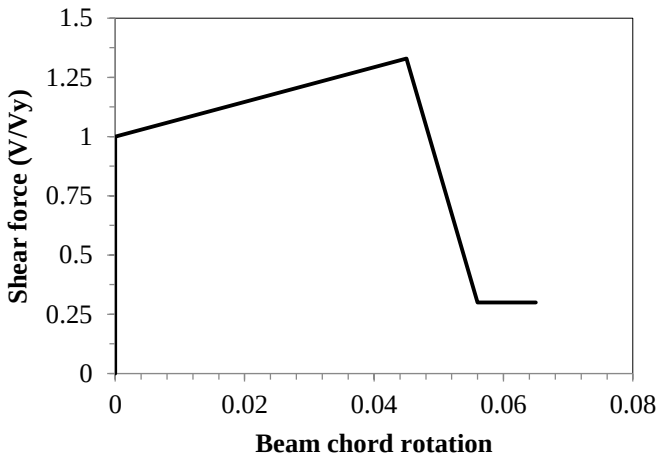

Figure 6.7 Tri-linear shear force-rotation back bone curve.

The yield shear strength, V_y of diagonally reinforced coupling beam is taken equal to nominal shear strength, V_n obtained from Eq. (21.9) of ACI 318-11 as presented here by Eq. (6.2).

$$V_n = 2A_{vd} f_y \sin\alpha \tag{6.2}$$

$$A_{vd} = \frac{V_{\max}}{2\phi_s f_y \sin\alpha}$$

$$V_n = \frac{V_{\max}}{\phi_s}$$

where A_{vd} is the total area of reinforcement in each group of diagonal bars, α is the angle between the diagonal bars and the longitudinal axis of the coupling beam, V_{max} is maximum seismic shear demand and ϕ_s is shear strength reduction factor equal to 0.85 according to section 9.3.4 of ACI 318-11.

The ultimate shear strength, V_u is estimated from V_y by assuming $V_u = 1.33V_y$ and the residual shear strength, V_r is taken as $V_r = 0.3V_u$ (Naish et al. 2013).

The displacement shear hinge is related to rotation of coupling beam by:

$$\Delta = \theta L_b \tag{6.3}$$

where θ is rotation in radian and Δ is equivalent displacement at a rotation, θ of coupling beam.

Modeling parameters and numerical acceptance criteria for diagonally-reinforced coupling beams proposed by Naish et al. (2013) are used as shown in Table 6.2. The cyclic degradation parameters to be used in PERFORM 3-D for modeling of RC coupling beam are shown in Table 6.3, proposed by Naish (2010).

Table 6.2 Modeling parameters and numerical acceptance criteria for nonlinear procedures- diagonally-reinforced coupling beams (Naish et al. 2013).

Conditions		Plastic Hinge Rotation (radians)		Residual Strength Ratio	Acceptable Plastic Hinge Rotation (radians)		
l_n/h	$\frac{V}{t_w l_w \sqrt{f_c'}}$	a	b	c	IO	LS	CP
≤ 2.0	≤ 6.0	0.045	0.065	0.30	0.007	0.020	0.045
≤ 2.0	≥ 8.0	0.035	0.055	0.30	0.006	0.018	0.035
≥ 3.0	≤ 6.0	0.050	0.070	0.30	0.009	0.022	0.050
≥ 3.0	≥ 8.0	0.045	0.065	0.30	0.007	0.020	0.045

Table 6.3 Cyclic degradation parameters for coupling beams (Naish 2010).

Model	Energy degradation factor					Unloading stiffness factor
	Y	*U*	*L*	*R*	*X*	
Moment-hinge (LCB)	0.50	0.45	0.40	0.35	0.35	0.5
Shear-hinge (SCB)	0.50	0.45	0.40	0.35	0.35	-

where *Y* is the first yield point, *U* is maximum strength point, *L* is ductile limit point, *R* is residual strength point and *X* is maximum deformation point as shown in Figure 6.8.

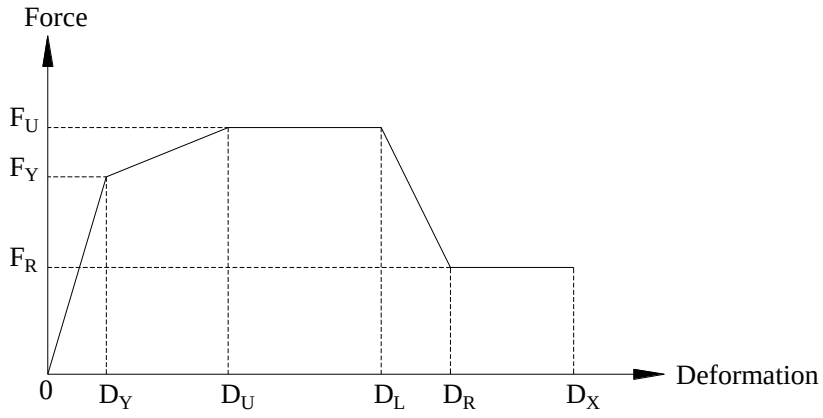

Figure 6.8 Inelastic force-deformation relationship in PERFORM-3D.

6.1.2.3 Long coupling beam

Long coupling beams (LCB) across the two core walls (span to depth ratio of 8) include rotational plastic hinge elements at both ends with modeling parameters given by ASCE 41-13. Tri-linear moment-hinge rotation relationship as shown in Figure 6.9 is utilized. The elastic modulus for bending of elastic portion is taken the same as SCB. LCB is connected to the walls using embedded element in the same way as SCB.

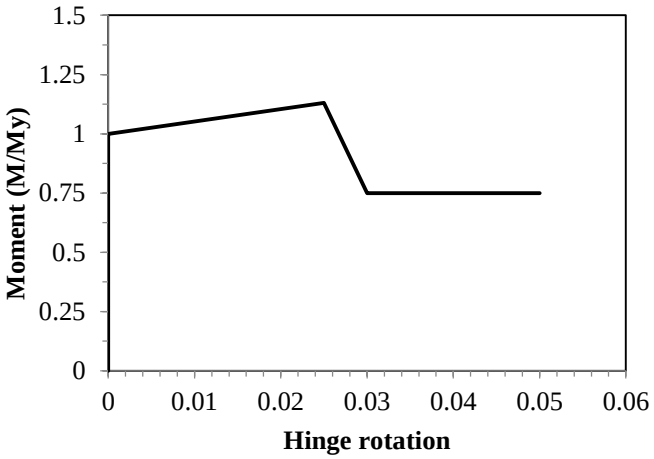

Figure 6.9 Tri-linear moment-hinge rotation back bone curve.

The flexural yield strength, M_y is taken equal to nominal flexural strength, M_n computed in Section 5.5.2. The capping strength, M_u is estimated from M_y by assuming M_u/M_y=1.13 suggested by Haselton et al. (2008).

The effective stiffness of structural members in nonlinear modeling is summarized in Table 6.4.

Table 6.4 Effective stiffness of structural members in nonlinear modeling.

Element	Stiffness	
	Flexural	Shear
Core wall	Fiber section	0.1 GA_g
Coupling beam	0.2 EI_g	1.0 GA_g

6.1.2.4 Tri-linear hysteresis loop

Tri-linear hysteresis loop model is used for cyclic behavior of reinforcing steels and coupling beams. The brief concepts of this model in PERFORM-3D are presented here.

PERFORM-3D accounts for energy degradation by adjusting the unloading and reloading stiffness to reduce the area under the loop. The loop properties are defined by the relationship between deformation of the component and the corresponding energy degradation factor which is defined as the ratio of the area of the degraded hysteresis loop to the area of the non-degraded loop. The tri-linear degraded loops are shown in Figure 6.10 and Figure 6.11.

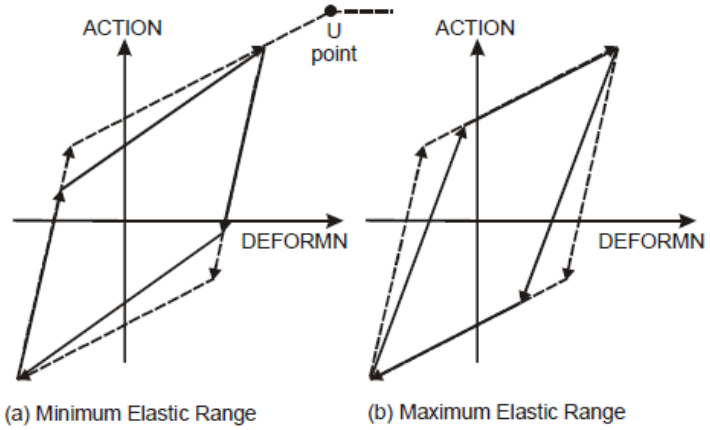

Figure 6.10 Degraded loop for tri-linear behavior before U point in PERFORM-3D.

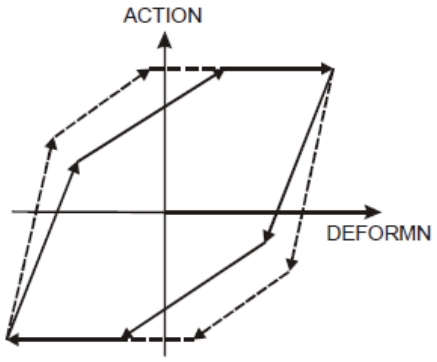

Figure 6.11 Degraded loop for tri-linear behavior after U point in PERFORM-3D.

Figure 6.10 shows the cyclic behavior before both positive and negative deformations reach the *U* point (maximum strength point). The dash lines represent the

first cyclic behavior for non-degraded loop whereas the solid lines are the second cyclic behavior in two extreme shapes for the degraded loop. Figure 6.10a provides minimum elastic range and maximum strain hardening range. The elastic stiffness remains the same as the first cycle. Figure 6.10b gives maximum elastic range and minimum strain hardening range. The hardening stiffness does not change while the elastic stiffness degrades. The degraded elastic and hardening stiffness are calculated to make the area of the degraded loop equal to energy degradation factor times the area of the non-degraded loop. Elastic range is controlled by unloading stiffness factor. Unloading stiffness factor of one and minus one give the behavior in Figure 6.10a and Figure 6.10b, respectively.

In Figure 6.11, the dash lines represent the first cyclic behavior after the positive and negative deformations of the components attain the *U* point whereas the solid lines are the second cyclic behavior for the degraded loop. The yield strength of the components degrades. The elastic and strain hardening stiffness also degrade in the manner that the area of the degraded loop is equal to the energy degradation factor times the area of the non-degraded loop.

6.2 Analysis considerations

NLRHA is conducted by using PERFORM-3D program (CSI 2011) in which three-dimensional nonlinear structural model is constructed as described in Section 6.1. Rayleigh damping is implemented with ζ damping ratio specified in the first and third modes suggested by Yathon (2011). The value of equivalent viscous damping ratio, ζ is calculated from Eq. (6.4) as recommended by PEER/ATC-72-1 (2010).

$$\zeta = \alpha / 30 \quad (\text{for } N<30) \qquad (6.4)$$
$$\zeta = \alpha / N \quad (\text{for } N>30)$$

where N is the number of stories, and α is a coefficient with a recommended range of 60 to 120. For reinforced concrete systems, $\alpha = 120$ is recommended.

NLRHA is performed using average-acceleration Newmark's method. The gravity load of $1.0D + 0.25L$ is applied before NLRHA. For Bangkok, seven ground motions described in Section 4.2.1 of Chapter 4 are used. For Chiang Mai, ten ground

motions selected from ten pairs of records as mentioned in Section 4.2.2 of Chapter 4 are employed. The ground motions are applied in each direction separately at a time.

6.3 Comparison of RSA and NLRHA seismic demands

The results presented below are the mean values of responses to the ground motions used in NLRHA. Earthquake excitations applied to the structures in X and Y directions are named as EQx and EQy, respectively. The results in Bangkok and Chiang Mai are named as BKK and CM, respectively. The comparisons of seismic demands determined from linear RSA and linear response history analysis (LRHA) are presented in Appendix C.

6.3.1 Base shear and base moment amplification of core wall

Base shear amplification (BSA) is defined as the ratio between shear force in a core wall from NLRHA and design shear force in RSA procedure. Base moment amplification (BMA) is defined as the ratio between bending moment in a core wall from NLRHA and design bending moment in RSA procedure. Base flexural over-strength (BFOS) is defined as the ratio between actual ultimate bending moment capacity of a core wall and design bending moment in RSA procedure. Bending moment strength of core wall is computed with the axial load of D+0.25L before running NLRHA.

- **Base shear amplification**

Figure 6.12 shows that base shear amplifications are generally greater than two. The results in both locations, Bangkok and Chiang Mai, are significantly different in Y direction (Figure 6.12b). In Y direction (EQy), in which core walls behave like cantilever walls, BSAs are as large as five for 20- and 25-story buildings in Bangkok while in Chiang Mai, BSAs are relatively smaller and are about three for 10- to 25-story buildings. In X direction (EQx), the behavior is like coupled walls, in which two core walls are coupled by LCB. In these cases, BSAs are smaller than in Y direction. BSAs in Bangkok are a little bit larger than in Chiang Mai (Figure 6.12a). From detail investigation, it is found that core walls in X direction do not yield much at the base while the coupling beams sustain wide spread yielding at several plastic hinges in the

upper stories dissipating much energy. This may be the reason why core walls suffer little yielding and smaller shear amplification.

The differences of BSAs in both locations come from mainly different base flexural over-strength (BFOS) of core wall (Figure 6.14) and higher-mode contributions due to different spectrum shape as explained in Section 5.3.3 of Chapter 5. The sensitivity effects of BFOS of core wall on BSA of core wall will be investigated in Section 6.5.

❖ **Base moment amplification**

Unlike base shear response, base moment response is contributed mainly from the first mode and the base moment is limited by actual flexural capacity of core wall which is dependent of the amount of axial load. Due to flexural over-strength which came from mainly: different axial load (D+0.25L for NLRHA and 0.9D, which governs the design, for RSA), strength reduction factors, hardening of the steel, and confinement effect of concrete, bending moments from NLRHA are larger than those from RSA procedure. As example shown in Figure 6.15 for the case of 15-story core wall in Chiang Mai, the bending moment demand of core wall from NLRHA is located at the actual P-M interaction surface and is larger than the design moment from RSA procedure. The design P-M interaction includes the strength reduction factors according to ACI 318-11 and the actual P-M interaction does not consider those strength reduction factors. Under EQx (Figure 6.13a), base moment amplifications are in the range of 1.2 to 2.2 for Bangkok and 1.2 to 1.5 for Chiang Mai. Under EQy (Figure 6.13b), BMAs are relatively larger in the range of 1.2 to 3 for Bangkok and 1.5 to 2.1 for Chiang Mai. The difference of BMAs and BFOS between the two directions of core wall comes from the design process. In designing the vertical reinforcement of the core walls, the bending moment demands due to EQx and EQy are considered. The bending moment demands due to EQx govern the design for most of the buildings and result in smaller BFOS in X direction than in Y direction for those buildings, as shown in Figure 6.14.

Moment amplification at mid-height of core wall is totally different from base moment amplification of core wall when the walls in upper stories are designed to remain elastic. This will be discussed in Section 6.6.

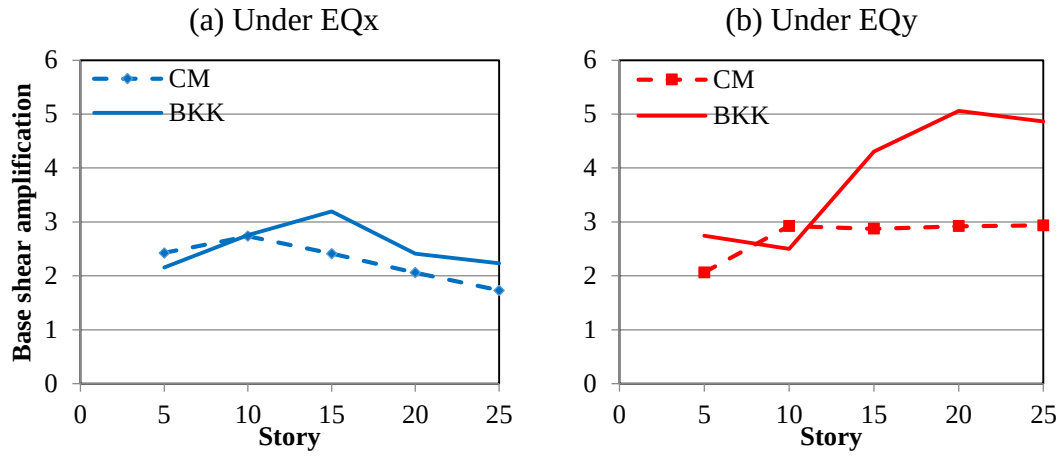

Figure 6.12 Base shear amplification of core wall: (a) under EQx and (b) under EQy.

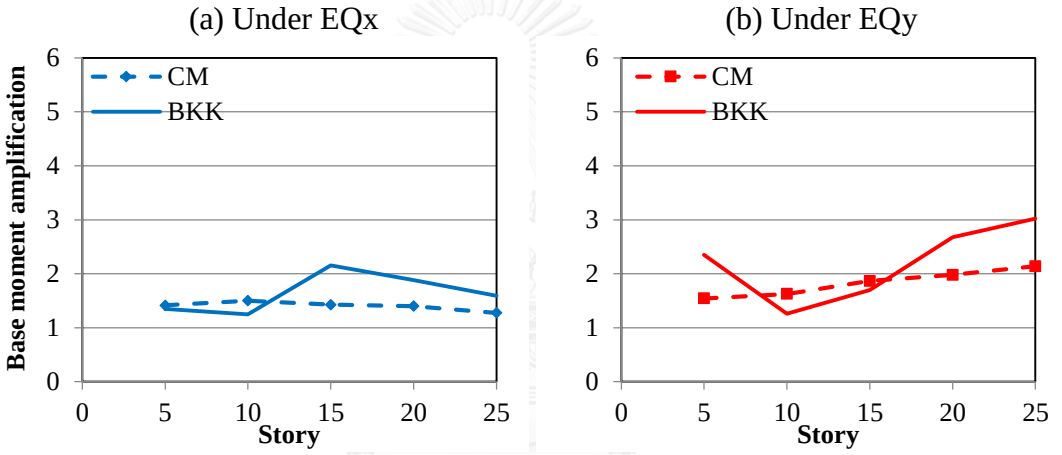

Figure 6.13 Base moment amplification of core wall: (a) under EQx and (b) under EQy.

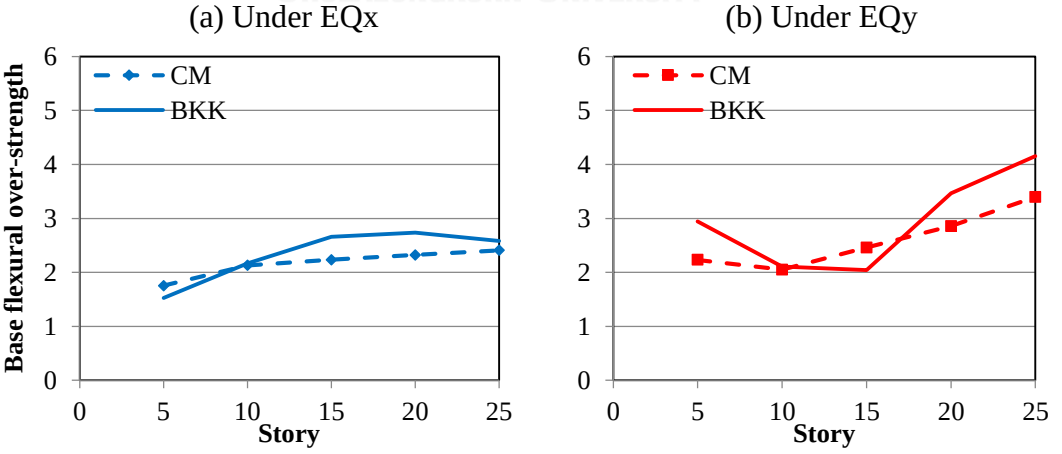

Figure 6.14 Base flexural over-strength of core wall: (a) under EQx and (b) under EQy.

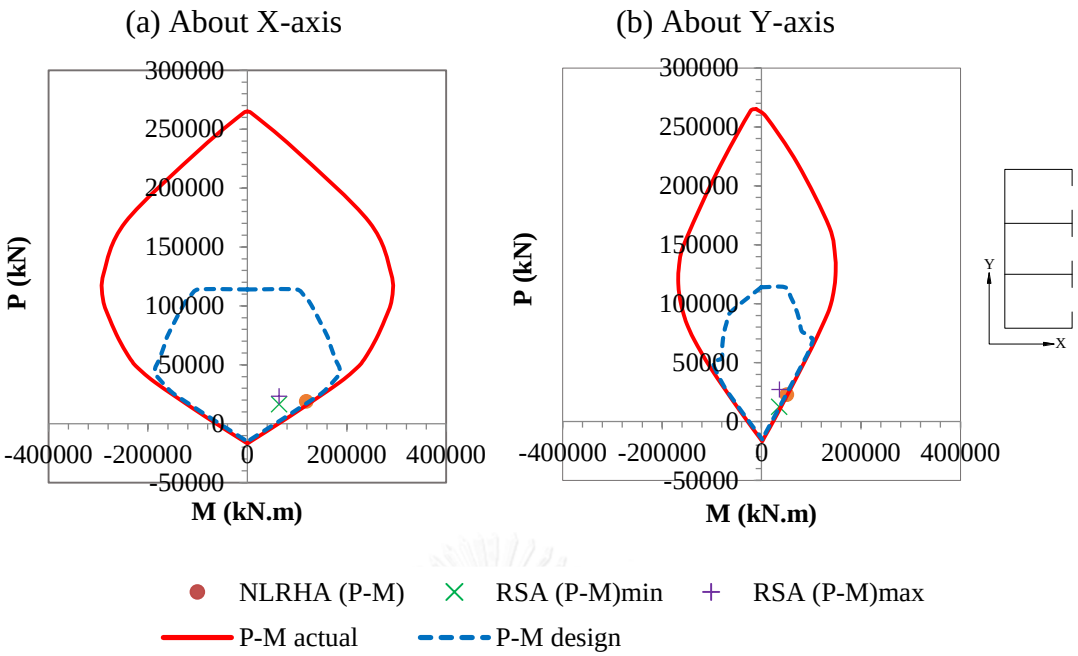

Figure 6.15 Comparison of actual and design P-M interaction diagram of 15-story core wall: (a) about X-axis and (b) about Y-axis.

6.3.2 Shear, bending moment and story drift along the height of structure

❖ Shear force of core wall

Shear forces along the height of 5- to 25-story core walls determined by NLRHA and RSA procedure are plotted in Figure 6.16 for both in Bangkok and Chiang Mai. It is found that shear demands determined by NLRHA are much larger than the design shear forces from RSA procedure along the height of core walls. The shear amplification in Y direction (cantilever walls) is smaller around mid-height of the core wall where the contribution from higher modes is smaller than that at the base of core wall. The shear amplification in X direction (coupled walls) is less than that in Y direction and rather uniform along the height of core wall for taller buildings (20- and 25-story).

(a) 5-story

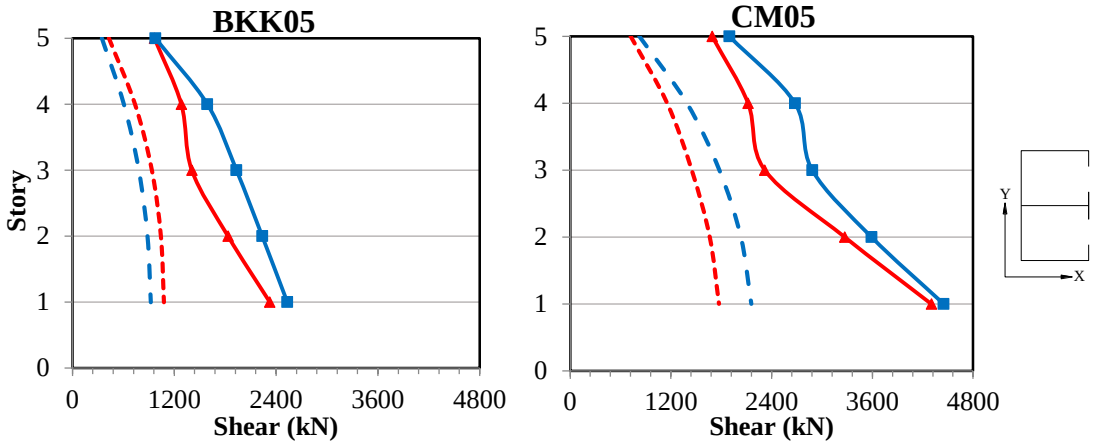

(b) 10-story

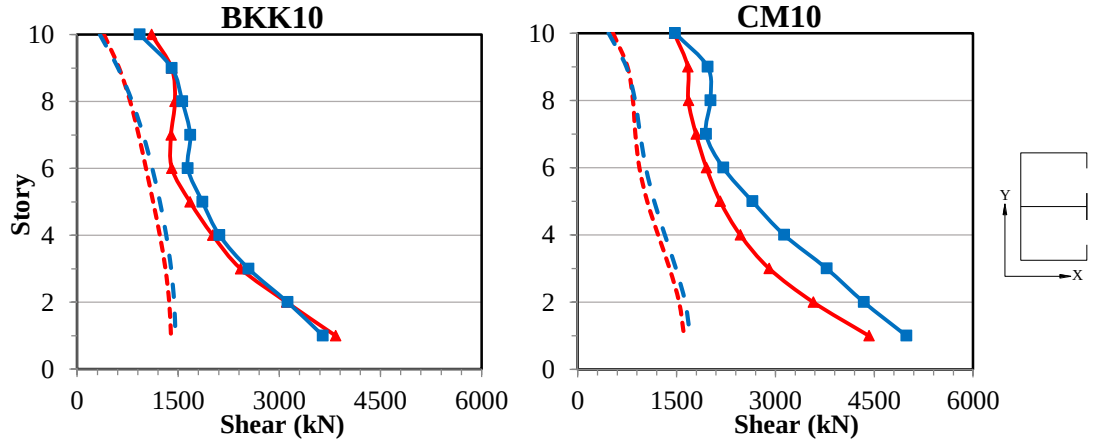

(c) 15-story

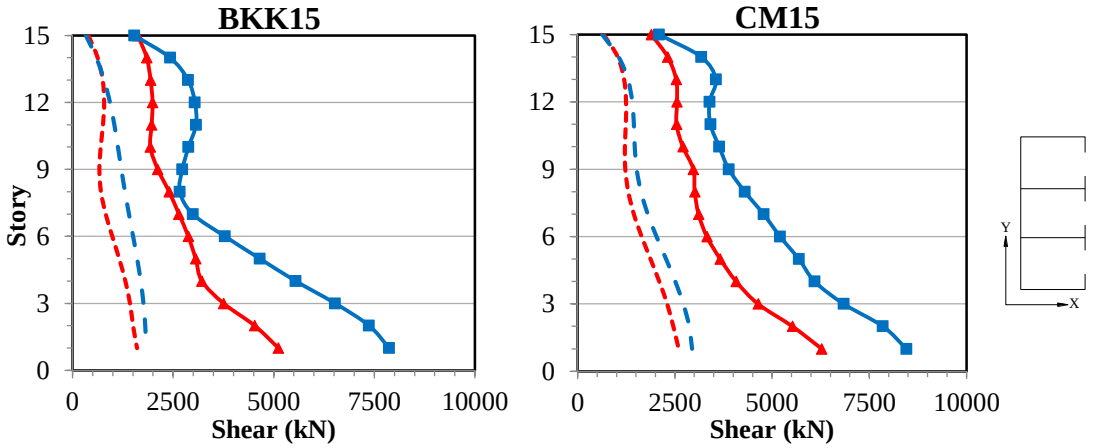

(d) 20-story

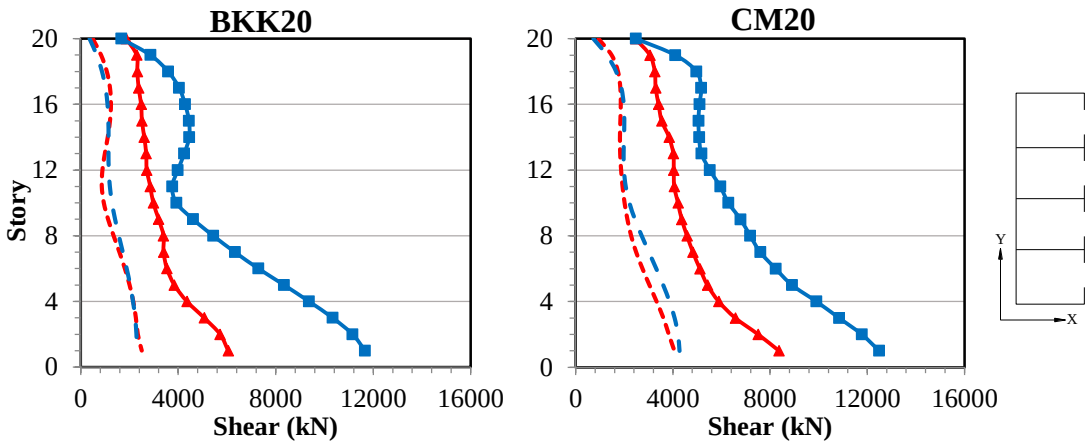

(e) 25-story

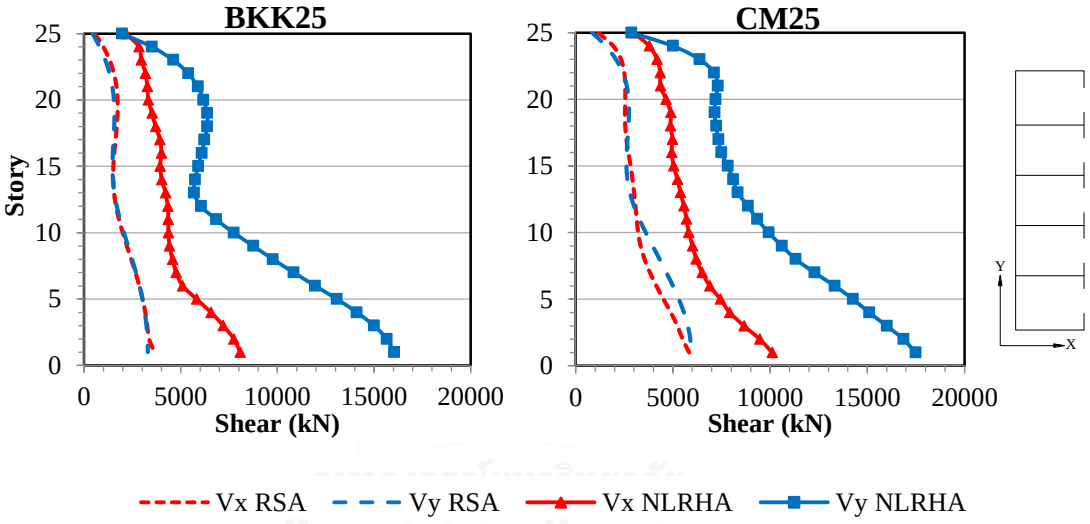

Figure 6.16 Comparison of shear forces along the height of core walls obtained from RSA procedure and NLRHA: (a) 5-story; (b) 10-story; (c) 15-story; (d) 20-story and (e) 25-story.

❖ **Bending moment of core wall**

Bending moments along the height of 5- to 25-story core walls determined by NLRHA and RSA procedure are plotted in Figure 6.17 for both in Bangkok and Chiang Mai. The results demonstrated that bending moment demands determined by NLRHA are much larger than the design moments computed by RSA procedure, significantly for taller buildings. However, designing flexural strengths of core walls by using flexural demands from RSA procedure does not mean that flexural failure occurs in core wall because these large bending moments from NLRHA are mainly due to

different axial load and flexural over-strength, as explained in base moment amplification above. The moment amplification of core wall is smaller in coupled direction because the flexural demands in that direction govern the design of core wall.

(a) 5-story

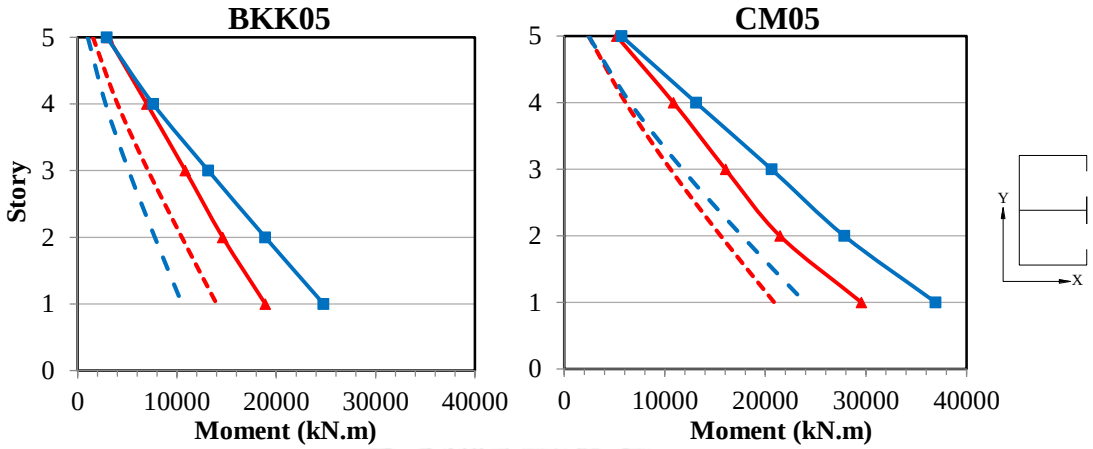

(b) 10-story

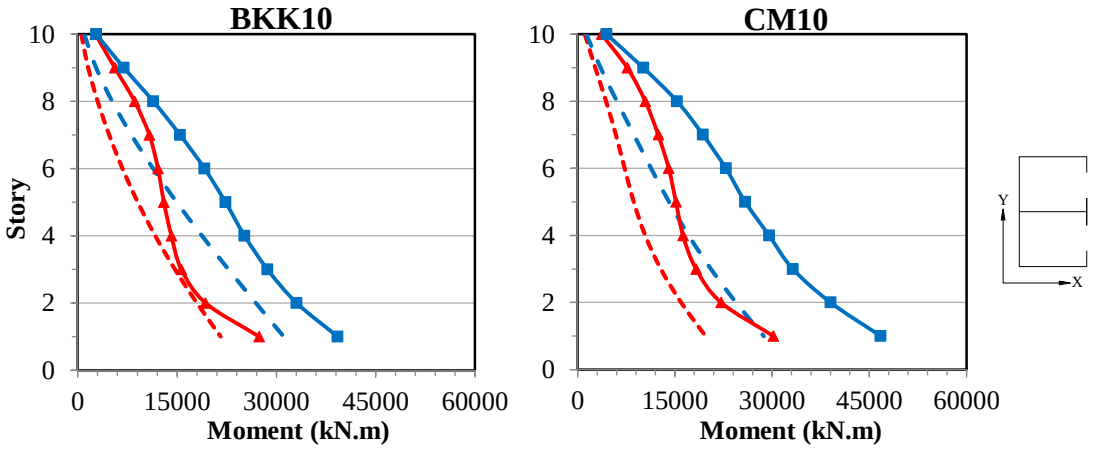

(c) 15-story

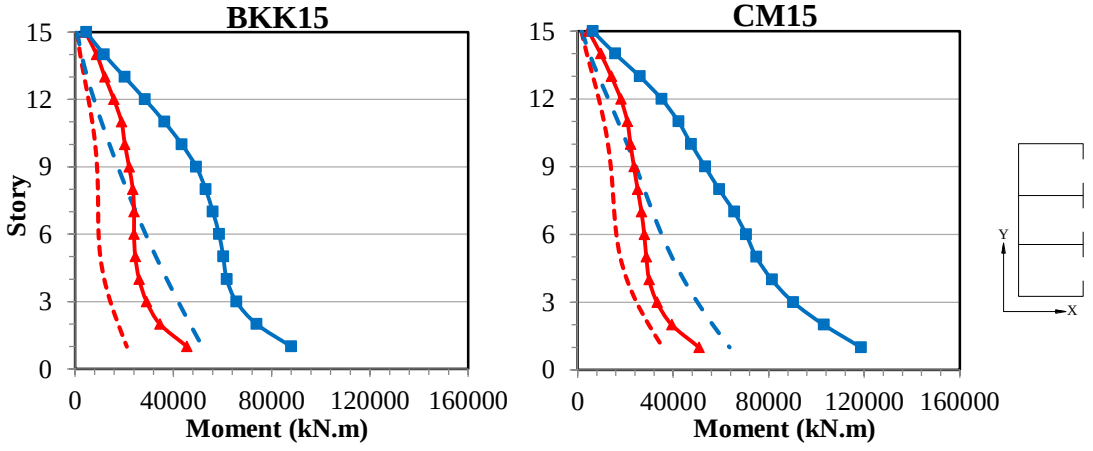

(d) 20-story

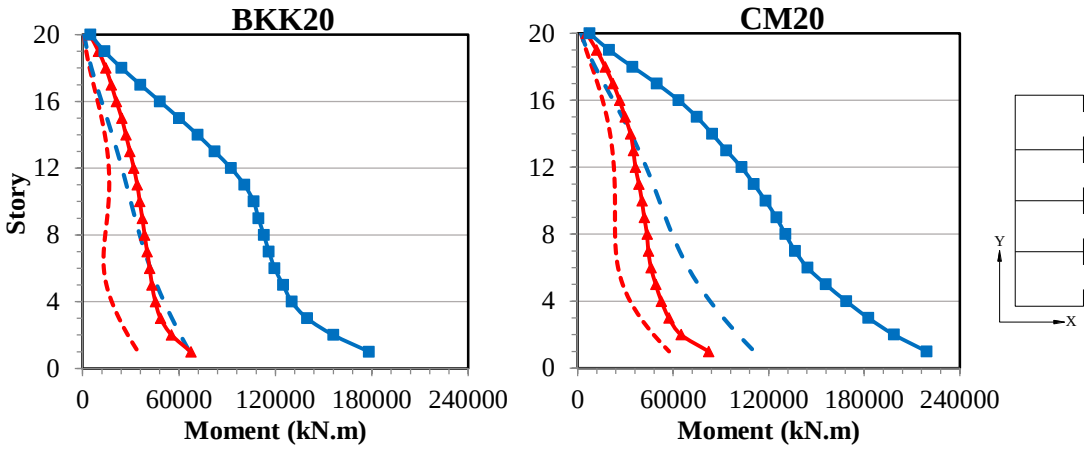

(e) 25-story

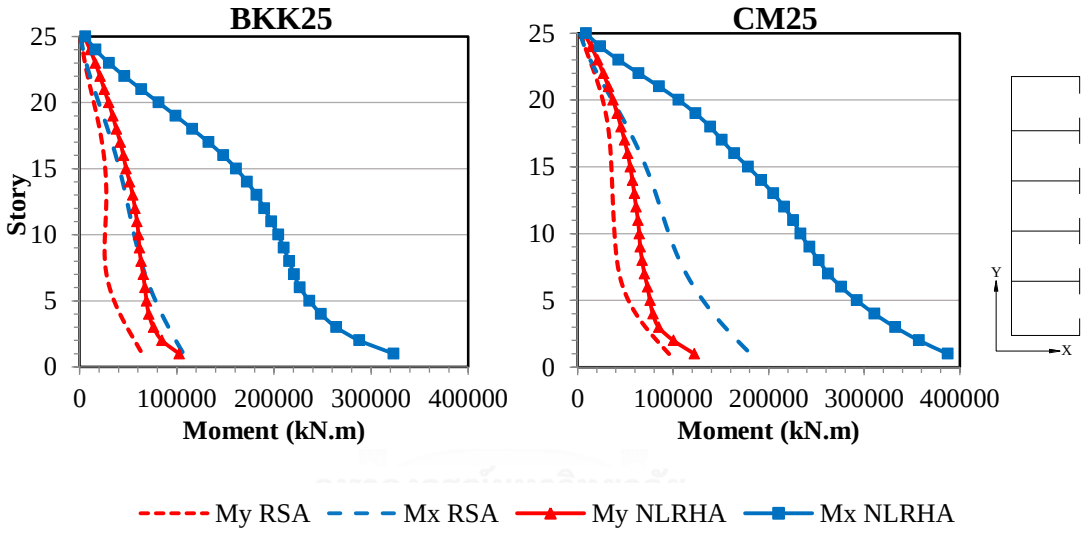

Figure 6.17 Comparison of bending moments along the height of core walls obtained from RSA procedure and NLRHA: (a) 5-story; (b) 10-story; (c) 15-story; (d) 20-story and (e) 25-story.

❖ **Story drift**

ASCE 7-10 employs deflection amplification factor (C_d) to multiply the story drift from linear analysis after reducing the elastic spectrum by response modification factor (R). The factor C_d in this standard is not larger than the factor R expecting that inelastic story drift is always smaller than elastic story drift. However, NLRHA results show that inelastic story drifts are larger than elastic story drifts computed from linear response history analysis (LRHA) and linear response spectrum analysis (LRSA), while

those computed by ASCE 7 procedure are the smallest (Figure 6.18). Therefore, elastic story drifts are more accurate than those obtained by ASCE 7 procedure. The difference of elastic story drifts from LRSA and LRHA is theoretically due to the different modal combinations used in both methods of analysis. Consequently, story drifts determined by NLRHA are larger than those computed by ASCE 7 procedure for all buildings as shown in Figure 6.19. However, all the story drift demands are still below the allowable limit which is 1.5%.

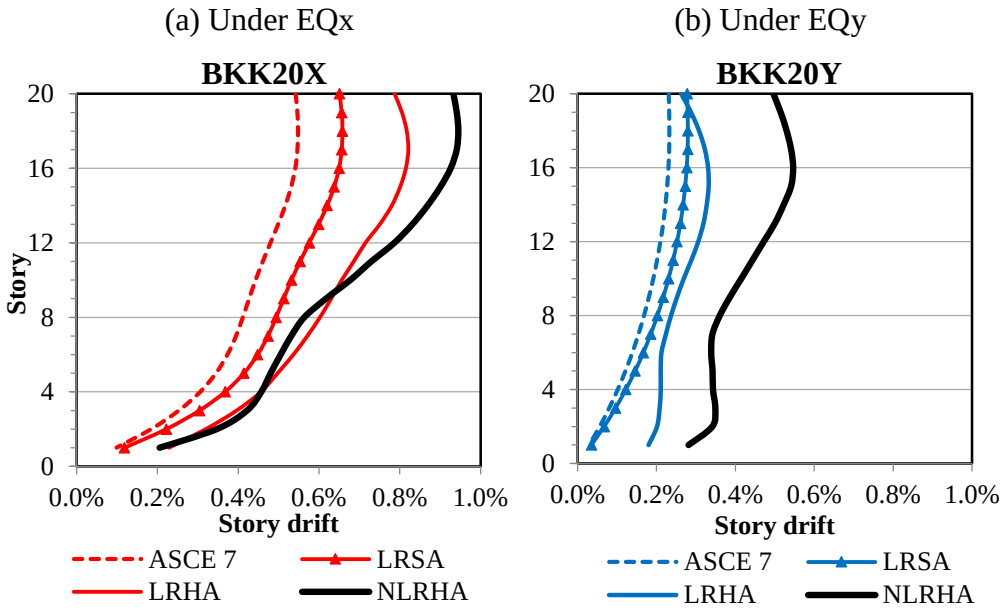

Figure 6.18 Comparison of story drifts obtained from ASCE 7-10, NLRHA, LRHA and LRSA: (a) under EQx and (b) under EQy.

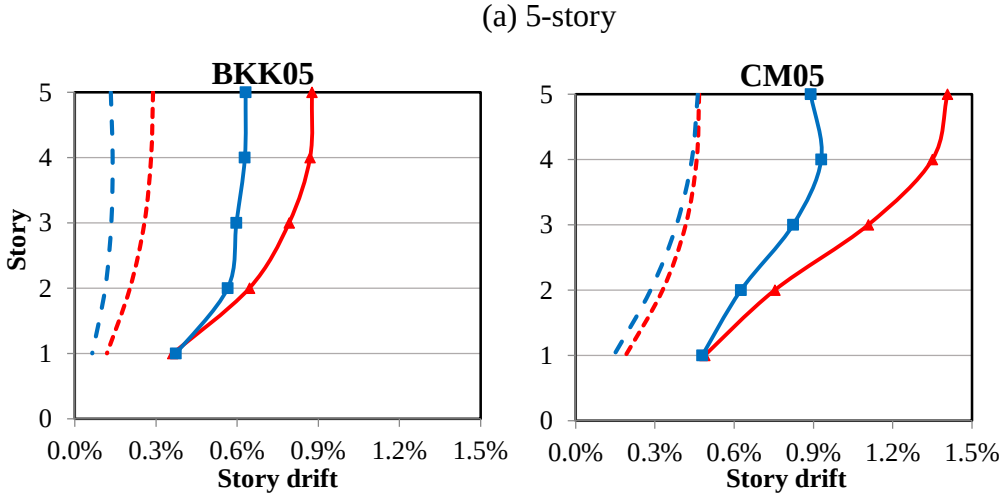

(b) 10-story

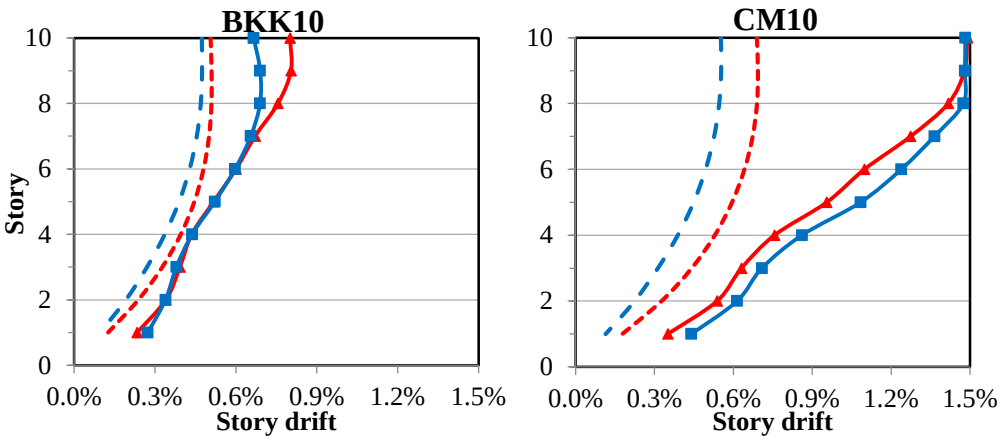

(c) 15-story

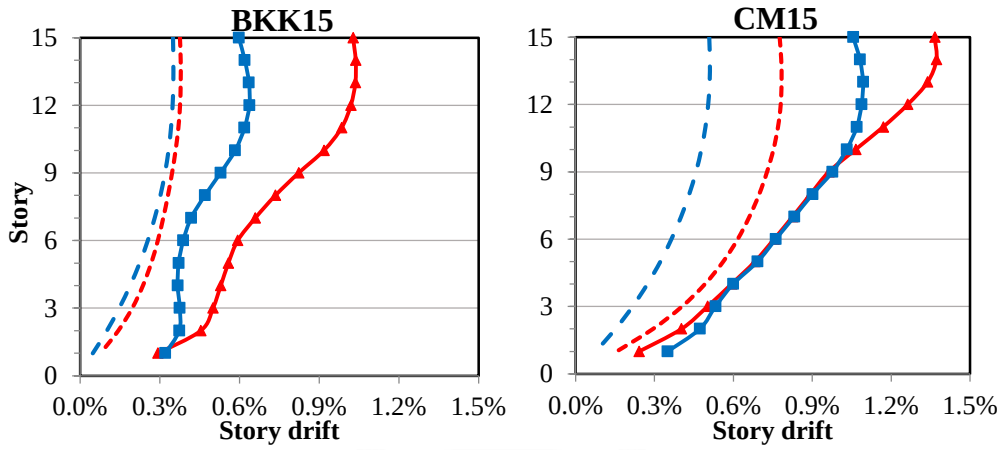

(d) 20-story

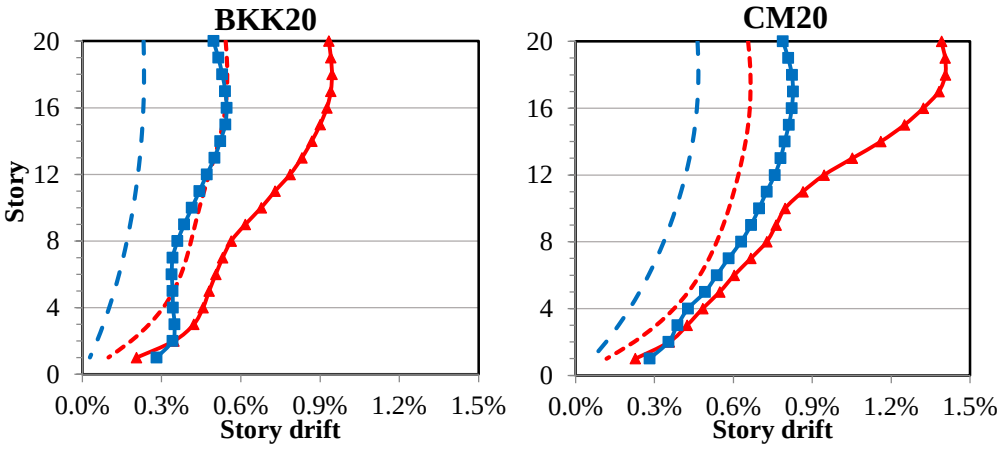

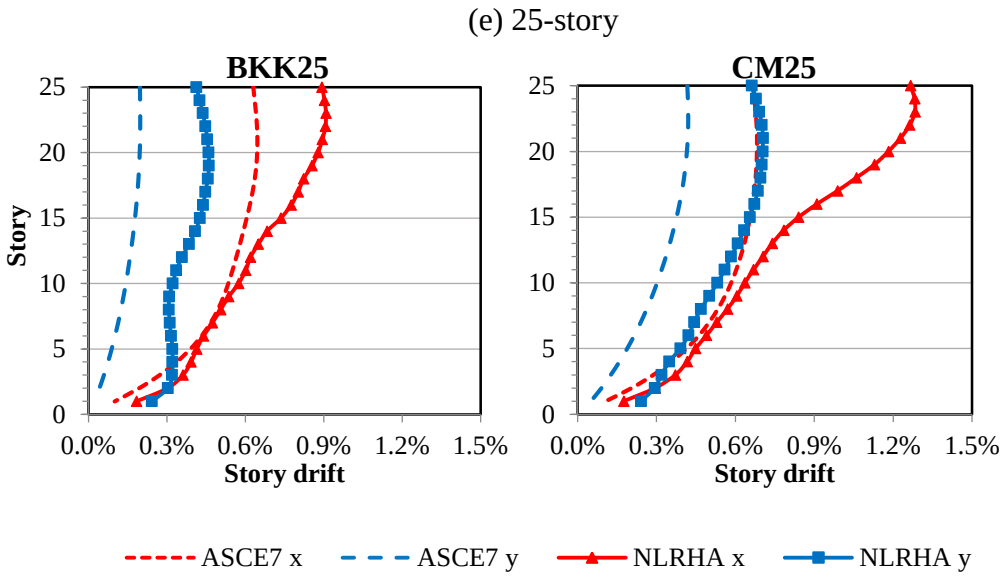

Figure 6.19 Comparison of story drifts obtained from ASCE 7-10 and NLRHA: (a) 5-story; (b) 10-story; (c) 15-story; (d) 20-story and (e) 25-story.

6.4 Evaluation of accuracy of various codes and previous researchers' formulas

The shear forces of core walls determined from various codes and previous researchers' formulas are taken to compare with those obtained from NLRHA in this study. To reasonably compare, the seismic force reduction factor, flexural over-strength at the base of the wall and other relevant parameters required for each formula are taken the same as those used in this study as described below:

For NZS, V_E was taken equal to the already scaled shear force from RSA and ϕ_o was equal to BFOS for computing base shear force of the wall. For Paulay and Priestley (1992), μ_Δ was considered to be the same as R_{eff}.

For EC8, q was considered equal to R_{eff} and $\gamma_{Rd}M_{Rd}/M_{Ed}$ was taken the same as BFOS. For Priestley (2003), the inelastic first mode shear force, V_{1i}, was taken the same as the first mode shear of Calugaru and Panagiotou (2012) as defined here by $V_{1i} = \gamma_w V_{1Ei}/R_{eff}$ where γ_w was equal to BFOS. For Rutenberg and Nsieri (2006), q was taken equal to R_{eff}. For Rejec et al. (2012), $m(z)$ was taken from Figure 2.5, q and $\gamma_{Rd}M_{Rd}/M_{Ed}$ were the same as those used in EC8's formula.

For CSA, $R_d R_o$ was taken equal to R_{eff} and "the ratio of base probable moment capacity to the base factored moment obtained from RSA" was taken equal to BFOS. For Yathon (2011), R_d was assumed equal to R_{eff}. For Boivin and Paultre (2012), $\left(M_p/M_f\right)_{base}$ was equal to BFOS. For Luu et al. (2014), γ_w was equal to BFOS and their proposed equation was assumed to be applicable for 20- and 25-story building in X direction even though its fundamental periods were greater than 3.5 second.

6.4.1 Base shear amplification of core wall

The base shear amplification (BSA) here is defined as the ratio between base shear force from NLRHA (or the already-amplified design shear force from various codes and previous researcher's formula) and the design shear force from RSA procedure. It should be noted that the design shear force of some researchers (Rutenberg and Nsieri 2006, Rejec et al. 2012) was amplified by different shear force while some others (Priestley 2003, Yathon 2011, Calugaru and Panagiotou 2012) proposed formula to determine the design shear force directly as described in Chapter 2. The mean value (mean) of BSA from NLRHA is presented along with mean plus and minus one standard deviation (mean±s) to show the variability of the shear amplification among different ground motions.

6.4.1.1 Various codes

Design shear forces of the walls computed from three seismic design codes: EC8, CSA and NZS as described in Chapter 2 are taken into comparison with shear demands determined from NLRHA in this study as shown in Figure 6.20. EC8 provides better results than other codes in Bangkok; although it slightly underestimates BSA in cantilever direction for 20- and 25-story core walls (Figure 6.20b). EC8 is quite conservative in Chiang Mai (Figure 6.20c and Figure 6.20d). CSA underestimates BSA in Bangkok, significantly in cantilever direction of core wall but it instead provides better results than other codes in Chiang Mai, even though it is a little bit underestimation in some buildings. NZS is much overestimation of BSA for most of the cases.

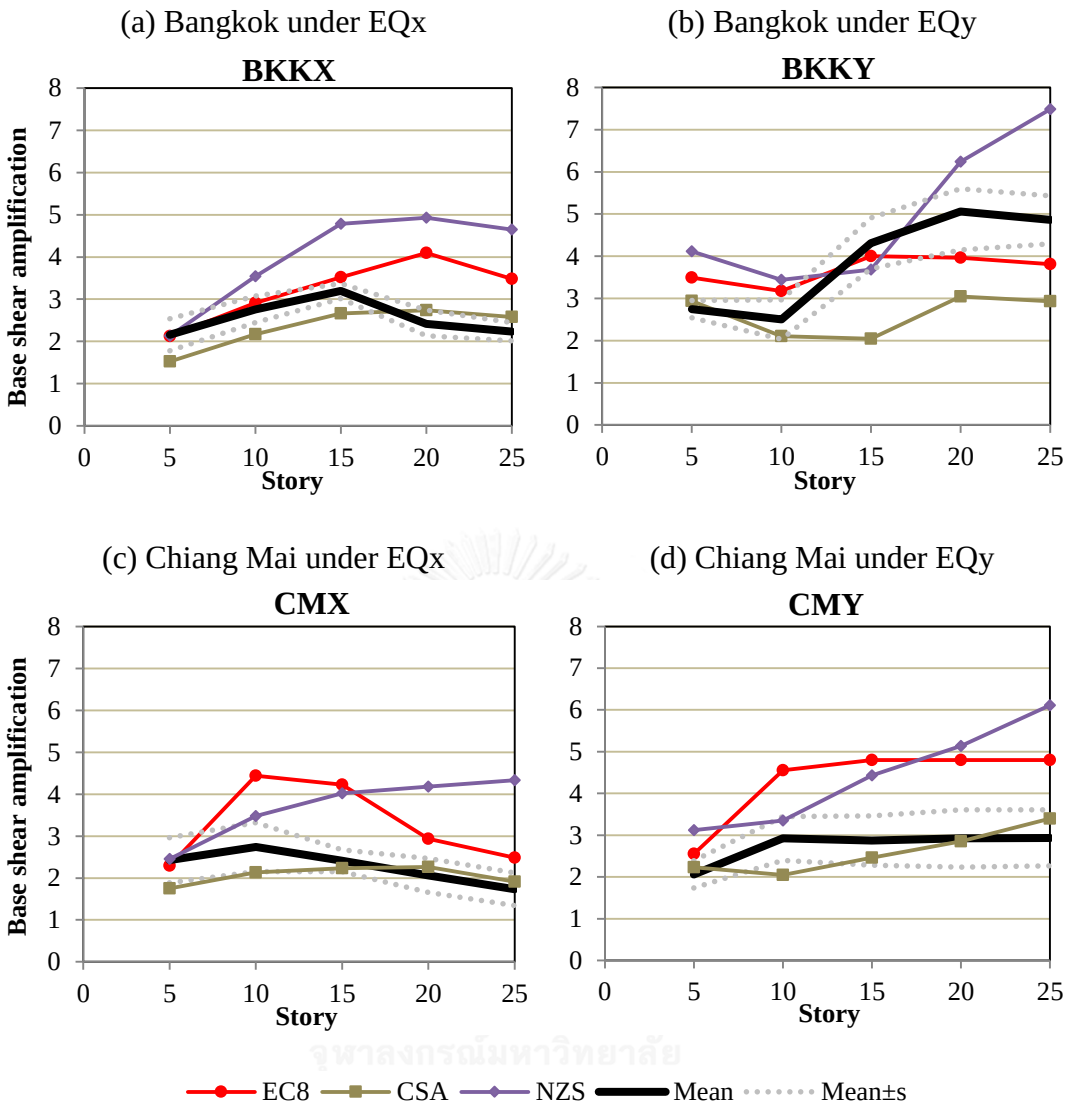

Figure 6.20 Comparison of BSA from NLRHA in this study and various codes: (a) Bangkok under EQx; (b) Bangkok under EQy; (c) Chiang Mai under EQx and (d) Chiang Mai under EQy.

6.4.1.2 Previous researchers' formulas

Design shear forces of the walls estimated from equations of three different groups of researchers (Group of EC8, Group of CSA and Group of NSZ) as described in Chapter 2 are compared with the shear demands obtained from NLRHA in this study. The MMRSA of Calugaru and Panagiotou (2012) is excluded in the comparison because it is not belong to any of the three groups and it is very similar to MMS method

of Priestley (2003). It should be noted that all the formulas in the comparison here are proposed for cantilever walls. They are not developed for coupled walls.

For group of EC8 (Figure 6.21), Rejec et al. (2012) provides a better agreement with base shear amplifications of core walls from this study than other researchers in cantilever direction (Figure 6.21b and Figure 6.21d), even though it is slightly conservative in Chiang Mai. For coupled direction (Figure 6.21a and Figure 6.21c), none of them could well predict the BSAs comparing to this study's results, as they always overestimate significantly for taller buildings.

Fro group of CSA (Figure 6.22) in the case of Bangkok, all of them considerably underestimate base shear amplifications in cantilever direction of core walls of taller buildings (Figure 6.22b) but they could estimate BSAs quite well in coupled direction of core walls (Figure 6.22a). In the case of Chiang Mai (Figure 6.22c and Figure 6.22d), all of them provide good comparable results with this study, among which Luu et al. (2014) could lead to the most accurate results in both directions of core walls.

For group of NZS (Figure 6.23), none of them could provide good comparison with this study, as they are underestimation of BSAs in cantilever direction of core walls in Bangkok (Figure 6.23b) and they are overestimation in the other cases.

❖ **Group of EC8**

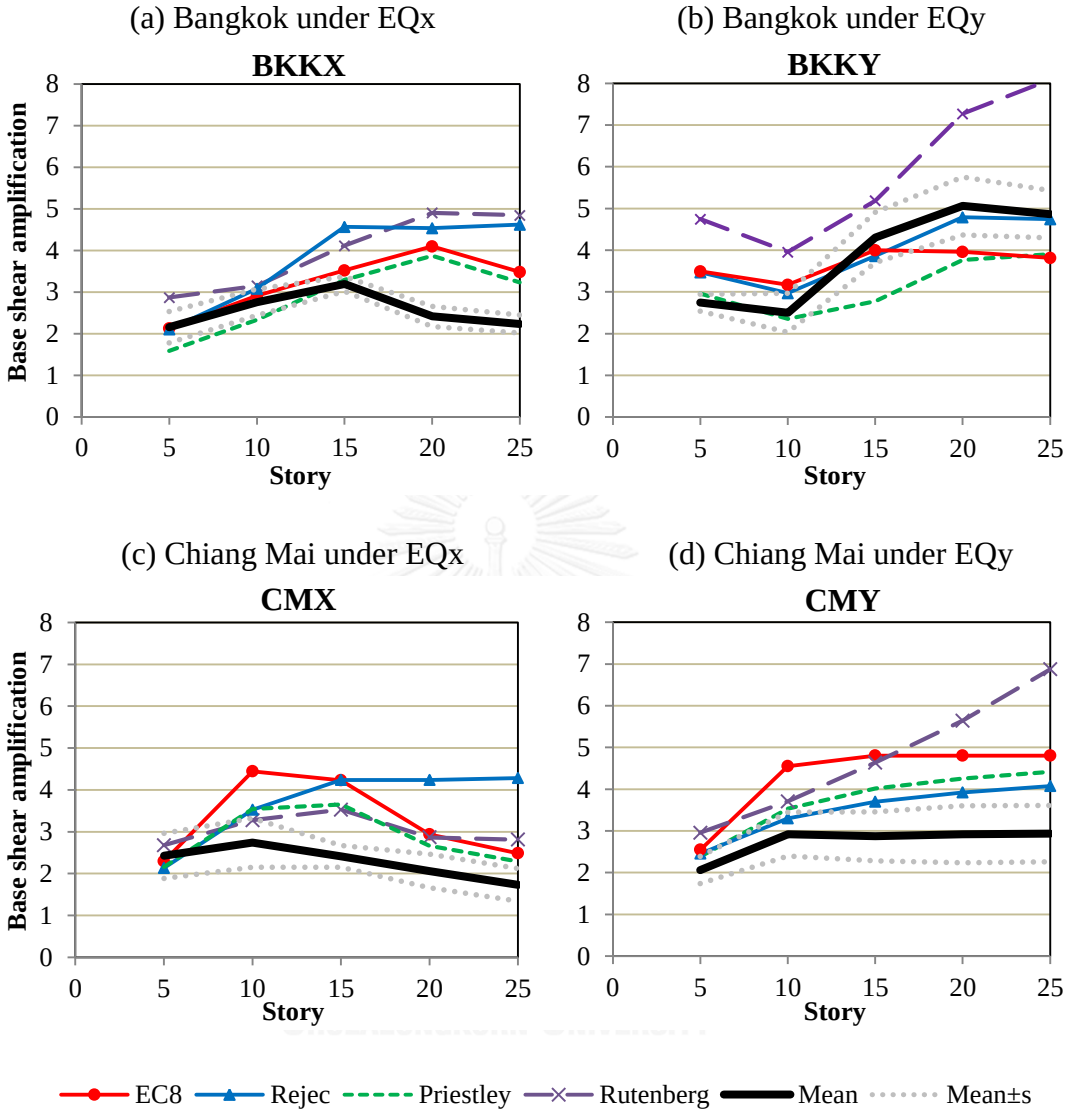

Figure 6.21 Comparison of BSA from NLRHA in this study and group of EC8: (a) Bangkok under EQx; (b) Bangkok under EQy; (c) Chiang Mai under EQx and (d) Chiang Mai under EQy.

❖ **Group of CSA**

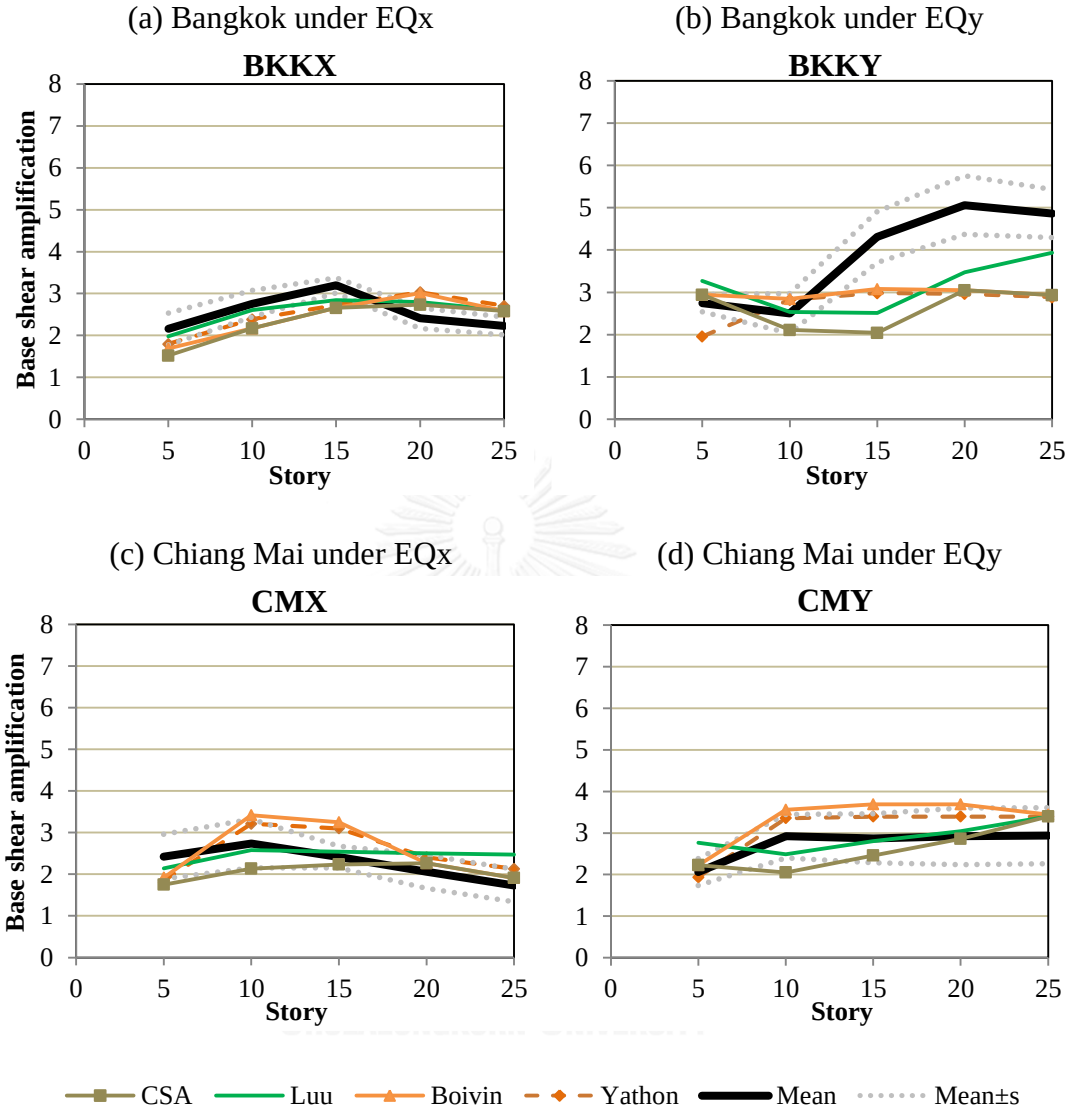

Figure 6.22 Comparison of BSA from NLRHA in this study and group of CSA: (a) Bangkok under EQx; (b) Bangkok under EQy; (c) Chiang Mai under EQx and (d) Chiang Mai under EQy.

❖ **Group of NZS**

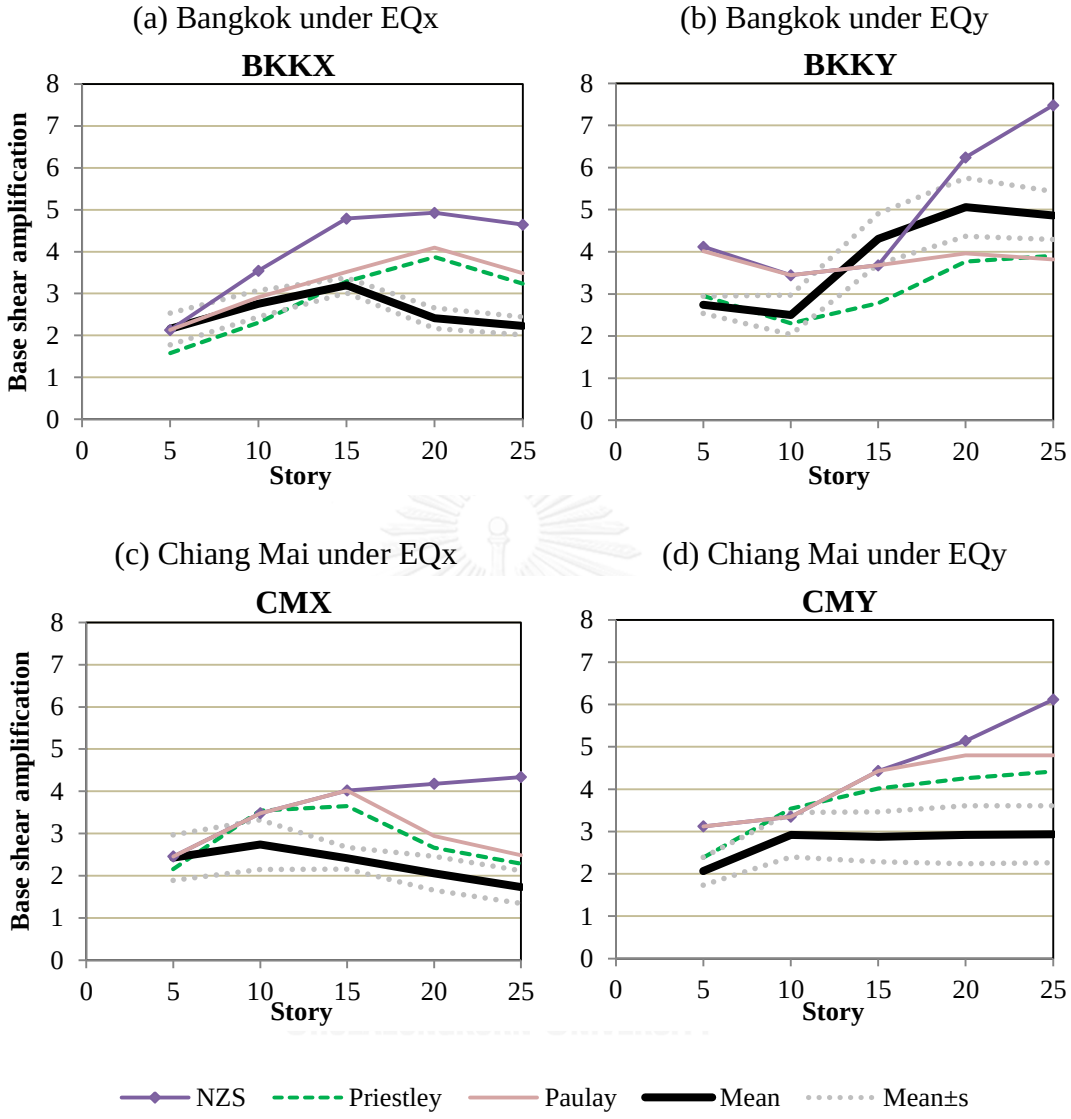

Figure 6.23 Comparison of BSA from NLRHA in this study and group of NZS: (a) Bangkok under EQx; (b) Bangkok under EQy; (c) Chiang Mai under EQx and (d) Chiang Mai under EQy.

6.4.2 Shear force along the height of core wall

Shear forces along the height of the 15- to 25- story core walls predicted by EC8, Priestley (2003), Rejec et al. (2012) and Luu et al. (2014)'s formulas are compared to the shear demands determined by NLRHA in this study. The mean value (mean) of shear demands from NLRHA is presented along with mean plus and minus one standard deviation (mean±s).

For Bangkok (Figure 6.24) in cantilever direction (EQy), Rejec et al. (2012)'s formula can well estimate the shear forces along the height of the core walls, while other formulas underestimate the shear forces of core walls at lower stories. In coupled direction (EQx), Luu et al. (2014)'s envelop can well follow the variation of shear forces along the height of core walls, whereas other formulas largely overestimate shear forces along the height of core walls.

For Chiang Mai (Figure 6.25), Luu et al. (2014)'s formula provides the best estimation of shear forces along the height of core walls in both directions, while other formulas over-predict significantly shear forces at the base of core walls.

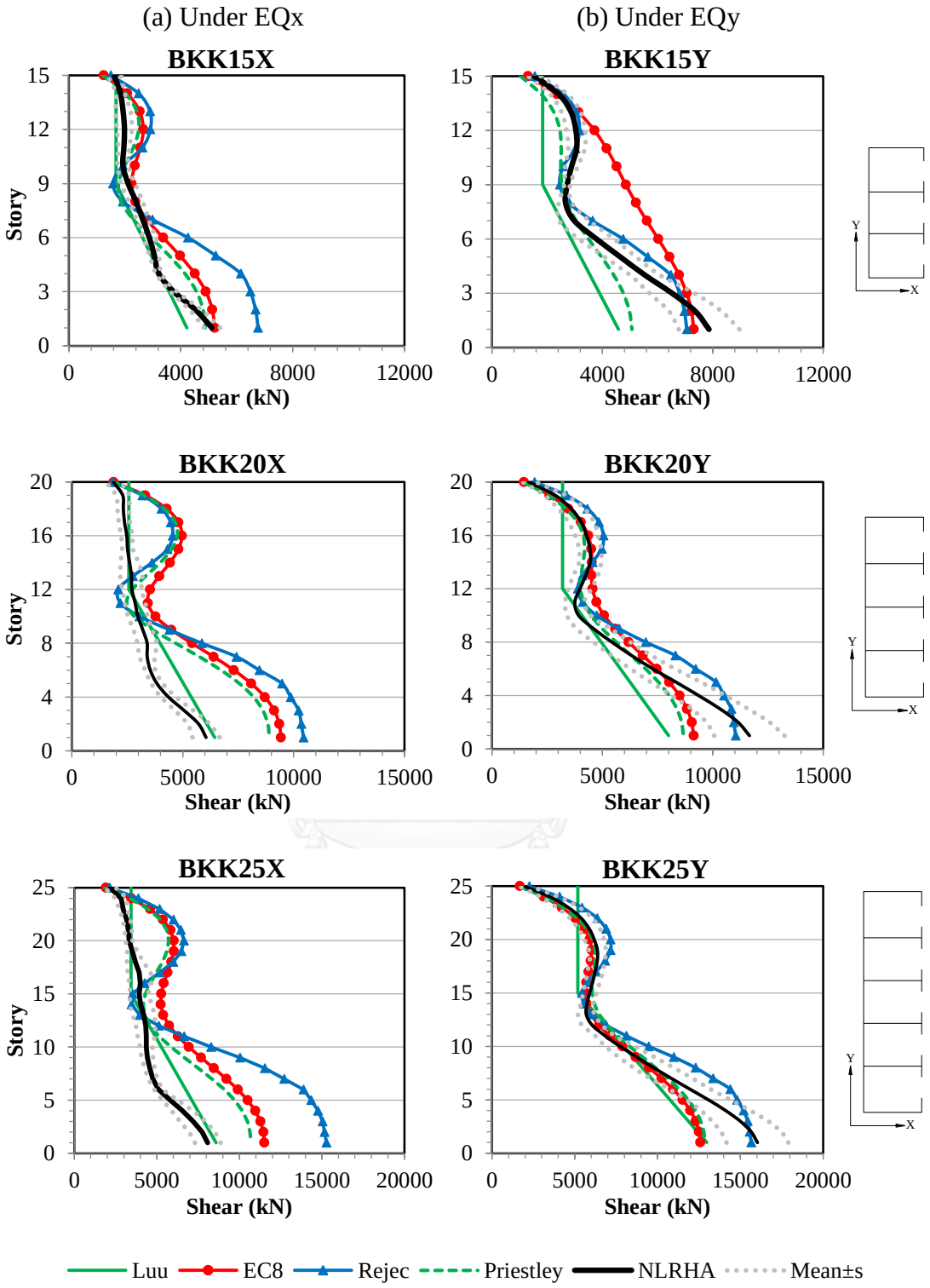

Figure 6.24 Comparison of shear forces along the height of core walls from NLRHA in this study and previously proposed formulas in Bangkok: (a) under EQx and (b) under EQy.

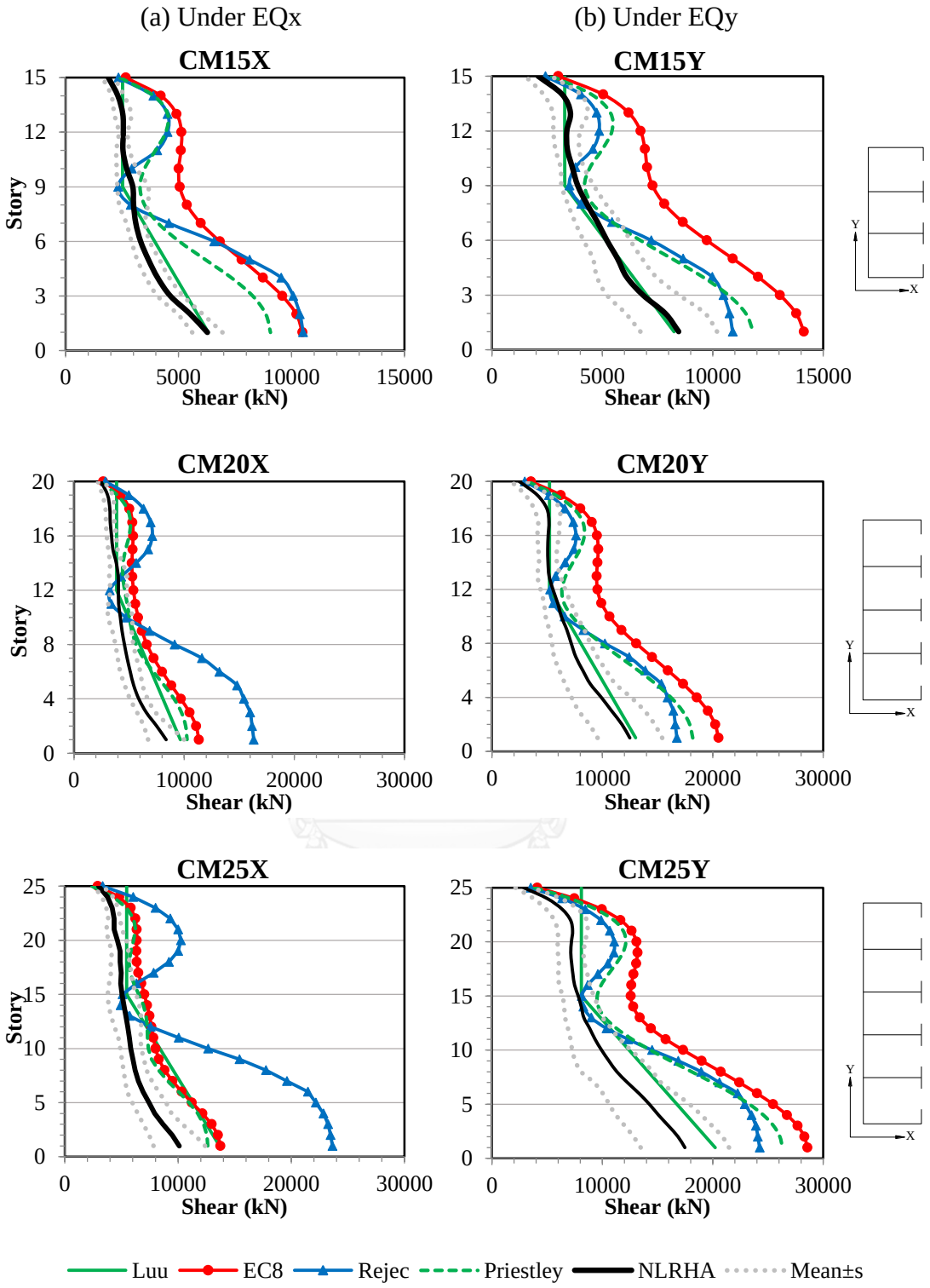

Figure 6.25 Comparison of shear forces along the height of core walls from NLRHA in this study and previously proposed formulas in Chiang Mai: (a) under EQx and (b) under EQy.

6.5 Sensitivity effects of flexural over-strength on shear demands of core walls

In practice, the structures are designed to have flexural strength much stronger than required by design. This extra strength is recognized as flexural over-strength inherent in the design. However, this flexural over-strength can increase shear forces of the structures. Therefore, its sensitivity effects on shear demands of core walls are investigated in this section. The followings are considered:

- Uniform vertical reinforcing ratio of core wall is used for all stories.
- Three different ratio of uniform vertical reinforcement assigned in core walls are used, which are taken equal to 50%, 100% and 150% of the reinforcing ratio at the base of core walls designed from RSA procedure as indicated by U50%, U100% and U150%, respectively in Figure 6.26.
- Coupling beam strengths are kept the same.
- All walls are allowed to yield at any location along the height of the building.

Using uniform reinforcing ratio (U100%) along the height of core wall leads to slightly increase of base shear amplifications of core walls comparing to non-uniform reinforcing ratio (N100%) which was the structures presented up to this section. Using U100% has little effect for taller buildings (20-and 25-story), as shown in Figure 6.27. Using U100% provides a little bit larger shear force along the height of core wall than N100% as illustrated in Figure 6.28. These results come from the case in Chiang Mai while there is no influence for the case in Bangkok because most core walls require minimum reinforcements that are already uniform along the height of core wall.

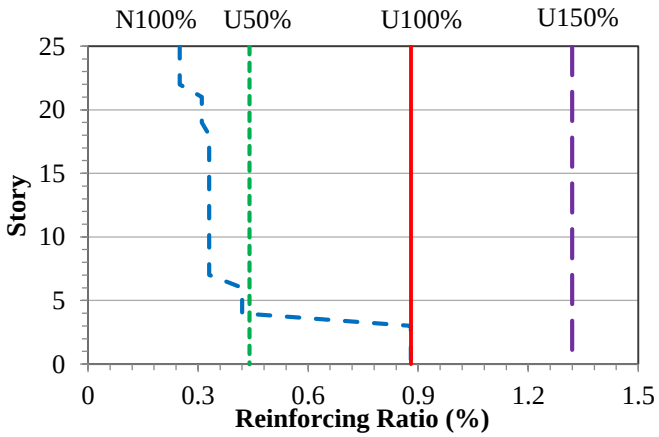

Figure 6.26 Reinforcing ratios of core wall in 25-story building.

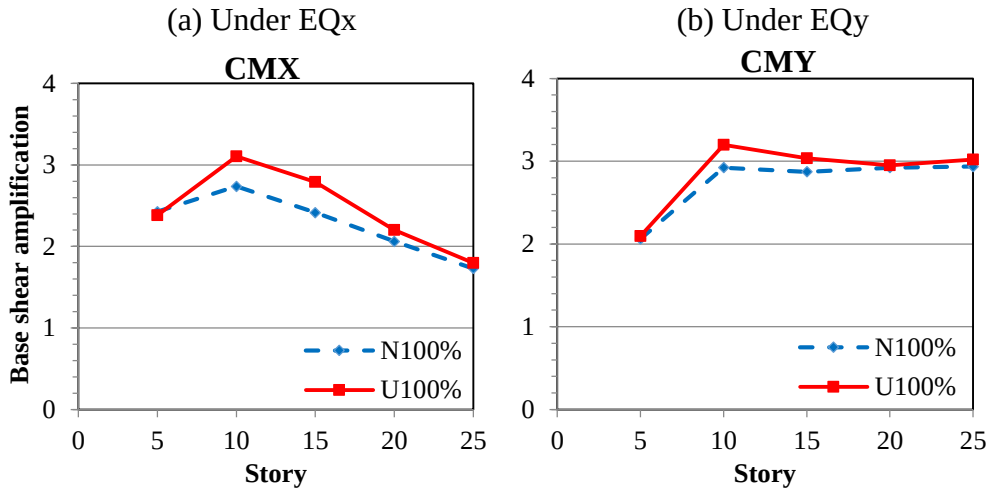

Figure 6.27 Comparison of BSA obtained from NLRHA by using non-uniform and uniform reinforcement: (a) under EQx and (b) under EQy.

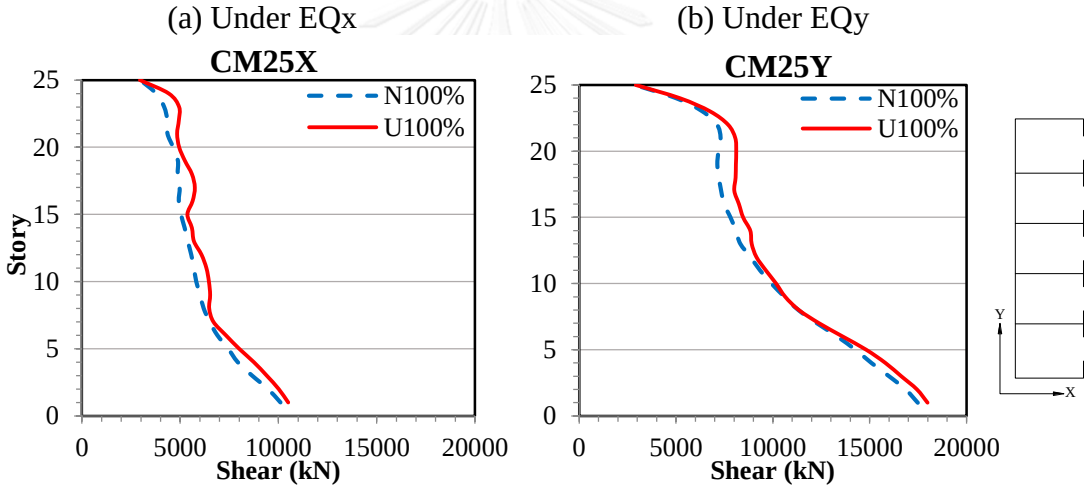

Figure 6.28 Comparison of shear force along the height of core wall from NLRHA by using non-uniform and uniform reinforcement: (a) under EQx and (b) under EQy.

Base shear amplification (BSA) is increased with increasing of base flexural over-strength (BFOS) of core walls for all buildings in both directions (Figure 6.29). The significant influence of BFOS on BSA is indicated by the slope of BSA as summarized in Table 6.5 . The larger slope means larger influence. The slopes of BSA in coupled direction (EQx) are larger than those in cantilever direction (EQy). This infers that BFOS has less effect on BSA in cantilever direction. The slopes of BSA in 5- to 15-story core walls are larger than those in 20- to 25-story core walls indicating that BFOS has larger influence on BSA in shorter buildings than in taller buildings. As

shown in Figure 6.30, increasing of reinforcing ratios of core wall has only little influence on shear force along the height of core wall in 25-story building.

Table 6.5 Slope of BSA due to increasing of BFOS of core wall.

No. story	Slope of base shear amplification (%)	
	Under EQx	Under EQy
5	0.27	0.33
10	0.62	0.32
15	0.65	0.35
20	0.34	0.16
25	0.20	0.13

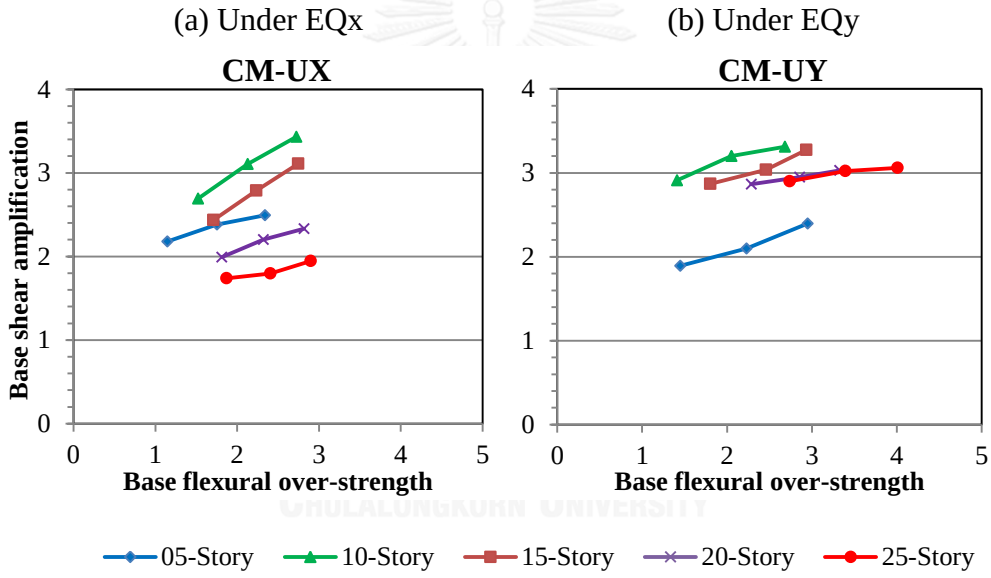

Figure 6.29 Effect of BFOS on BSA of core wall: (a) under EQx and (b) under EQy.

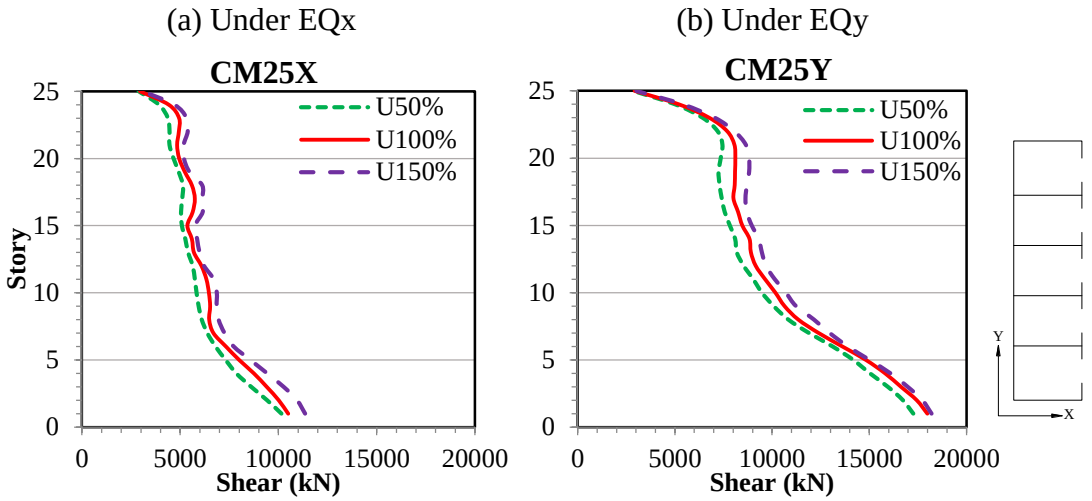

Figure 6.30 Comparison of shear force along the height of core wall from NLRHA by using three different reinforcing ratios: (a) under EQx and (b) under EQy.

6.6 Effects of elastic wall in upper stories on seismic demands of the structure

All the results presented above are based on the design concept that flexural strengths of the walls in every story are designed according to the flexural demands of the walls determined from RSA procedure. Hence, the walls can yield at any location along the height of the building. This design concept is named as distributed plastic hinge (DPH) of the walls. However, in another design concept, the walls in upper stories are provided enough strength to prevent any yielding in upper stories and yielding is allowed to occur only at the base of the walls. This design concept is defined as single plastic hinge (SPH) of the walls. The effects of elastic walls in upper stories on seismic demands of the structure are investigated here.

For SPH in this study, yielding can only occur at the first-story core wall and all coupling beams along the height of the building. The demands obtained from SPH of core wall are compared with those determined from DPH which were the results presented in Section 6.3. The flexural strengths of 25-story core wall about X-axis for SPH and DPH are indicated in Figure 6.31 as example of the difference between SPH and DPH modeling concept. Only the results of 20- and 25-story buildings in the case of Chiang Mai are discussed here.

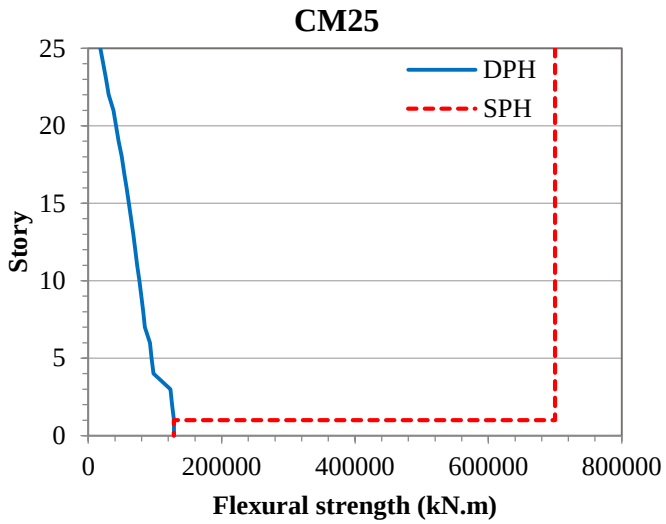

Figure 6.31 Flexural strength of core wall in DPH and SPH design concept.

Designing the walls in upper stories to remain elastic could lead to increase of base shear amplification (BSA) in coupled direction of core wall in about 1.4 times comparing to BSA obtained from DPH design concept (Figure 6.32a) but this has little influence on BSA in cantilever direction of core wall (Figure 6.32b). SPH results in significantly larger shear forces than DPH at upper stories in both directions of core wall (Figure 6.33).

Preventing the walls from yielding in upper stories causes significantly large bending moment at mid-height of core wall in both directions (Figure 6.34). This large bending moment at the mid-height is closed to the bending moment at the base of core wall. Hence, designing the mid-height walls to behave elastic requires excessive vertical reinforcement. The bending moments at mid-height of core wall from SPH are considerably larger than those from DPH because bending moment demands from DPH are limited by flexural strengths of core wall as indicated in Figure 6.31. At the base of core wall, there are not much difference of bending moments computed from SPH and DPH because core walls could easily yield, and then bending moment demands are limited by flexural strengths of core wall.

Designing the walls in upper stories to behave elastic results in decreasing of story drifts at upper stories (Figure 6.35). The roof drifts from SPH could reduce up to about 30% comparing to those from DPH where the wall in upper stories could yield at any level of the building. While at lower stories near the base, story drifts from SPH

are slightly larger than those from DPH. These kinds of differences between story drifts from SPH and DPH come from the fact that elastic story drifts are smaller than inelastic story drifts as discussed in Section 6.3.2.

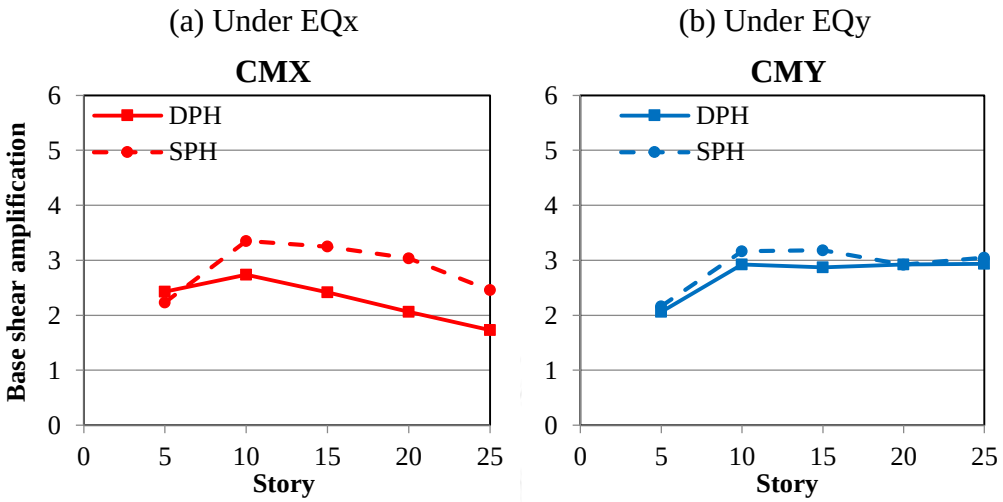

Figure 6.32 Comparison of base shear amplifications of core walls obtained from NLRHA for SPH and DPH design concepts: (a) under EQx and (b) under EQy.

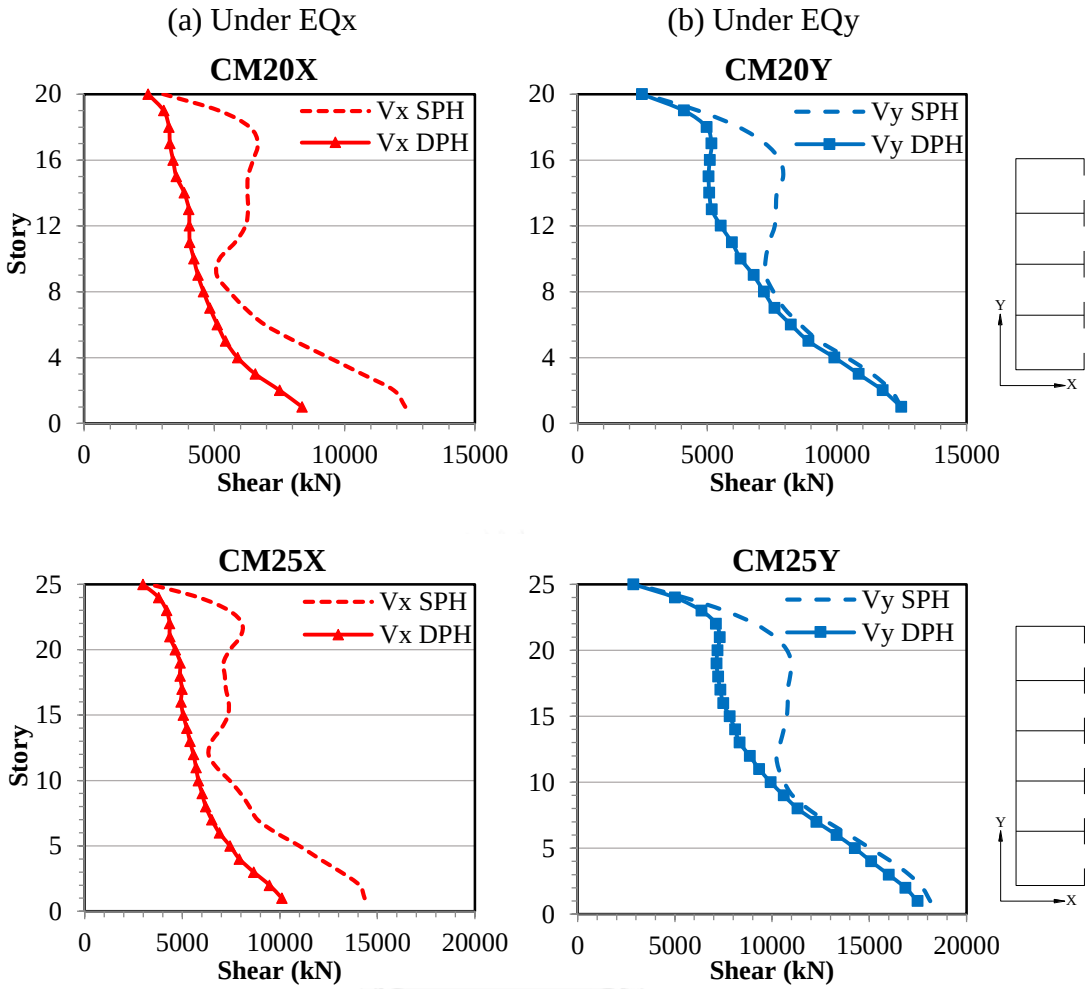

Figure 6.33 Comparison of shear demands of core walls obtained from NLRHA for SPH and DPH design concepts: (a) under EQx and (b) under EQy.

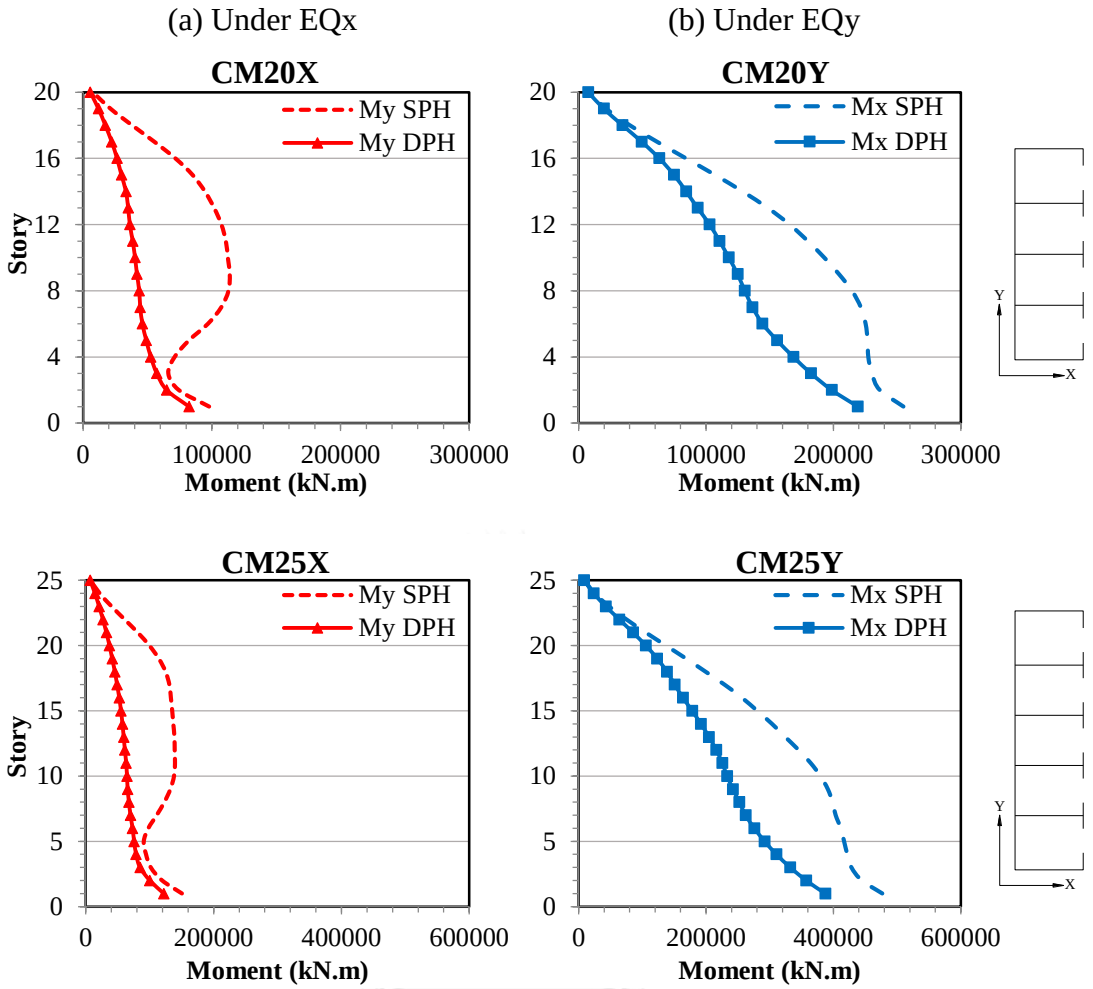

Figure 6.34 Comparison of bending moment demands of core walls obtained from NLRHA for SPH and DPH design concepts: (a) under EQx and (b) under EQy.

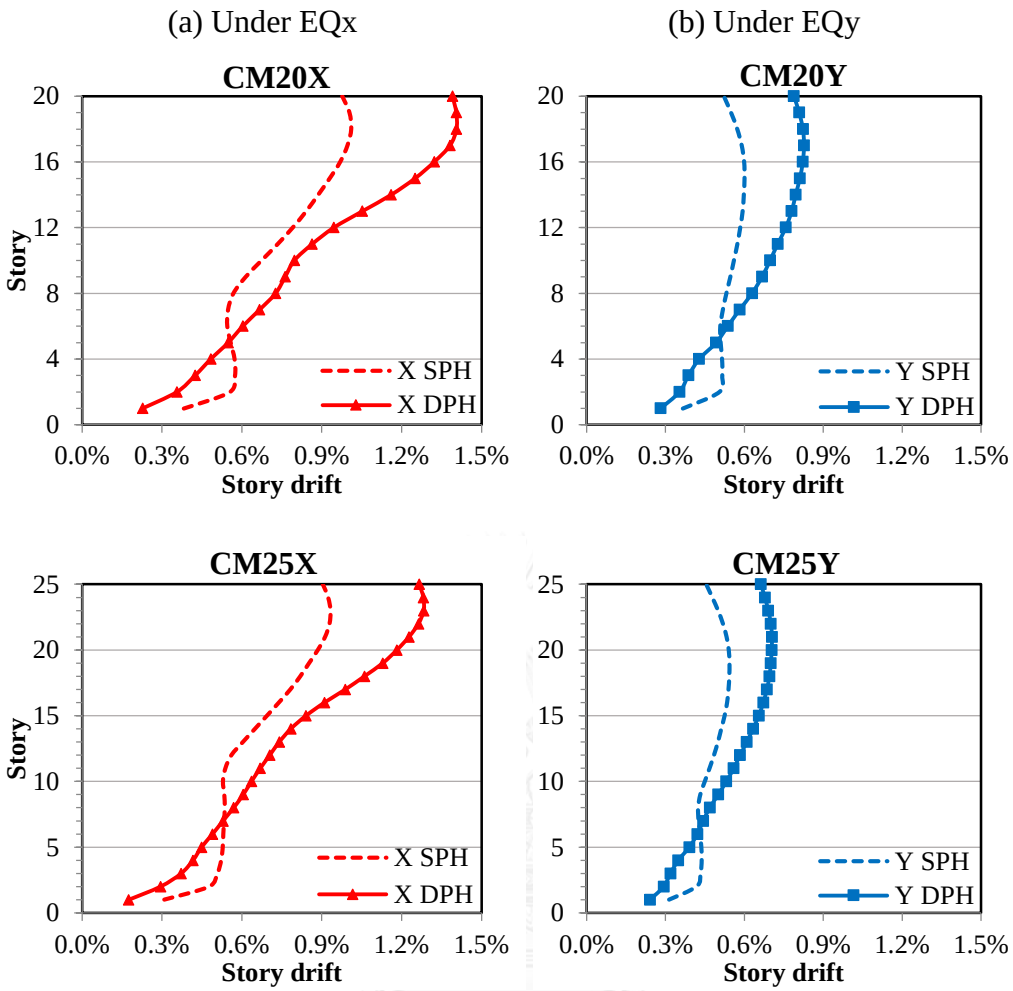

Figure 6.35 Comparison of story drifts obtained from NLRHA for SPH and DPH design concepts: (a) under EQx and (b) under EQy.

CHAPTER 7
CONCLUSIONS

7.1 Summary

This study has evaluated the seismic shear demands of RC core walls determined from response spectrum analysis (RSA) procedure in ASCE 7-10 by nonlinear response history analysis (NLRHA). RC split core walls in five buildings varying from 5 to 25 stories, which were subjected to ground motions in two different cities, Bangkok and Chiang Mai in Thailand, were employed. Two directions of core wall whose behaviors are different as it behaves like cantilever wall in Y direction and coupled wall in X direction were studied. The accuracy of various codes and previously proposed formulas for estimating the design shear force of RC wall was evaluated. The following conclusions could be drawn:

1. The shear demands in core walls determined by NLRHA are significantly larger than the design shear forces used in RSA procedure. In Y direction where core wall behaves like cantilever wall, the base shear amplifications could be as high as 2 to 5 in Bangkok and 2 to 3 in Chiang Mai, but they are relatively lower in X direction where core wall behaves as coupled wall.
2. Different locations having different spectrum shapes lead to different shear amplification.
3. The accuracy of various codes and previous researchers' formulas for estimating the design shear forces of RC walls comparing to shear demands from NLRHA in this study is described below:

- For Bangkok, EC8 provides better results than other codes, although it slightly underestimates base shear demands computed from NLRHA in cantilever direction of 20- and 25-story core walls, and it is conservative in coupled direction of core walls. For Chiang Mai, EC8 is significant overestimation in both directions of core walls.
- For Bangkok, Rejec et al. (2012)'s equation provides good estimation of shear forces in cantilever direction of core walls, while it significantly overestimates

the shear forces in coupled direction of core walls computed from NLRHA. For Chiang Mai, it is conservative for both directions of core walls.

- For Chiang Mai, Luu et al. (2014)'s equation provides good agreement with the shear forces determined from NLRHA in both directions of core walls. It could well follow the trend of shear forces along the height of core walls in Chiang Mai. However, it significantly underestimates the shear forces in cantilever direction of core walls computed from NLRHA in Bangkok.

4. Sensitivity effects of flexural over-strength on shear demands of core walls are summarized below:

- Shear demands in both directions of core walls are increased with increasing of flexural over-strength of core walls for all buildings.
- Flexural over-strength of core walls has less effect on shear demands of core walls in cantilever direction comparing to those in coupled direction.
- Flexural over-strength of core walls has larger influence on shear demands of core walls in shorter buildings than those in taller buildings.

All of the above conclusions are based on the design concept that flexural strengths of the walls in every story are designed according to the flexural demands of the walls determined from RSA procedure. This design concept is named as distributed plastic hinge (DPH) of the walls. However, in another design concept, the walls in upper stories are provided enough strength to prevent any yielding in upper stories and yielding is allowed to occur only at the base of the walls. This design concept is defined as single plastic hinge (SPH) of the walls. The effects of designing the wall in upper stories to behave elastic are summarized below:

- Shear demands in coupled direction of core walls at the base floor are increased about 1.4 times larger than those from DPH.
- Bending moments in both directions of core walls are increased significantly at mid-height. These large bending moments at the mid-height are closed to the bending moments at the base of core walls. Designing the mid-height walls to remain elastic requires excessive amounts of vertical reinforcement.
- Roof drifts are reduced up to 30% of those from DPH in both directions of the building.

7.2 Suggestions for modifying shear demands determined from RSA procedure

Due to different locations having different spectrum shapes, which affected the shear amplification intensity, an empirical equation cannot be applied for every location. For Chiang Mai, Luu et al. (2014)'s equation is appropriate to be adopted to modify shear demands in both directions of core walls determined from RSA procedure. For Bangkok, Rejec et al. (2012)'s equation is suggested to be adopted to modify shear demands of core walls computed from RSA procedure. However, Rejec et al. (2012)'s formula can well estimate the design shear forces only in cantilever direction of core walls, while it significantly overestimates in coupled direction of core walls; hence, one should be careful when applying such an equation to compute the design shear forces of the walls.

Beside these two equations, the shear magnification factor equation in EC8 is recommended to be adopted to multiply with the shear forces from RSA procedure before using them as design shear forces of RC core walls. The shear magnification factor equation in EC8 is more convenient to apply than Rejec et al. (2012)'s equation for design engineers. EC8 uses constant shear magnification factor for entire height of the walls and EC8 generally provides conservative results for both cantilever and coupled core walls in both locations, Bangkok and Chiang Mai, with the exception that it slightly underestimates the base shear force in cantilever direction of 20- and 25-story core walls in Bangkok.

7.3 Recommendations for future research

The following suggestions are recommended for further study:

- The results presented in this study were based on split core-wall buildings having regular plan and uniform stiffness over the entire height of the buildings in which torsional effects and interaction from gravity systems were not considered. Other lateral resisting system configurations where the torsional effects are significant are required for future research. Interaction from frames in resisting earthquake loading is suggested to be studied.

- The current study focused on soft soil class in downtown area of Bangkok and site class D in Chiang Mai. Other site classes which strongly affect the spectral shape should be observed.
- This current research ignored wind load effects when designing the structural systems. For high-rise buildings, wind load might govern the design and leads to large over-strength factor. The effects of wind load on shear demand amplification of structural walls are recommended to be investigated.

REFERENCES

ACI Committee 318 (2011). Building code requirements for structural concrete (ACI 318M-11) and commentary. Farmington Hills, USA.

Adebar, P., J. Mutrie, R. DeVall and D. Mitchell (2014). Seismic design of concrete buildings: The 2015 Canadian Building Code. 10th US National Conference on Earthquake Engineering. Anchorage, Alaska.

American Society of Civil Engineers (2010). Minimum design loads for buildings and other structures. ASCE standard ASCE/SEI 7-10. Reston, Virginia.

American Society of Civil Engineers (2013). Seismic rehabilitation of existing buildings. ASCE Standard ASCE/SEI 41-13. Reston, Virginia.

Blakeley, R. W. G., R. C. Cooney and L. M. Megget (1975). "Seismic shear loading at flexural capacity in cantilever wall structures." Bulletin of the New Zealand Society for Earthquake Engineering **8**: 278-290.

Boivin, Y. and P. Paultre (2012). "Seismic force demand on ductile reinforced concrete shear walls subjected to western North American ground motions: Part 1 - parametric study." Canadian Journal of Civil Engineering **39**(7): 723-737.

Boivin, Y. and P. Paultre (2012). "Seismic force demand on ductile reinforced concrete shear walls subjected to western North American ground motions: Part 2 - new capacity design methods." Canadian Journal of Civil Engineering **39**(7): 738-750.

Building Seismic Safety Council (2007). FEMA 415B Notes: NEHRP Recommended provisions for new buildings and other structures: training and instructional materials: inelastic behavior of materials and structures. Washington, USA.

Calugaru, V. and M. Panagiotou (2012). "Response of tall cantilever wall buildings to strong pulse type seismic excitation." Earthquake Engineering and Structural Dynamics **41**(9): 1301-1318.

Canadian Standard Association (2004). Design of concrete structures. CSA standard A23.3-04. Ontario, Canada.

Chopra, A. K. (2012). Dynamics of structures: Theory and applications to earthquake engineering. 4th Edition. Pearson Prentice Hall, Upper Saddle River, NJ.

Computers and Structures, Inc. (2011). PERFORM-3D, Nonlinear analysis and performance assessment of 3D structures, Version 5.0.0. Berkeley, California.

Computers and Structures, Inc. (2013). ETABS, Integrated building design software, Version 13.2.0. Berkeley, California.

EduPro Civil System, Inc. (2004). ProShake ground response analysis program, User's Manual, Version 1.1. Redmond, Washington.

Eibl, J. and E. Keintzel (1988). Seismic shear forces in RC cantilever shear walls. 9th World Conference on Earthquake Engineering. Tokyo-Kyoto, Japan.

European Committee for Standardization (2004). Eurocode 8: Design of structures for earthquake resistance - Part 1: General rules, seismic actions and rules for buildings. Brussels, Belgium.

Ghosh, S. K. and V. P. Markevicius (1990). Design of earthquake resistant shear walls to prevent shear failure. 4th US National Conference on Earthquake Engineering. Palm Springs, California.

Haselton, C. B., A. B. Liel, S. Taylor Lange and G. G. Deierlein (2008). Beam-column element model calibrated for predicting flexural response leading to global collapse of RC frame buildings. PEER Report No. 2007/03. Pacific Earthquake Engineering Research Center, University of California, Berkeley, California.

Imbsen Software Systems (2006). XTRACT, Cross sectional analysis of structural components, Version 3.0.5. Sacramento, California.

Luu, H., P. Léger and R. Tremblay (2014). "Seismic demand of moderately ductile reinforced concrete shear walls subjected to high-frequency ground motions." Canadian Journal of Civil Engineering **41**(2): 125-135.

Mander, J. B., M. J. Priestley and R. Park (1988). "Theoretical stress-strain model for confined concrete." Journal of Structural Engineering **114**(8): 1804-1826.

Minchainant, P. (2012). Ground motion database for seismic design. Master Thesis, Chulalongkorn University, Bangkok, Thailand.

Moehle, J. P., Y. Bozorgnia, N. Jayaram, P. Jones, M. Rahnama, N. Shome, Z. Tuna, J. W. Wallace, T. Y. Yang and F. Zareian (2011). Case studies of the seismic performance of tall buildings designed by alternative means, Task 12 Report for the Tall Buildings Initiative. PEER Report No. 2011/05. Pacific Earthquake Engineering Research Center, University of California, Berkeley, California.

Munir, A. and P. Warnitchai (2012). "The cause of unproportionately large higher mode contributions in the inelastic seismic responses of high-rise core-wall buildings." Earthquake Engineering and Structural Dynamics **41**(15): 2195-2214.

Naish, D., A. Fry, R. Klemencic and J. Wallace (2013). "Reinforced Concrete Coupling Beams—Part II: Modeling." ACI Structural Journal **110**(06).

Naish, D. A. B. (2010). Testing and modeling of reinforced concrete coupling beams. Doctoral Dissertation, University of California, California, USA.

National Building Code of Canada (2010). Commission on building and fire codes, National Research Council of Canada. Ottawa, Canada.

New Zealand Standard (2006). NZS 3101: Part 2: Commentary on the design of concrete structures. Wellington, New Zealand.

Orakcal, K. and J. W. Wallace (2006). "Flexural modeling of reinforced concrete walls-experimental verification." ACI Structural Journal **103**(2).

Palasri, C. and A. Ruangrassamee (2010). "Probabilistic seismic hazard maps of Thailand." Journal of Earthquake and Tsunami **4**(04): 369-386.

Paulay, T. and M. J. N. Priestley (1992). Seismic design of reinforced concrete and masonry buildings. John Wiley and Sons, New York, USA.

PEER/ATC-72-1 (2010). Modeling and acceptance criteria for seismic design and analysis of tall buildings. Applied Technology Council, Redwood, California.

Powell, G. (2007). Detailed example of a tall shear wall building using CSI's Perform 3D nonlinear dynamic analysis. Computers and Structures Inc., Berkeley, California.

Priestley, M. J. N. (2003). "Does capacity design do the job? An examination of higher mode effects in cantilever walls." Bulletin of the New Zealand Society for Earthquake Engineering **36**(4): 276-292.

Priestley, M. J. N., G. M. Calvi and M. J. Kowalsky (2007). Displacement-based seismic design of structures. IUSS Press, Pavia, Italy.

Rejec, K., T. Isaković and M. Fischinger (2012). "Seismic shear force magnification in RC cantilever structural walls, designed according to Eurocode 8." Bulletin of Earthquake Engineering **10**(2): 567-586.

Rutenberg, A. (2013). "Seismic shear forces on RC walls: review and bibliography." Bulletin of Earthquake Engineering **11**(5): 1727-1751.

Rutenberg, A. and E. Nsieri (2006). "The seismic shear demand in ductile cantilever wall systems and the EC8 provisions." Bulletin of Earthquake Engineering **4**(1): 1-21.

Yathon, J. S. (2011). Seismic shear demand of reinforced concrete cantilever walls. Master Thesis, University of British Columbia, Vancouver, Canada.

APPENDIX

APPENDIX A

Floor plans of the buildings

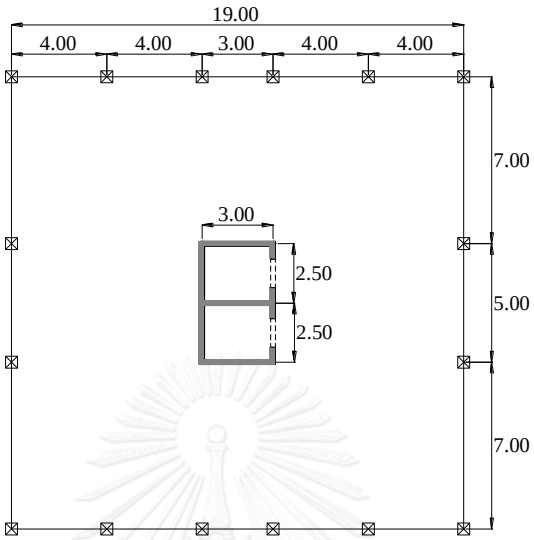

5-story building

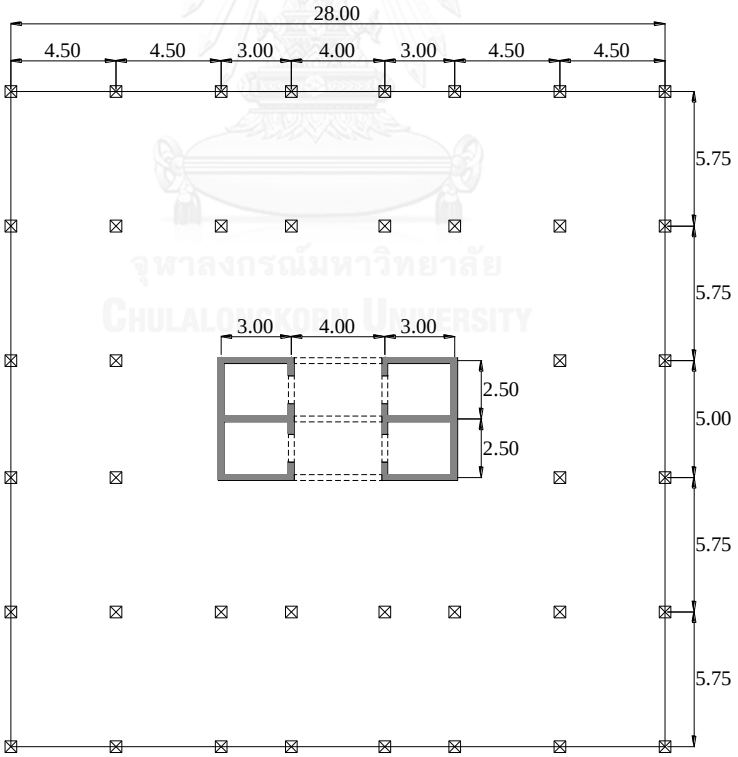

10-story building

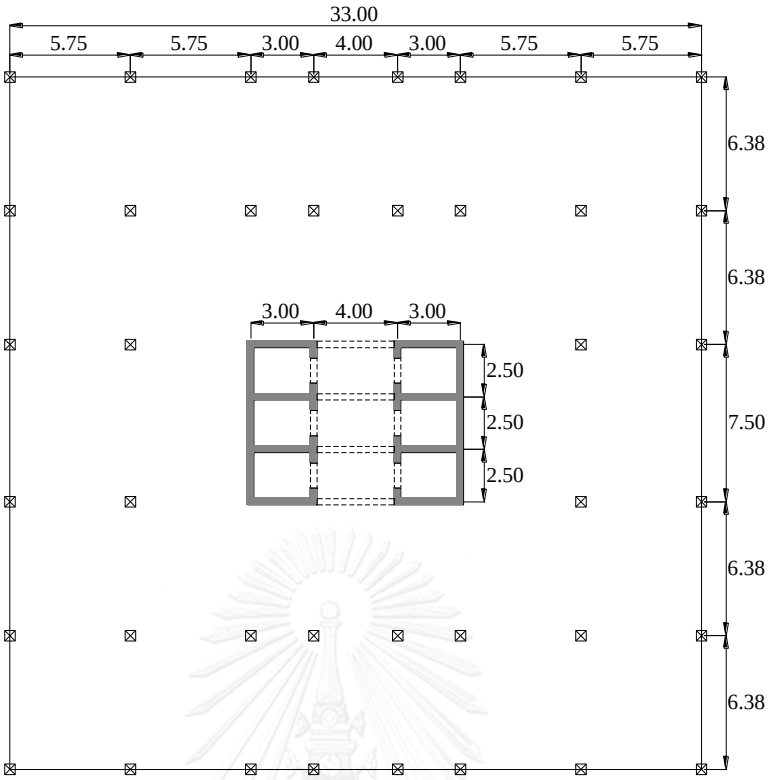

15-story building

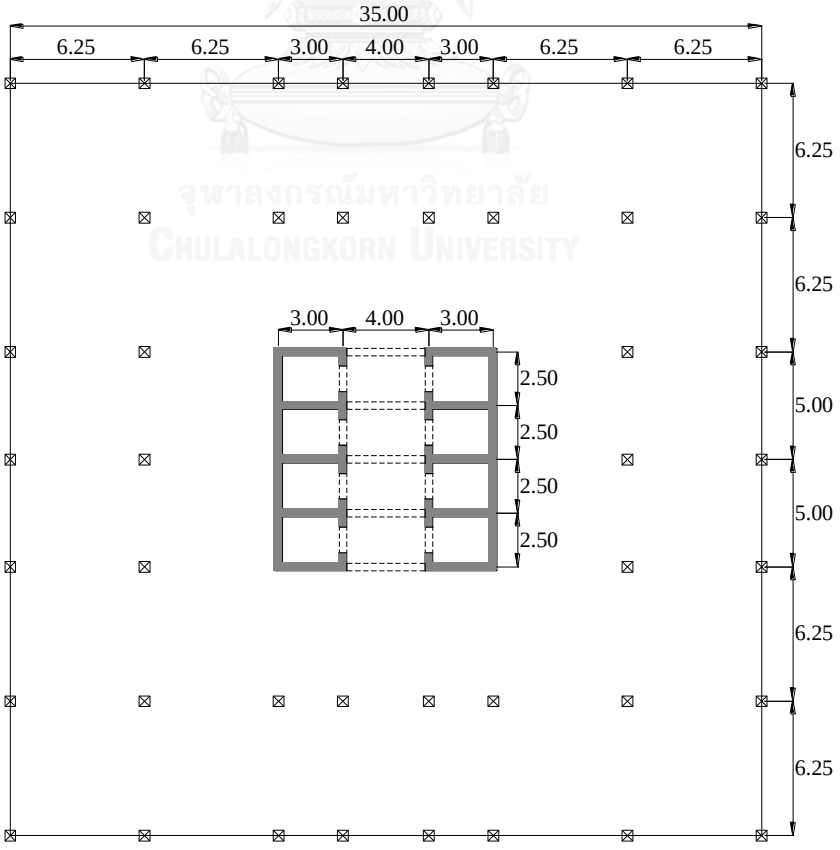

20-story building

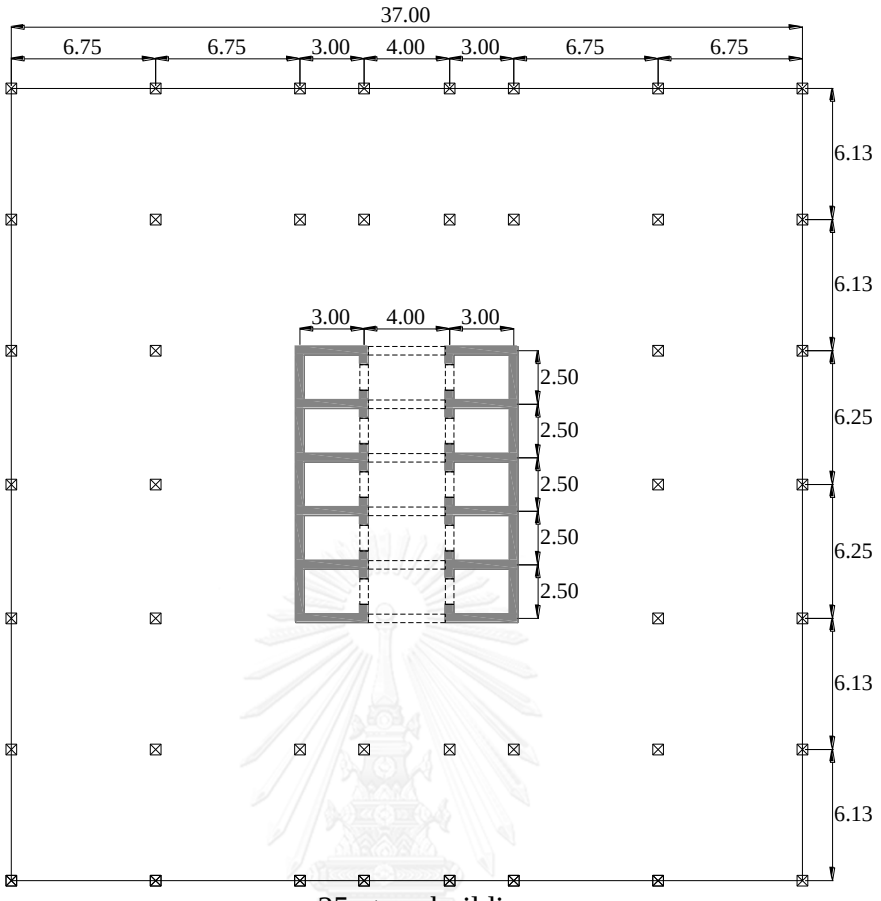

25-story building

All unites are in meter.

Figure A.1 Floor plans of the five buildings used in this study

APPENDIX B

Time history of ground accelerations in Bangkok and Chiang Mai

B.1 Bangkok

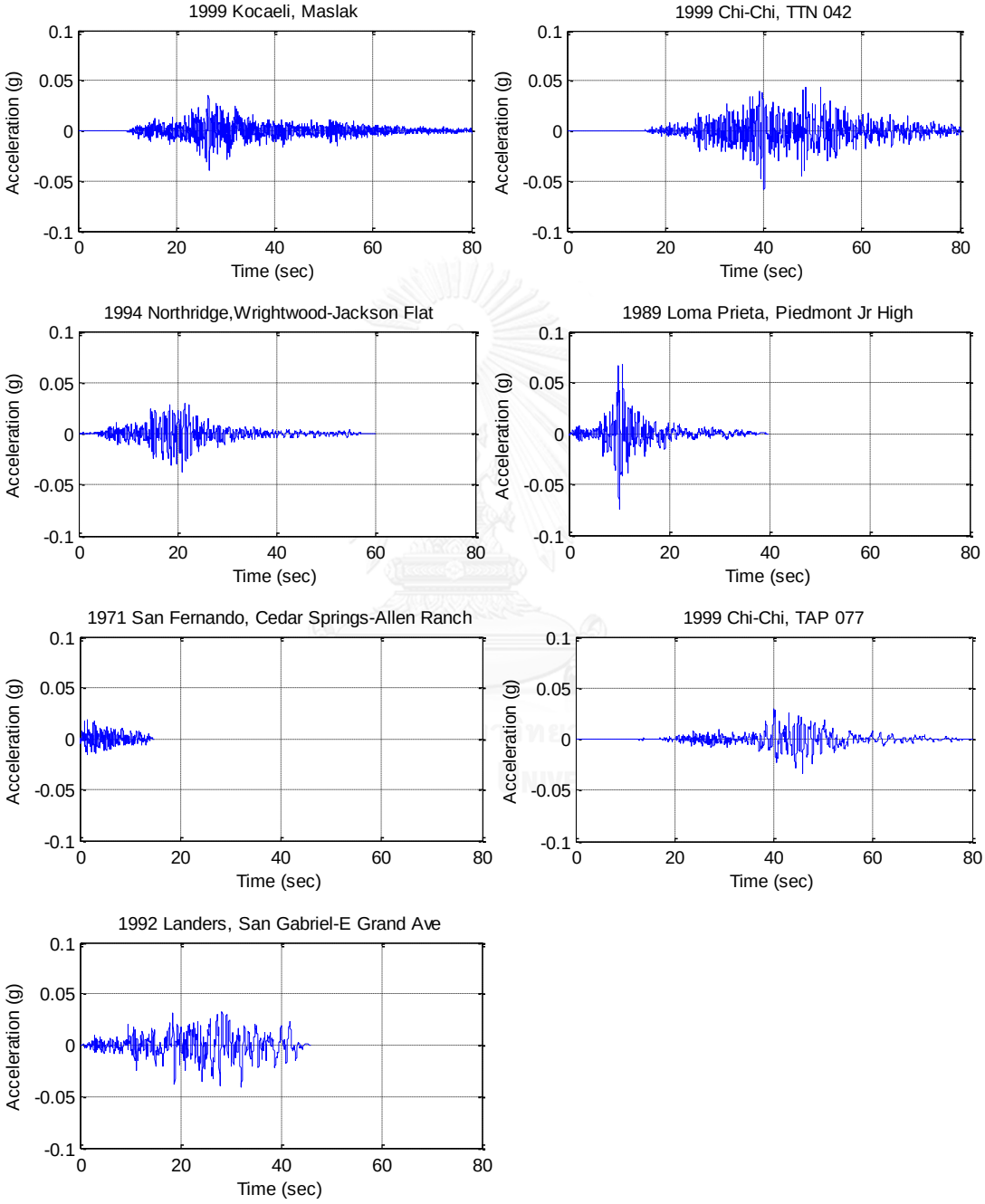

Figure B.1 Ground accelerations of the seven records modified to match the target spectrum before running through ProShake.

Table B.1 Average shear velocity and standard deviation along the depth of the soft soil profile underlying downtown area of Bangkok.

Depth (m)	Average shear velocity (m/s)	Standard deviation
0	74	0.15
3.3	79	0.15
4.8	78	0.15
6.3	80	0.15
7.8	79	0.17
9.3	107	0.17
12.3	107	0.17
13.8	301	0.17
15.3	271	0.17
15.8	198	0.17
16.8	307	0.17
18.3	326	0.17
21.3	423	0.17
22.8	234	0.17
24.3	261	0.17
25.8	369	0.17
27.3	280	0.17
28.8	280	0.17
30.3	400	0.17
60	450	0.07
120	550	0.07
300	600	0.07
600	600	0.07

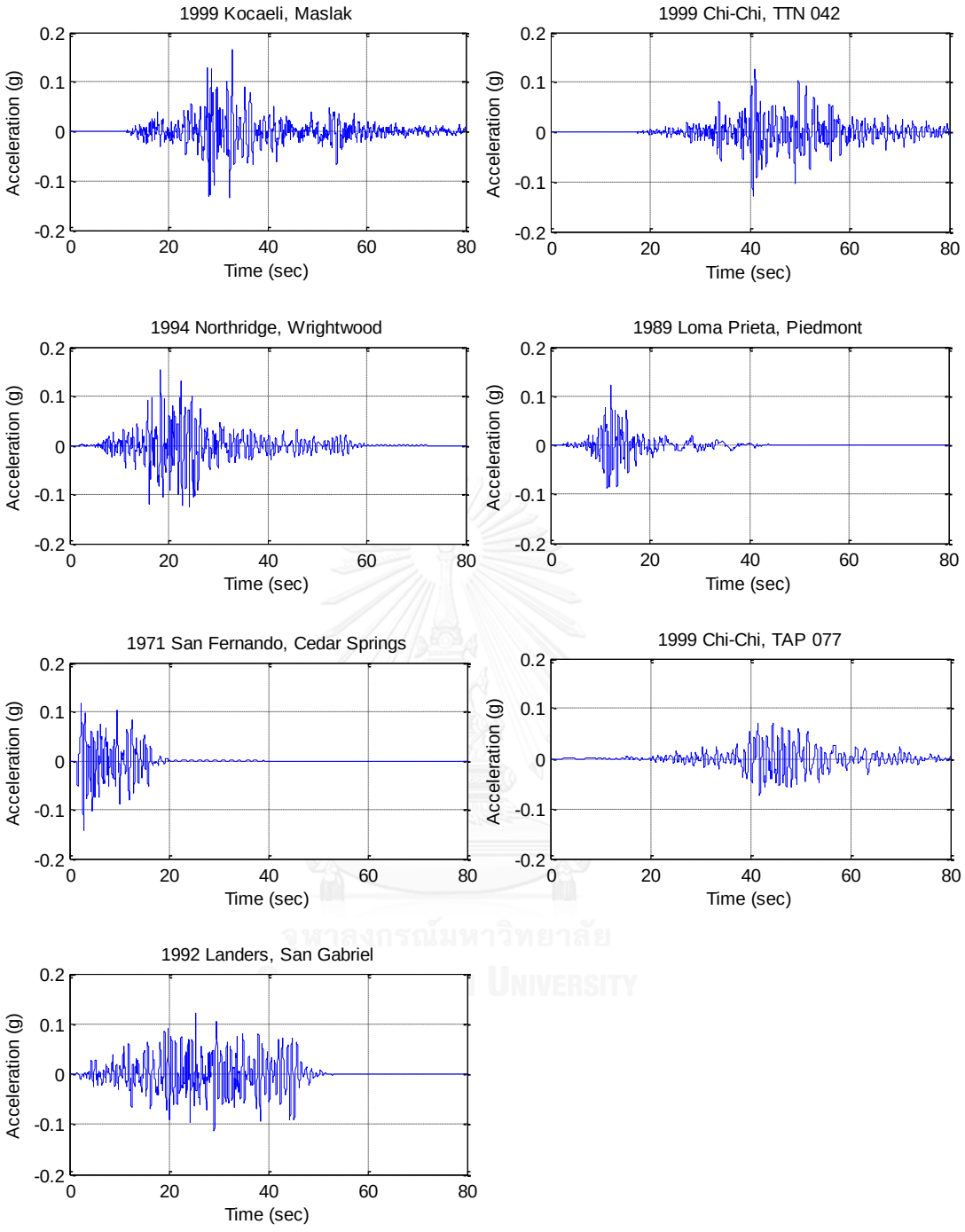

Figure B.2 Soft-soil ground accelerations of the seven records after running through ProShake.

B.2 Chiang Mai

NGA No.30

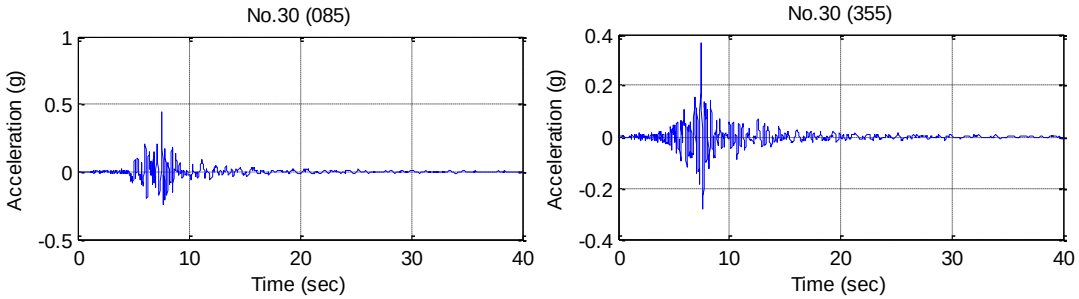

NGA No.95

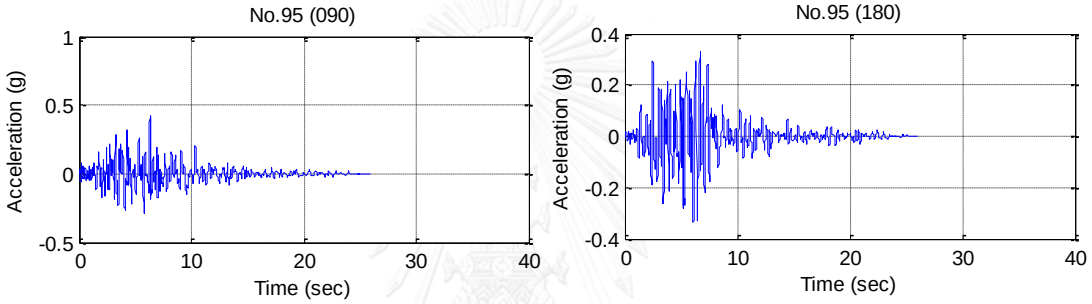

NGA No.147

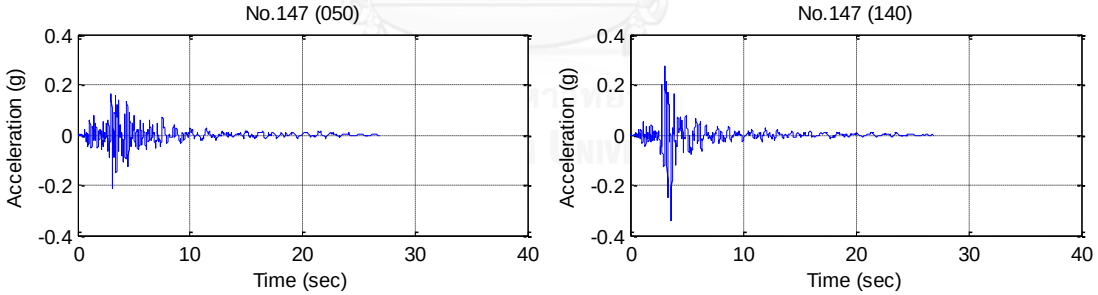

NGA No.148

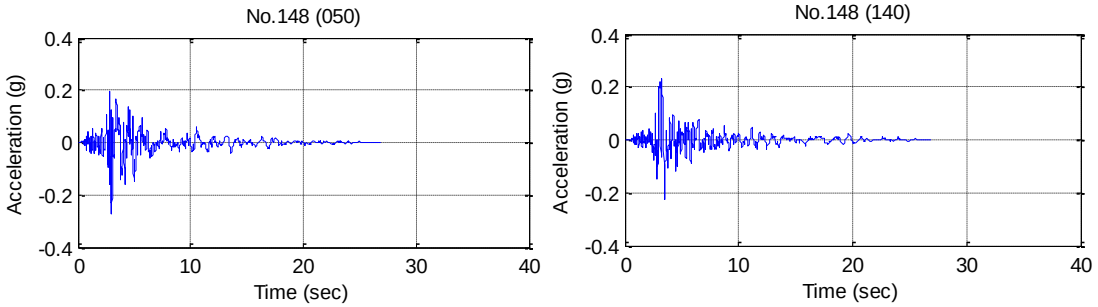

NGA No.149

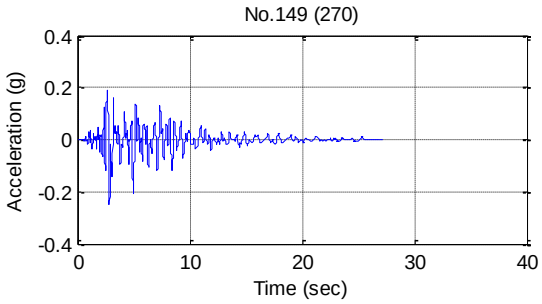

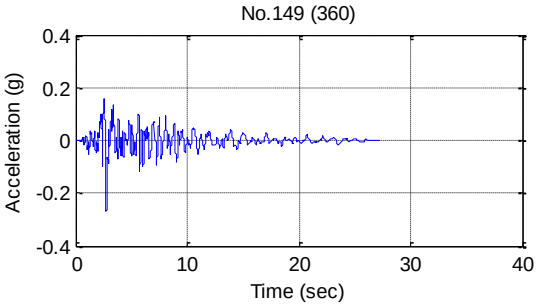

NGA No.159

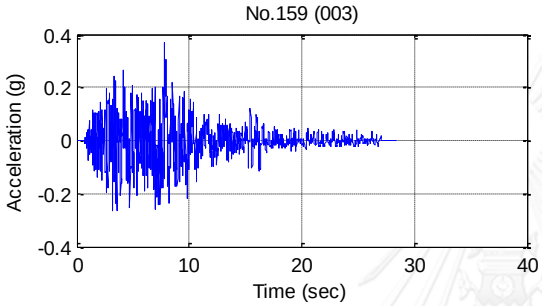

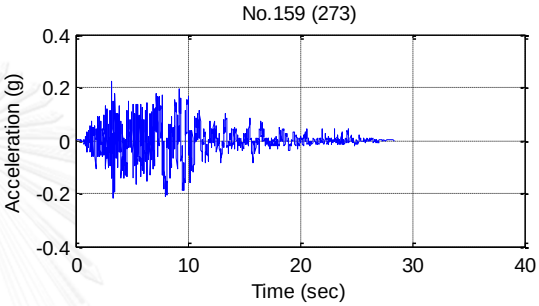

NGA No.161

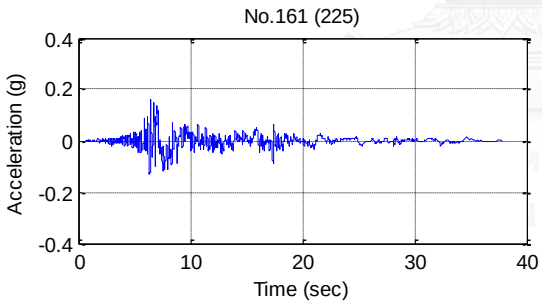

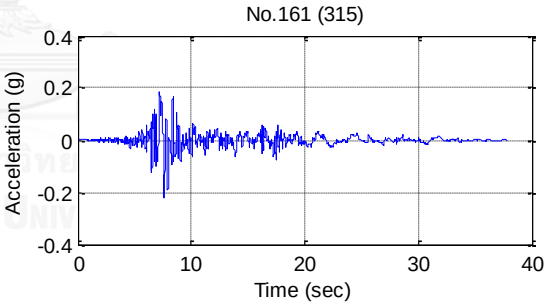

NGA No.162

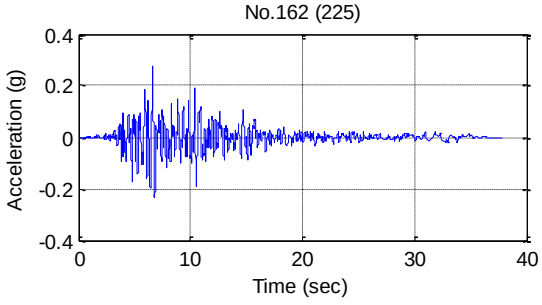

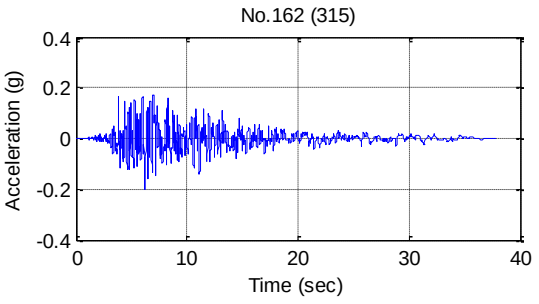

NGA No.179

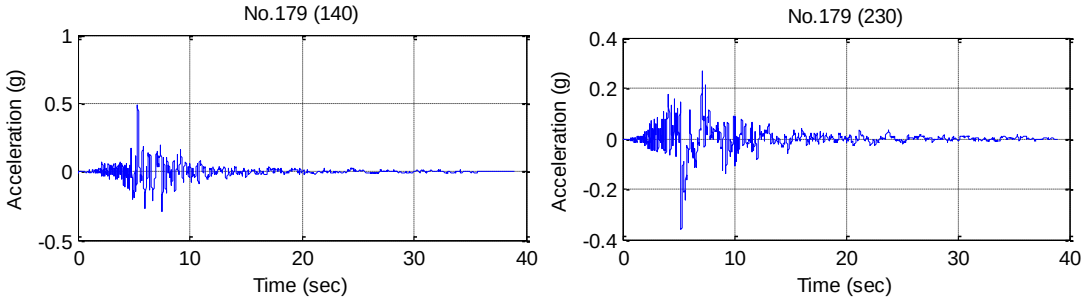

NGA No.185

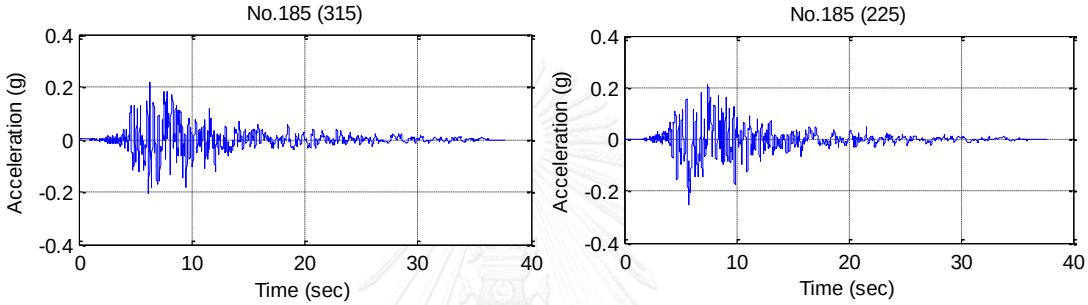

Figure B.3 Ten pairs of ground accelerations before scaling.

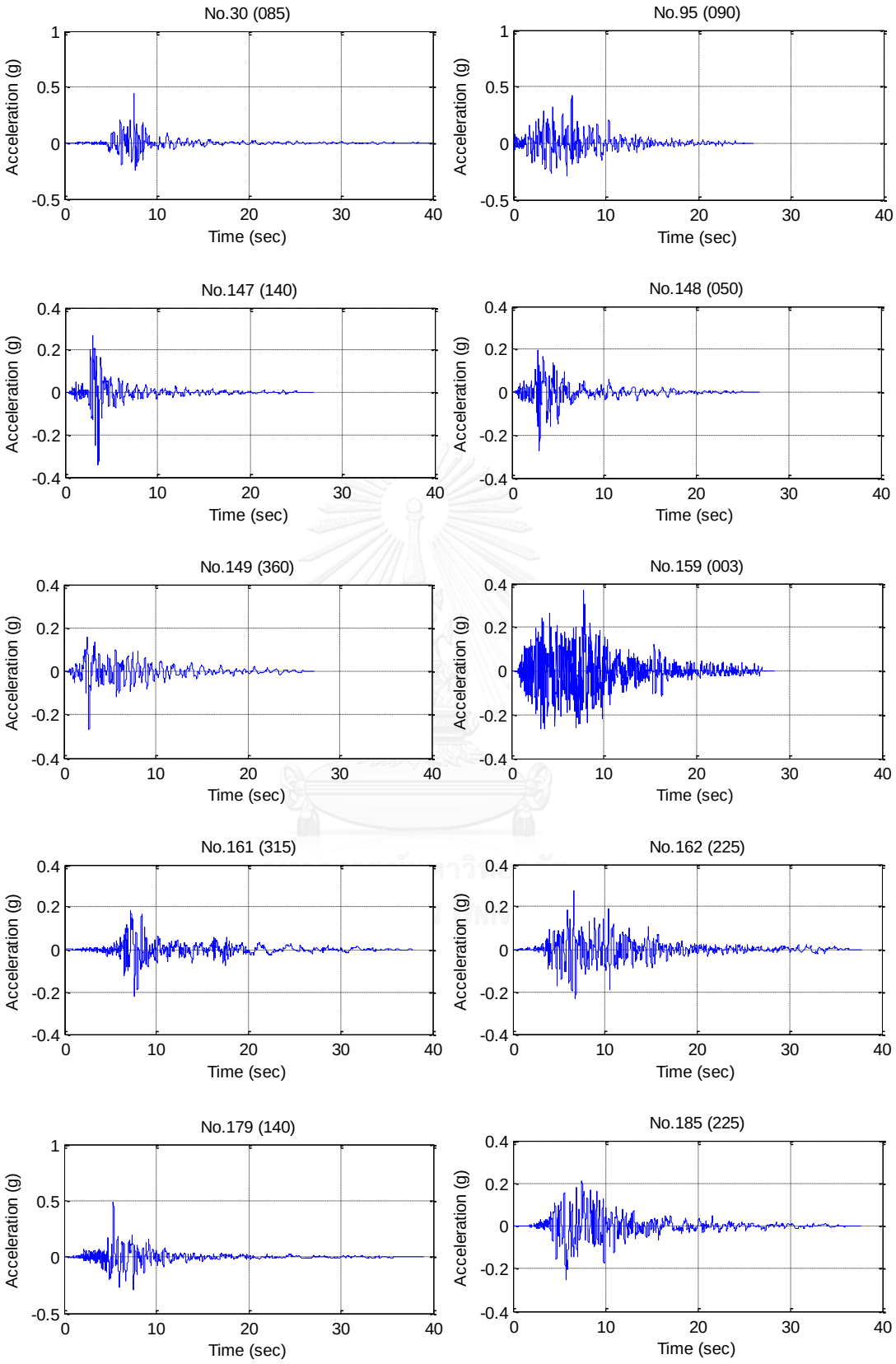

Figure B.4 Ten ground accelerations employed in NLRHA.

APPENDIX C

Comparison of elastic demands determined from RSA and LRHA

C.1 Comparison of modal properties of the building obtained from ETABS and PERFORM-3D program

To accomplish the objective of this research, this study tries to conduct RSA procedure in the same way as practical engineers in Thailand do but for NLRHA, this study adopts to the recommendations from literatures. This leads to different assumptions of effective stiffness of structural members in linear modeling (constructed in ETABS program) and nonlinear model (constructed in PERFORM-3D program). Due to these different assumptions, the modal properties of the structures determined from both programs are slightly different. The fundamental periods and modal participating mass ratios of the structures from PERFORM-3D program are a little bit larger than those from ETABS program as shown in Table C.1. The fundamental periods in both directions of the five buildings computed from both programs are plotted in Figure C.1. The elastic seismic demands of the structures computed by RSA in both programs are compared in Section C.2.

Table C. 1 Modal properties of the buildings obtained from ETABS and PERFORM-3D program.

No. story	Fundamental periods (s)				Modal participating mass ratios			
	ETABS		PERFROM-3D		ETABS		PERFORM-3D	
	X	Y	X	Y	X	Y	X	Y
5	0.57	0.43	0.68	0.70	69%	73%	79%	83%
10	1.62	1.28	1.70	1.45	66%	66%	70%	75%
15	2.68	1.71	2.80	1.90	65%	65%	67%	73%
20	3.72	2.05	3.89	2.27	66%	64%	67%	72%
25	4.60	2.27	4.83	2.46	66%	64%	66%	71%

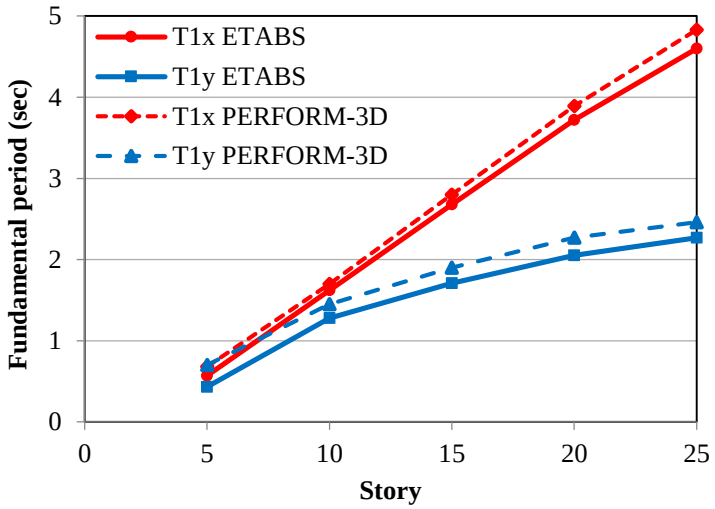

Figure C.1 Comparison of fundamental periods of the buildings obtained from ETABS and PERFORM-3D.

C.2 Comparison of elastic demands computed from RSA and LRHA

The elastic demands (story drift, shear force and bending moment of RC core wall) computed from RSA in ETABS program are compared with those determined from RSA in PERFORM-3D program. The elastic demands from RSA in PERFORM-3D program are also compared with those from linear response history analysis (LRHA) of the same structural model in PERFORM-3D program. LRHA is conducted by using modal damping of 5% in the same way as RSA.

The elastic demands obtained from RSA in ETABS, RSA and LRHA in PERFORM-3D are plotted in the same graphs as shown in Figures C.3 to C.5 for the case in Bangkok and Figures C.6 to C.8 for the case in Chiang Mai. The results from RSA in both programs are quite similar to each other, except for 5-story building where there are significant difference. This resulted from the difference of fundamental period of the building from the two programs, which leads to quite large different spectra acceleration of the first mode as shown in Figure C.2. The elastic demands from RSA and LRHA in PERFROM-3D are reasonably closed enough for all responses in all cases.

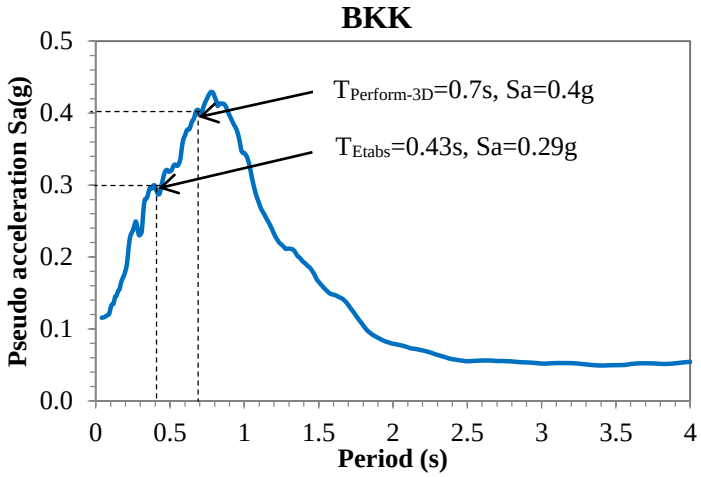

Figure C.2 Comparison of the first mode spectra acceleration of 5-story building modeled in ETABS and PERFORM-3D.

❖ **Shear force of core wall**

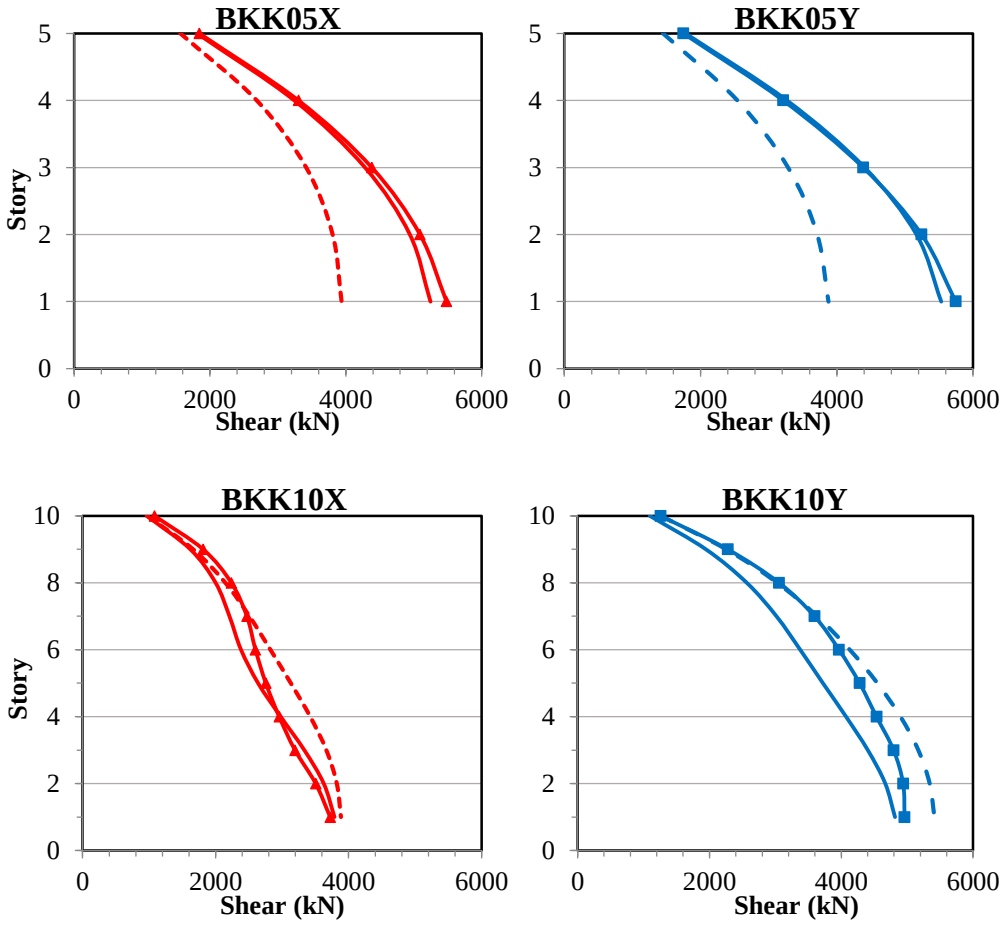

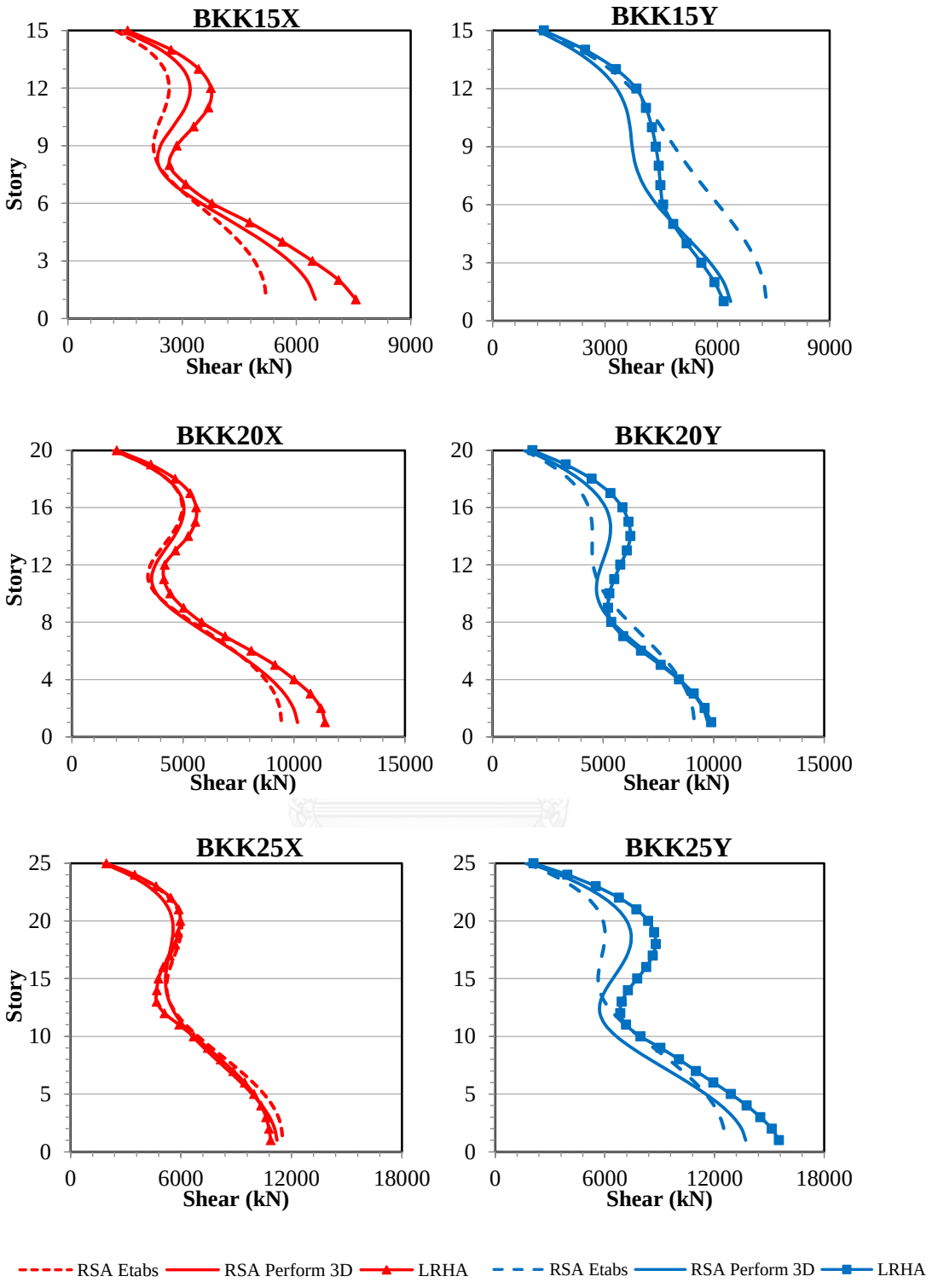

Figure C.3 Comparison of elastic shear forces of core walls computed from RSA in ETABS, RSA and LRHA in PERFROM-3D in Bangkok.

❖ **Bending moment of core wall**

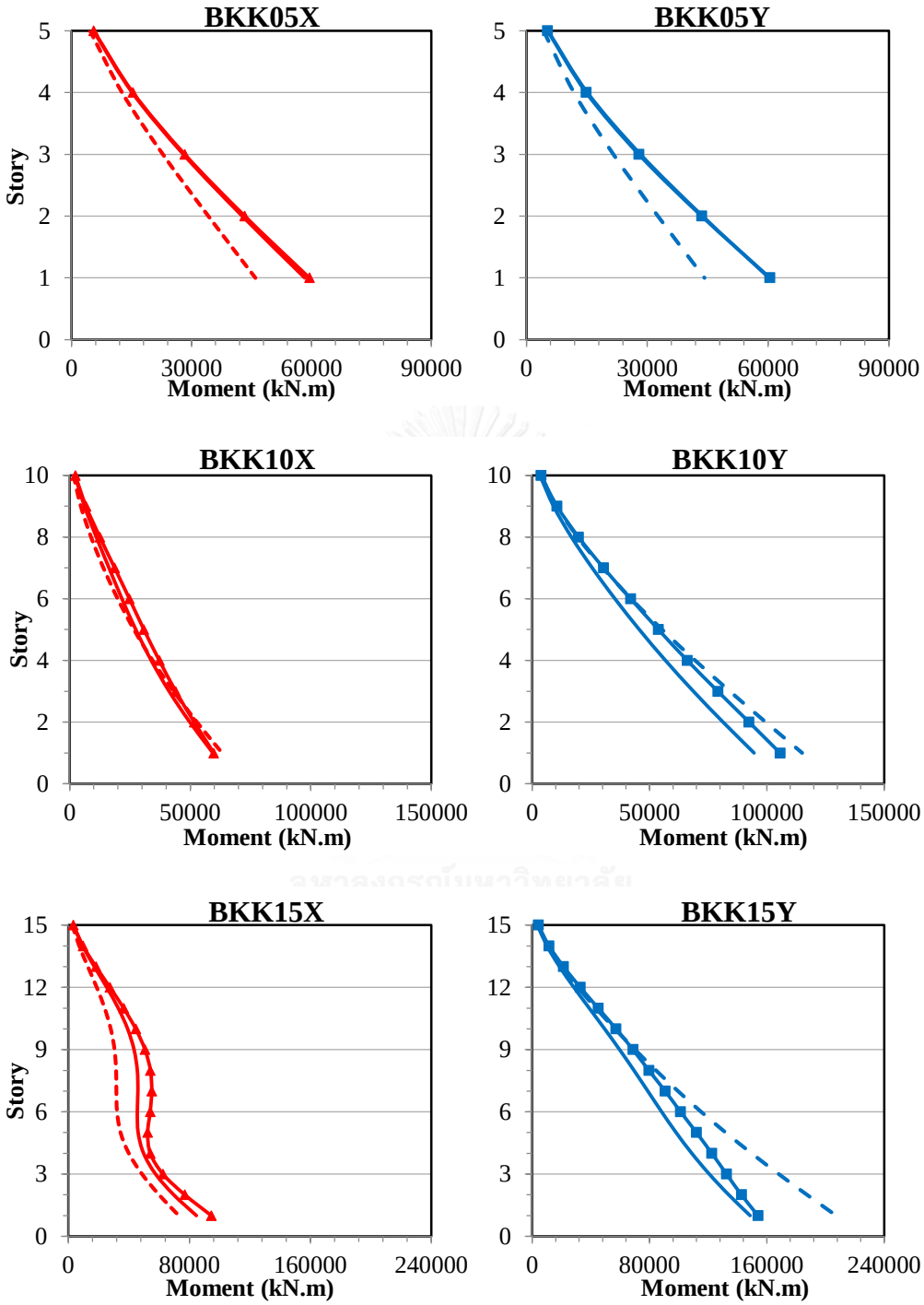

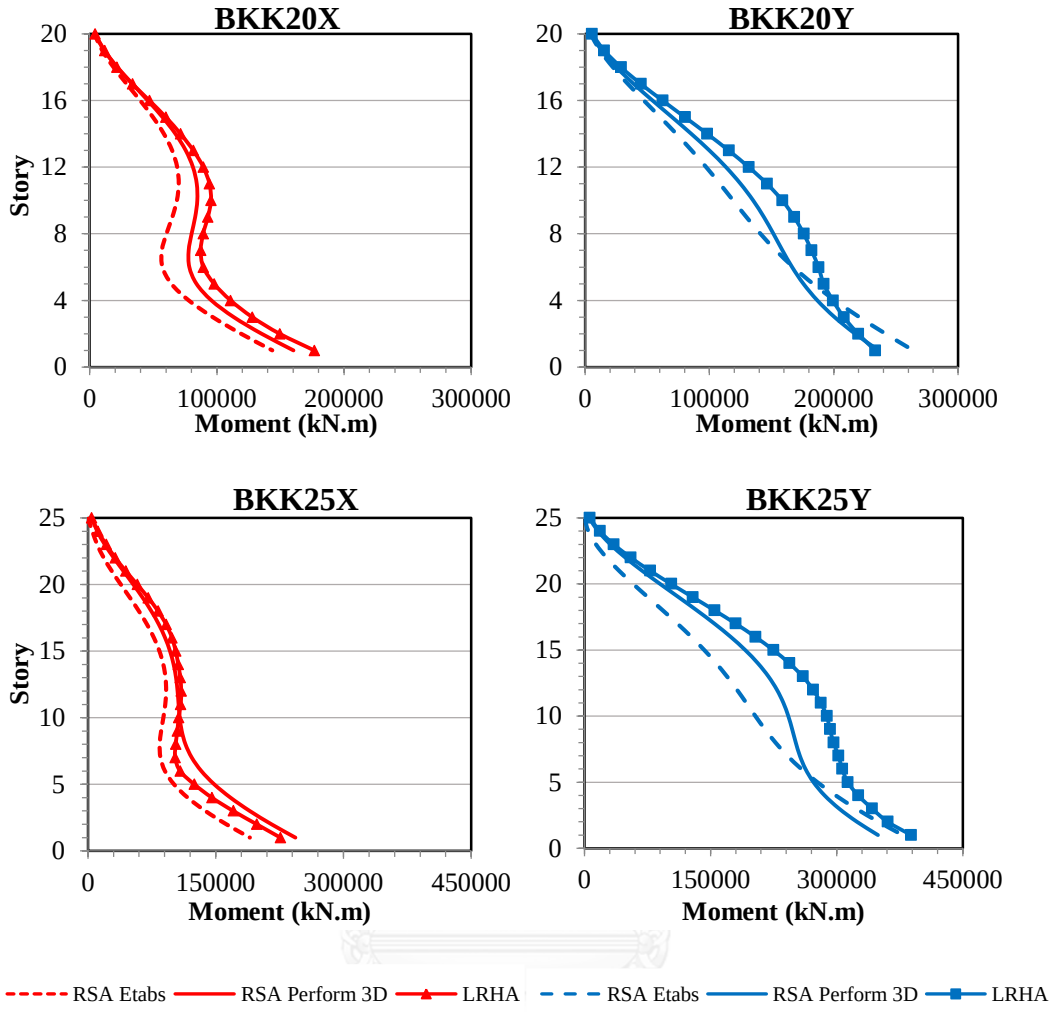

Figure C.4 Comparison of elastic bending moment of core walls computed from RSA in ETABS, RSA and LRHA in PERFROM-3D in Bangkok.

❖ **Story drift**

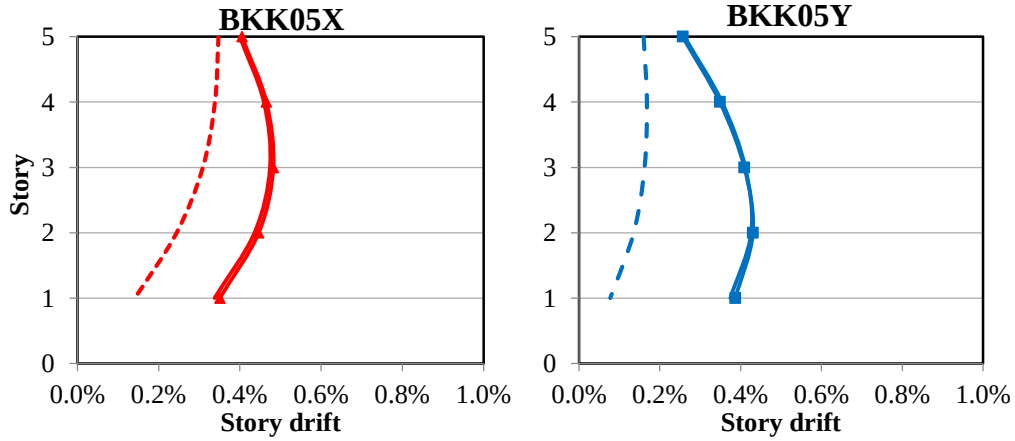

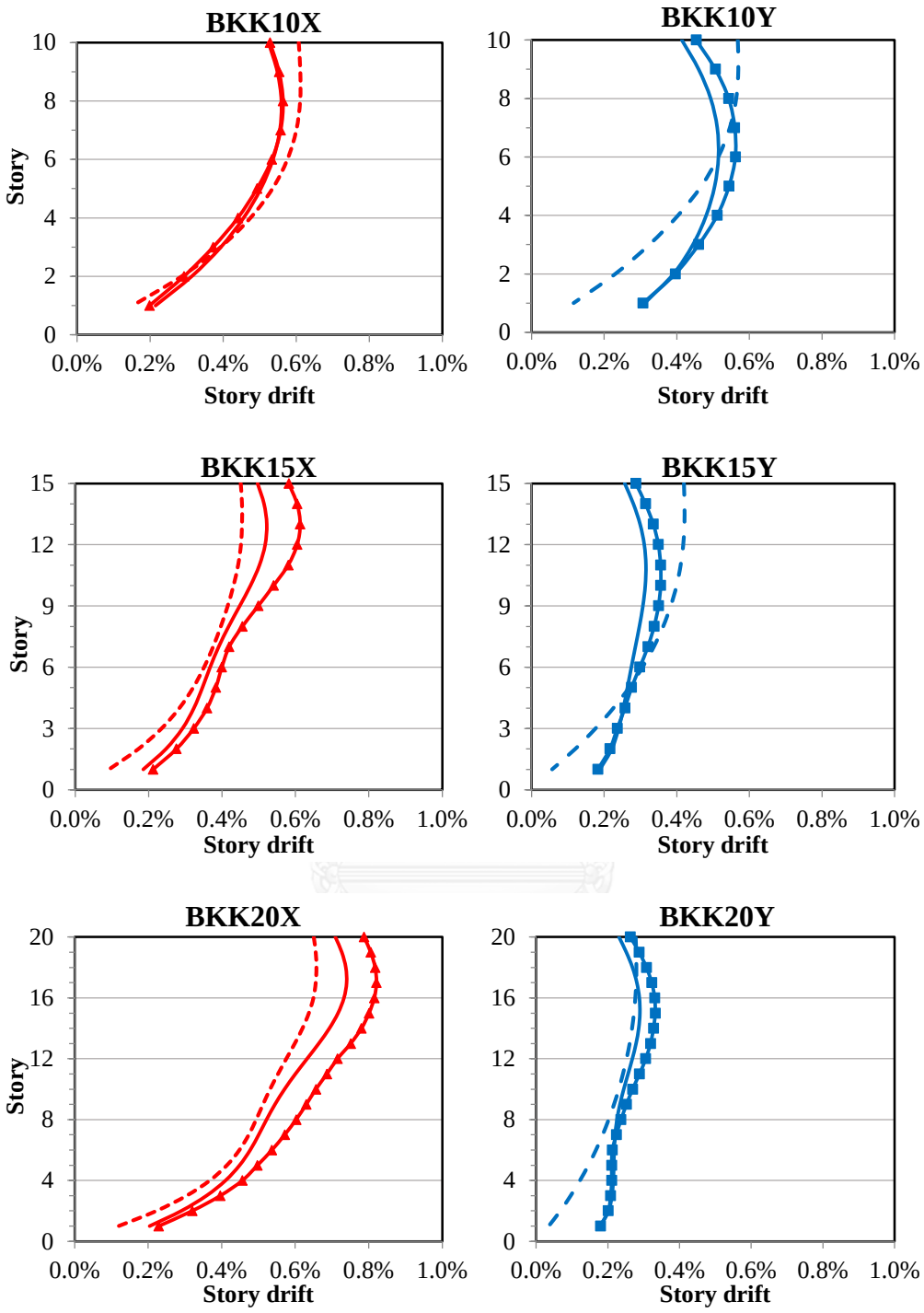
BKK10X
BKK10Y
BKK15X
BKK15Y
BKK20X
BKK20Y
Story
Story drift
0.0%
0.2%
0.4%
0.6%
0.8%
1.0%

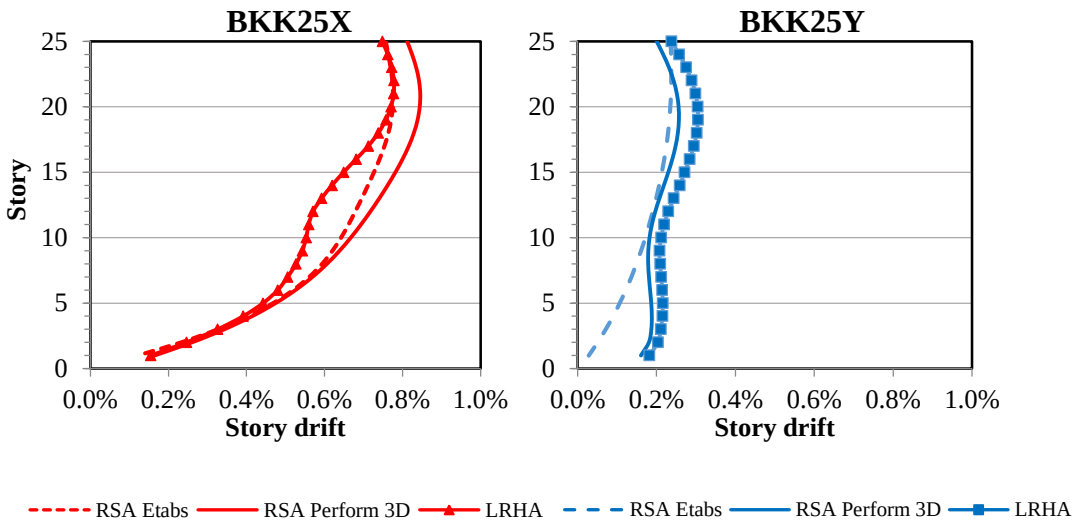

Figure C.5 Comparison of elastic story drifts computed from RSA in ETABS, RSA and LRHA in PERFROM-3D in Bangkok.

❖ **Shear force of core wall**

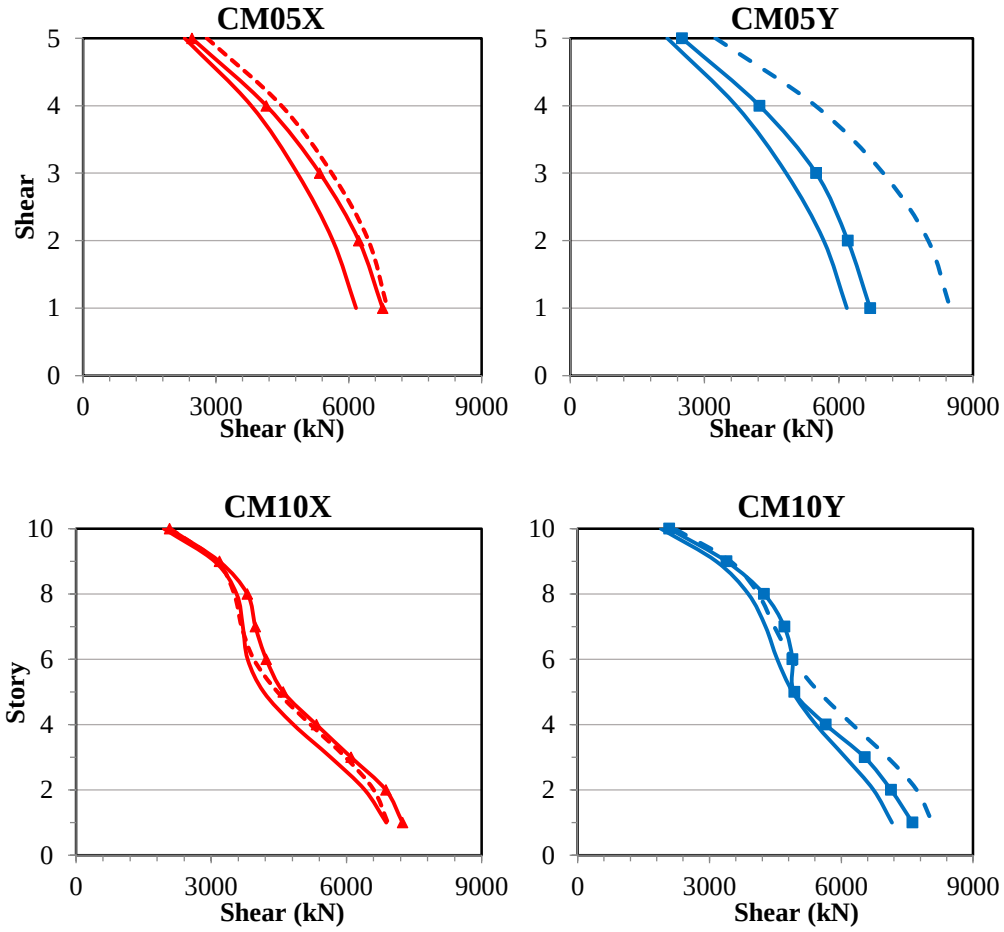

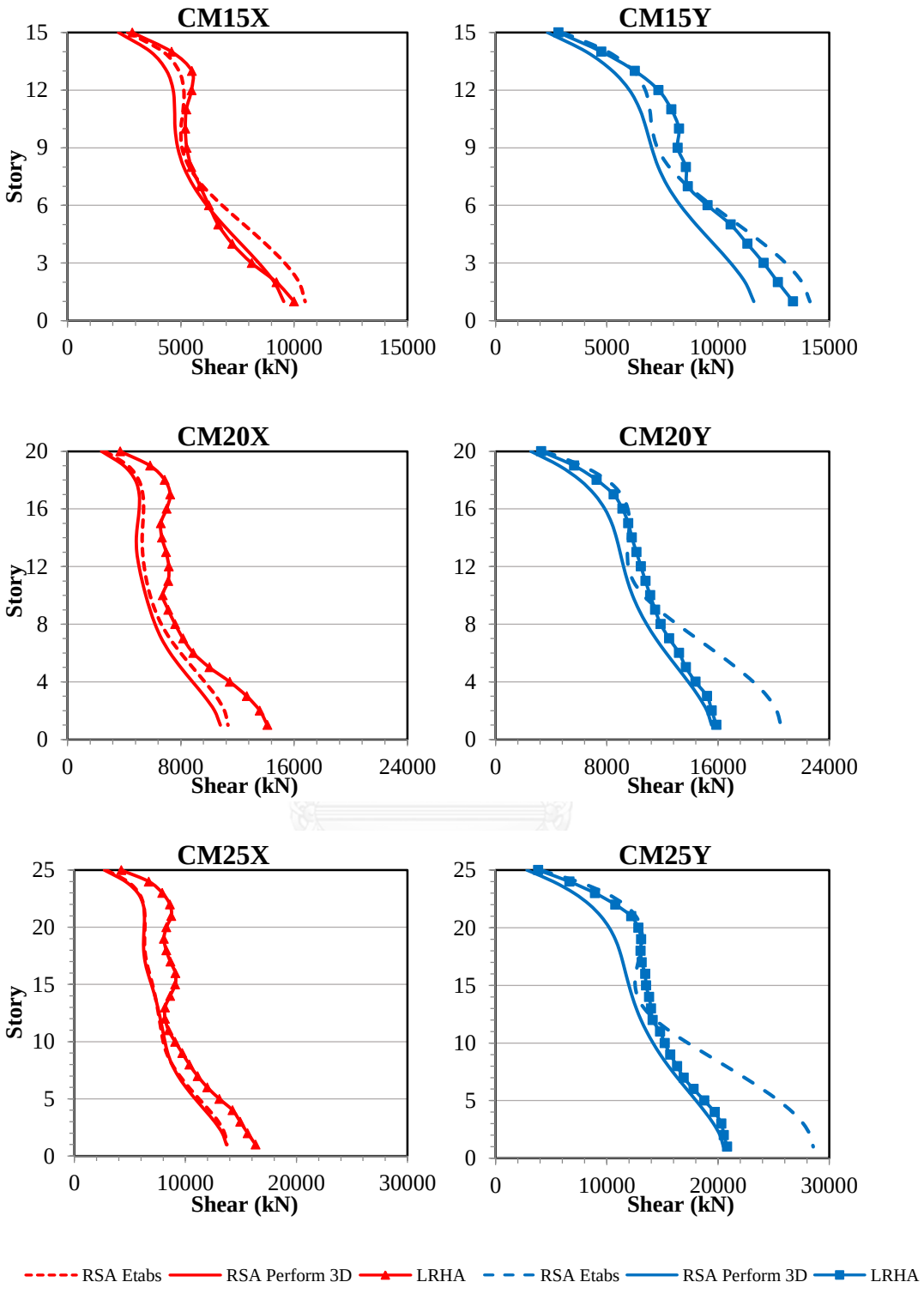

Figure C.6 Comparison of elastic shear forces of core walls computed from RSA in ETABS, RSA and LRHA in PERFROM-3D in Chiang Mai.

❖ **Bending moment of core wall**

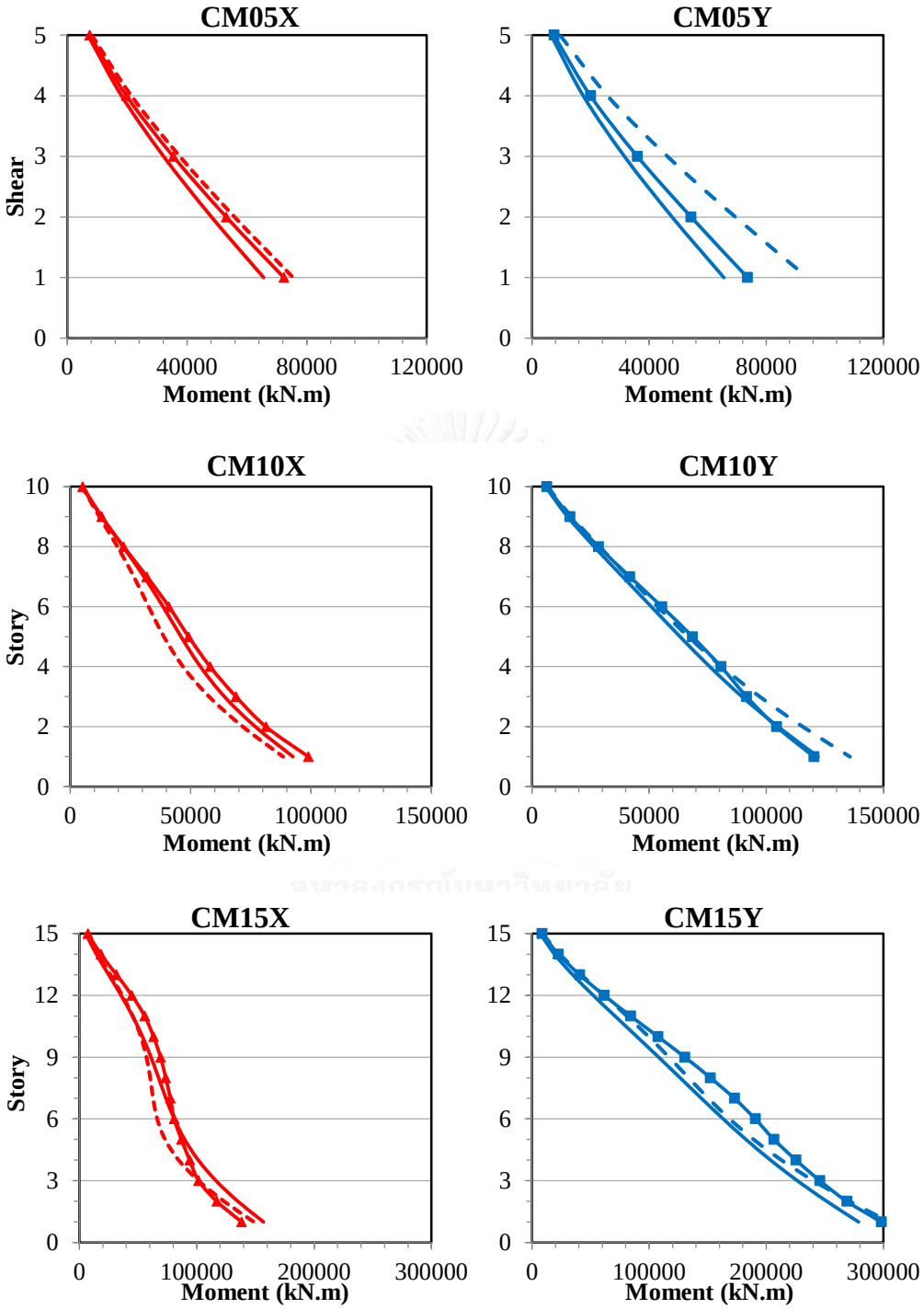

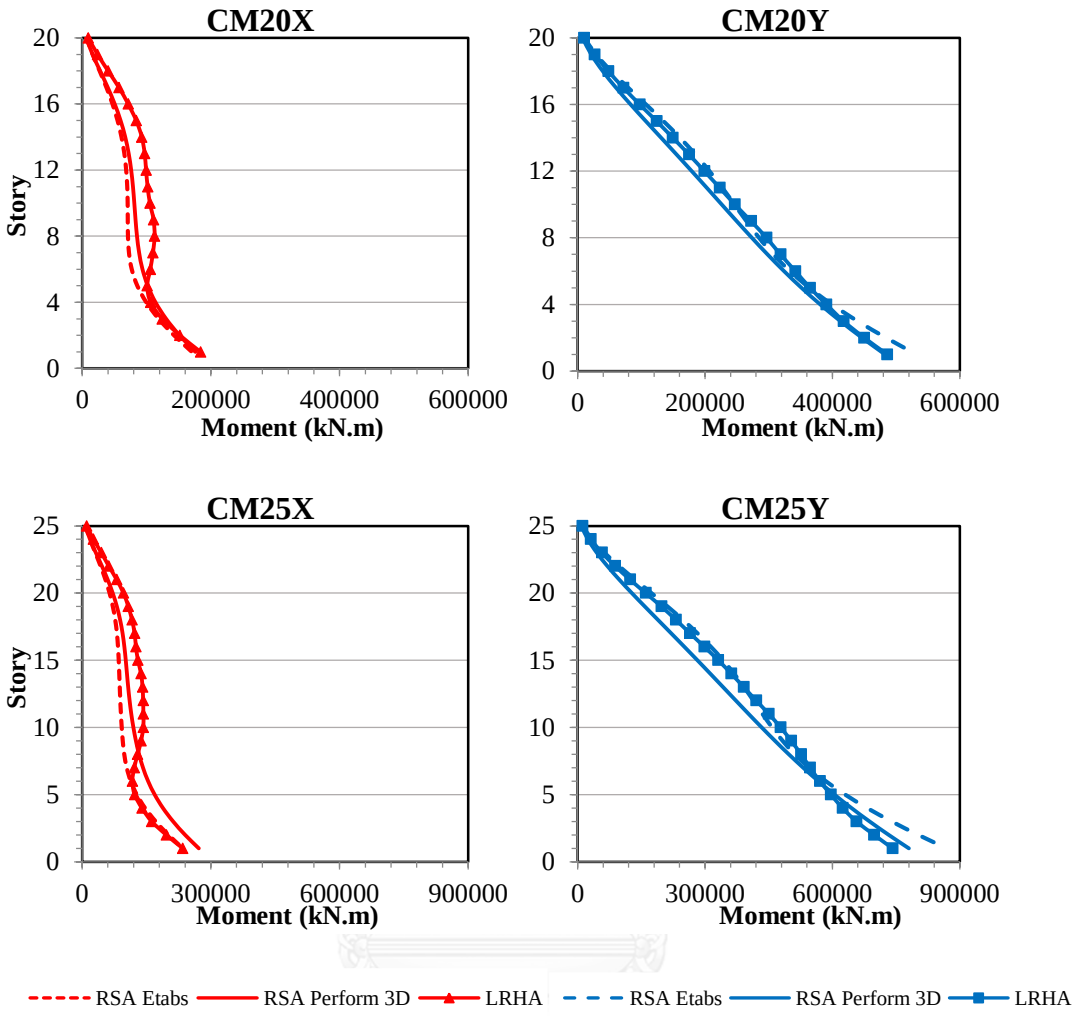

Figure C.7 Comparison of elastic bending moment of core walls computed from RSA in ETABS, RSA and LRHA in PERFROM-3D in Chiang Mai.

❖ **Story drift**

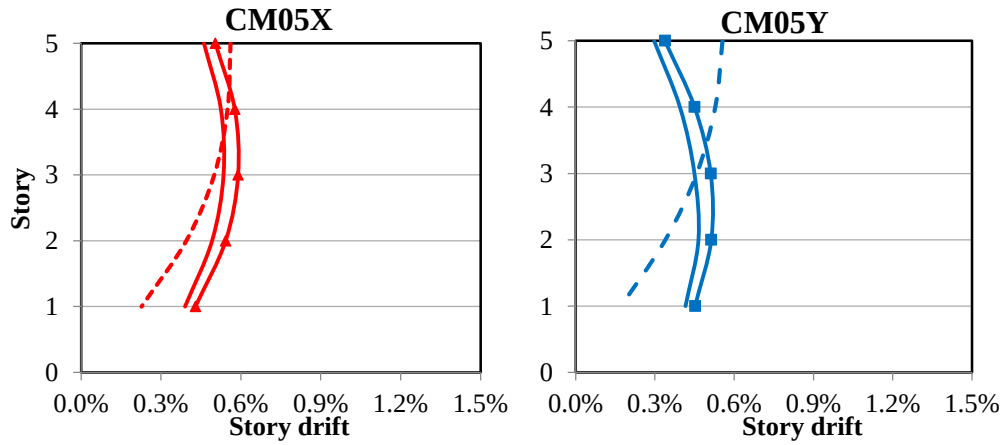

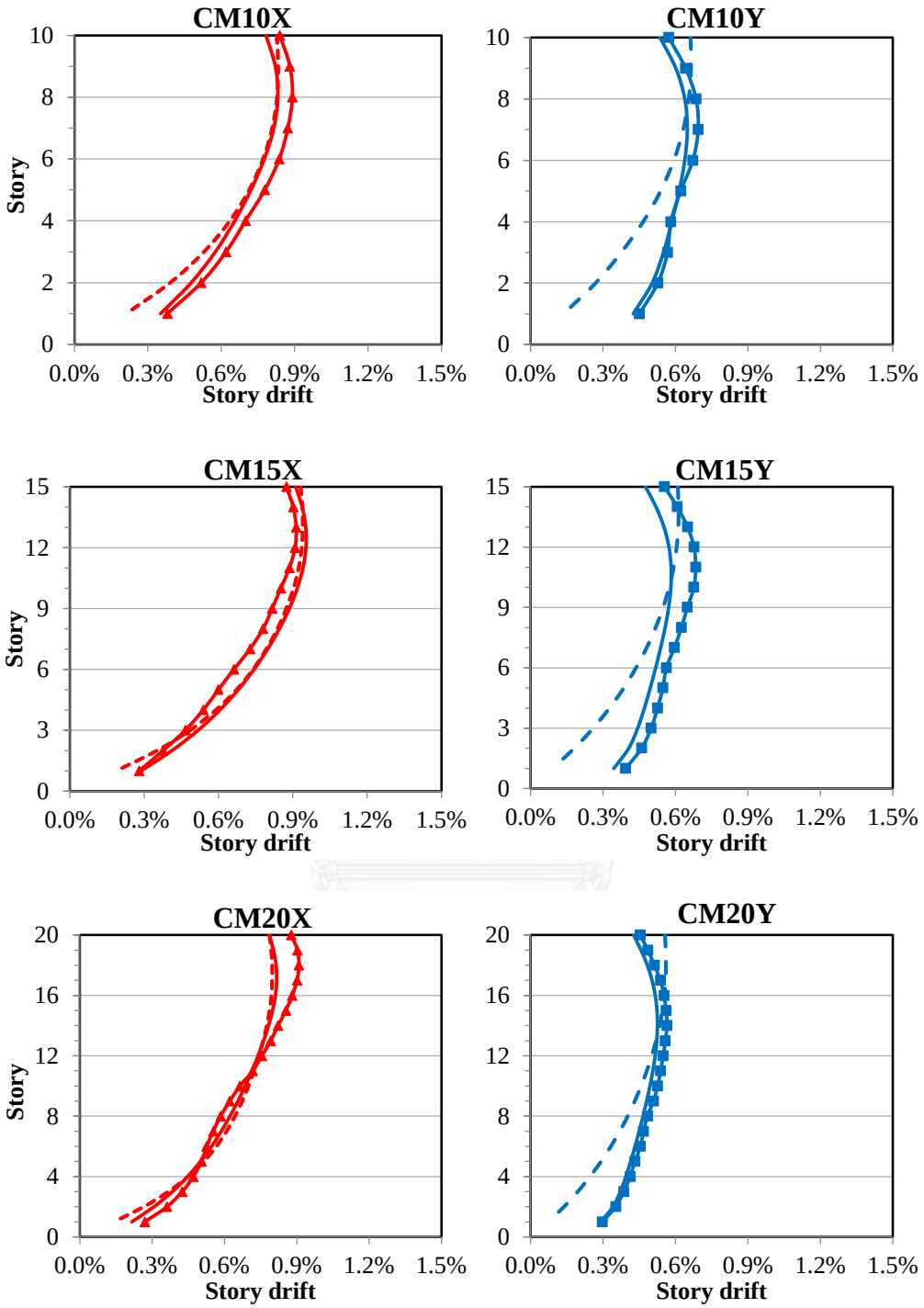
CM10X
CM10Y
CM15X
CM15Y
CM20X
CM20Y
Story
Story drift
0.0%
0.3%
0.6%
0.9%
1.2%
1.5%

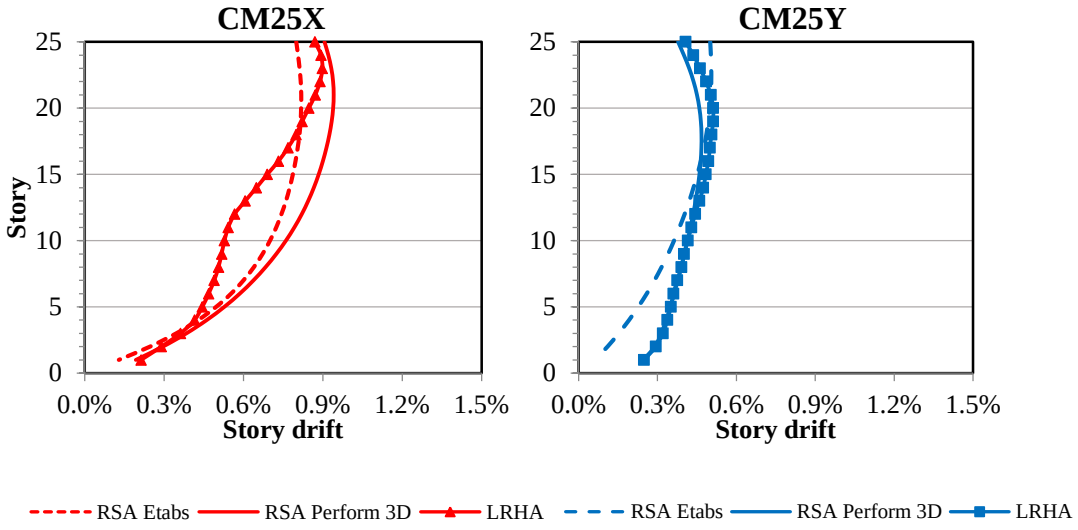

Figure C.8 Comparison of elastic story drifts computed from RSA in ETABS, RSA and LRHA in PERFROM-3D in Chiang Mai.

VITA

Kimleng Khy was born on 1st February 1991 in Kampot province, Cambodia. He finished his high school degree at Preah Reach Samphea High School in 2008. After that, he got a scholarship from government to pursue his Bachelor degree in Civil Engineering at Institute of Technology of Cambodia (ITC) in Phnom Penh for five years. During the final year in ITC, he worked as an assistant design engineer in a local company for seven months. In 2012, he got Honda Young Engineers and Scientists Award in Cambodia which was organized by Honda Company in Japan. He successfully graduated his Bachelor degree in Civil Engineering in 2013. At the end of 2103, he was awarded the scholarship from ASEAN University Network/Southeast Asia Engineering Education Development Network (AUN/SEED-Net) to pursue his Master's degree in Structural Engineering at Chulalongkorn University for two years.